Morphological and ecophysiological diversity of Mulga (*Acacia aneura* complex) in the Hamersley Ranges

Gerald Francis Miles Page
BSc. (Hons)

This thesis is presented for the degree of Doctor of Philosophy
of The University of Western Australia

School of Plant Biology

2013

Abstract

High diversification of growth forms within the Mulga species complex (*Acacia aneura* F.Muell. ex Benth. and close relatives) is characteristic of the mulga woodlands and shrublands of the Hamersley Ranges of the Pilbara region of northwest WA. However, it is unknown if particular growth forms predominate in different parts of the landscape and if their distribution is reflected in their ecophysiological functioning. The research presented in this thesis thus sought to: (a) determine if there were any identifiable trends or gradients in the morphological diversity within Mulga, particularly across landscape gradients, (b) if community patterns in morphological diversity reflected patterns in underlying growth conditions, and (c) investigate whether differences in ecophysiological adaptations among Mulga might explain patterns in community composition. I first surveyed 792 trees across 28 sites stratified into six discrete landscape positions; upper slope, lower slope, low open woodland, banded woodland, low woodland, and drainage line. I assessed variation of morphological attributes including branching habit and phyllode shape and size in relation to a range of physiographic attributes and soil physico-chemical properties across the landscape. I also conducted a series of field and lab based experiments to investigate the diversity of a variety of anatomical and physiological adaptations within the Mulga complex at the cellular, phyllode and branch level.

This research identified landscape scale trends in the composition and functional diversity of mulga woodlands. Mulga with terete to sub-terete phyllodes were more common on shaded hillslopes (south facing) while broader phyllode forms were more common in the valley woodlands. Single-stemmed growth forms were more common on hills, whereas the valleys had more multi-stemmed forms. Valley woodlands were also more diverse than hill slopes in both phyllode shapes and branching architectures. Soil chemical attributes and the differentiation among six landscape positions only explained a small proportion in the variance in the density of phyllode variants across the landscape, indicating that neither landscape position or soil chemistry are the major drivers of the morphological diversity of Mulga ‘types’ across the woodlands of the Hamersley Ranges.

During drought, the minimum branch water potential of *A. aneura* with terete phyllodes was - 8.13 MPa, compared to co-occurring broader phyllode variants of *A. aneura* and *A. ayersiana* (more negative than -10 MPa). However, all three phyllode variants showed a large and rapid (i.e., 1 – 3 days) rehydration response to 80 mm of simulated rainfall. Differences in the rates of water use were reflected by the size of the soil-to-leaf water potential gradient at midday ($\Delta\Psi$). Terete *A. aneura* had consistently less negative Ψ at midday than either of the other two phyllode variants most likely as a consequence of a larger one-sided leaf area to sapwood area ratio (*Hv*) that translated into lower overall rates of water use. Differences in water potential and phyllode shape were not reflected in the accumulation of stable osmotica. The contribution of soluble carbohydrates and inorganic ions to cellular osmolarity was relatively small (~ -1 MPa) in *A. catenulata* and three phyllode variants of *A. aneura*, which was surprising given the extreme degree of cellular dehydration (44% relative water content) and branch water potential (<-10 MPa) in many trees at the time of sampling. These data indicate a lack of coordination between the degree of drought severity (inferred from RWC, Ψ_{pd} and Ψ_{md}) and the accumulation of osmolytes in the phyllodes of either *A. aneura* or *A. catenulata*.

I also used a novel method of X-ray microtomography (micro-CT) to demonstrate three dimensional xylem connectivity was conserved across all trees regardless of phyllode shape or minimum water potential. This result suggests that differences in phyllode anatomy, and not xylem connectivity, likely explain diversity of drought tolerance among closely related *Acacia* species.

Overall, this study clearly demonstrates that the morphological diversity within *A. aneura* and the closely related species of the Mulga complex is mirrored by differences in their capacity to tolerate prolonged periods without rain but to also rapidly respond to rainfall events. These inherent but often subtle differences in physiology among Mulga types may also partly explain the co-occurrence of different species and morphotypes at the local scale; micro-site variability in underlying substrates and shading translate to small yet significant differences in the timing and availability of water to individual trees, thus creating multiple "functional niches" even within a site.

Table of Contents

List of Figures

List of Tables

Acknowledgements

Dr Pauline Grierson was my primary supervisor and it is to her that I owe the biggest thanks. Pauline has patiently allowed me to develop my own ideas, and consequently to make my (many) own mistakes. Pauline has kept me employed in various ways for several years since my scholarship expired and it has been a slow but rewarding experience - I have certainly learned the most during this period. Pauline has also shouldered the majority of editing and proof reading of this thesis, and I know its quality is a reflection of her skill at scientific writing and editing. Thanks also to my supervisor Dr Louise Cullen. Lou was intricately involved in the first two years of my project, which involved many weeks and months spent traversing the hills and valleys of West Angelas kicking the dirt and measuring many hundreds of Mulga. Lou's input was instrumental in the development of the foundations of this thesis. Thanks also to my supervisor Dr Stephen van Leeuwen for his involvement early on to establish this project and for providing an alternative perspective – that of the regulator in a rapidly changing Pilbara environment.

This project was funded by Rio Tinto. Without their support, both financial and in-kind, this project would never have happened. I would like to make special mention of Nev Havelberg and Sally Madden for particularly large and significant contributions to providing financial and logistic support and for getting things done. Many other staff at Rio Tinto also contributed, in particular site staff at West Angelas: Tracy Hagen, Melissa Thoday, John Wynn, Steve Tauro, Shaaron Stevenson, Cally Uren, Martin Burns and the site emergency response team of Dave, Peter and Chris. Thanks to Sam Luccitti for ongoing involvement in pieces of related research that have come about as a result of this thesis. Thanks to my colleagues at Rio Tinto during my brief secondment – it was a fascinating learning experience.

Dr Andrew Merchant provided advice on many aspects of tree physiology and the complications of remote field work during this project. I am extremely grateful for his ongoing mentoring. Andrew also came on a field trip and kindly hosted me at Creswick to do the osmotic analysis for Chapter 5. Dr Jie Liu was extraordinary helpful with the micro-CT analysis, and was always willing to discuss ways we could apply her amazing code to new and novel applications – hopefully we can continue this. Thanks also to Dr

Matthias Boer who provided many hours of advice on digital terrain modelling and many other aspects of my project.

Douglas Ford and Kaitlyn Height were ever-reliable and unflappable in their cooperation on long and trying camping trips. We travelled long distances, worked some very long hours carrying gas bottles up and down rocky slopes and hiking in the dark, yet still had a laugh around the fire – they were definitely good times!

Thanks also to Bruce Maslin, Jordan Reid and Joe Miller from the West Australian Herbarium and the Understanding Mulga Project for much advice regarding the peculiarities of Mulga.

All members of the Ecosystems Research Group, many past and present, contributed in a variety of ways to this project. Thanks to the honours students who broadened my research interests and also contributed to field work at West Angelas: Sharon Perks and Kaitlyn Height and their ants, Justin Fairhead and his termites and Rachel Butler and her dusty leaves. Dr Rebecca McIntyre helped in the field. Dr Alison O'Donnell helped on an early field trip and did a meticulous job of proof-reading this document. Thanks also to Kate Bowler, Chloe Flaherty, Greg Cawthray, Hai Ngo, Gary Cass, Jemima Rogers, Jessie Kalic and Trent Marwick for laboratory assistance. I also thank Dr Grzegorz Skrzypek for technical advice on stable isotope analysis, and for being patient with me during the period I worked in his lab. Dr Rohan Sadler provided invaluable statistical advice. Dr Jason Fellman was great company on field trips and I am particularly grateful to him for letting me be a field assistant on an incredible field trip to the Kimberley. My sincere apologies to anyone that I have thoughtlessly left out of these acknowledgements.

I am especially thankful to my family and friends. Wade, Kris, Jaymie, Bones, Ali, Justin, Doug, Chloe and Liz in particular have been fantastic mates around the lab. A big thanks to Mum and Dad for always encouraging me to keep studying, and sisters Bronwyn and Wendy for some great holidays.

Finally, thanks to Belinda. You met me three years into my PhD, about to run out of scholarship and with no end in sight. You've patiently heard me promise to finish "this year" each year since and never let it bother you. You're incredible.

x

Statement of Candidate Contribution

This thesis is my own work, except where otherwise acknowledged. This thesis was completed during the course of my enrolment in the degree of Doctor of Philosophy at The University of Western Australia and has not previously been accepted for any other degree at this or any other institution.

This thesis is presented as a series of manuscripts (Chapters 2-6) that have either been published (Chapters 2, 6), or are intended to be submitted for publication in peer-reviewed journals (Chapters 3 - 5). Acknowledgement for contributions to each chapter and publications details for Chapters 2 and 6 are given below. I was the primary author on both published chapters and was the main contributor for all chapters including data collection, analysis and manuscript preparation. I have permission from all co-authors to include this work in my thesis.

Chapter 2 (Published): Dr Louise Cullen and Dr Pauline Grierson are co-authors; they participated in field data collection and provided editorial advice on the manuscript. Dr Stephen van Leeuwen is a co-author and participated in manuscript development. Chapter 2 has been published as:

Page G.F.M., Cullen L.E., van Leeuwen S. & Grierson P.F. (2011) Inter- and intra-specific variation in phyllode size and growth form among closely related Mimosaceae *Acacia* species across a semiarid landscape gradient. *Australian Journal of Botany*, **59**, 426-439.

Chapter 3: Ms Kaitlyn Height and Ms Chloe Flaherty provided technical assistance with soil chemical analyses. Ms Kaitlyn Height and Mrs Kate Bowler processed extracts on the auto-analyzer for nitrogen and phosphorus fractions. Dr Matthias Boer provided advice on the digital terrain modelling and landscape classification analysis outlined in Appendix A.

Chapter 4: Stable isotope analyses were processed by Dr Grzegorz Skrzypek and Mr Douglas Ford at the Western Australia Biogeochemistry Centre at The University of Western Australia.

Chapter 5: Extraction and determination of carbohydrates in leaf extracts were conducted in collaboration with Dr Andrew Merchant (University of Sydney), who also provided editorial comment on the Chapter. Mr Michael Smirk processed leaf cation extracts on the ICP. Ms Kaitlyn Height provided technical assistance with pressure-volume curves.

Chapter 6 (Published): Dr Jie Liu was a co-author and processed the xylem network models using algorithms she had previously developed; she also assisted with manuscript development. Dr Pauline Grierson was a co-author, helped conceptualise the study and provided editorial advice on the manuscript. Chapter 6 has been published as:

Page G.F.M., Liu J. & Grierson P.F. (2011) Three-dimensional xylem networks and phyllode properties of co-occurring Acacia. *Plant, Cell & Environment*, **34**, 2149-2158.

Signed _____ Date_____

Gerald Page

Signed _____ Date_____

Pauline Grierson (coordinating supervisor)

Chapter 1: General Introduction

Introduction

This thesis aims to increase understanding of the morphological and ecophysiological diversity of the Mulga species complex and the significance of this diversity to the persistence of long-lived perennials in arid landscapes. My research sought to quantify the morphological diversity within the species complex found in the Hamersley Ranges of the Pilbara region of northwest Australia and to determine whether different morphotypes are also functionally differentiated. In this introductory chapter, I provide an overview of the current understanding of the morphological diversity in Mulga and introduce the influence of underlying variability in habitat and climate on plant ecophysiology, before identifying the knowledge gaps this study addressed.

Mountain ranges, even when only a few hundred metres higher than the surrounding plains, are recognised as hotspots of diversity in the arid and semi-arid landscapes of Australia (Byrne *et al.* 2008). Complex topography generates specialized niches that are particularly pronounced under the water limited conditions that characterize arid and semi-arid environments (Noy-Meir 1973). Consequently, mountain ranges provided important refugia during arid zone expansions and contractions during the Pleistocene, which also contributes to the complicated patterns of speciation and distribution often observed in these areas (Byrne *et al.* 2008). The mountains and valleys of the Hamersley Ranges of the Pilbara are a prime example of such hotspots. Here, highly localised variation in soils and their underlying geology, set within a landscape comprised of a mosaic of gorges, plateaux and plains, has generated a topographic and geological complexity that has contributed to significant localized speciation (Pepper *et al.* 2008), and with greater endemism than the surrounding arid regions (González-Orozco, Laffan & Miller 2011). Approximately 1,750 plant species occur in the Pilbara, 7% of which are endemic to the region and 40% are growing at the edge of their range (Stephen van Leeuwen, pers. com. 2013). However, these estimates are likely to be conservative as the flora of the Pilbara remains largely unstudied and new species are regularly described (McKenzie, van Leeuwen & Pinder 2009, Maslin & Reid 2012).

In addition to the high degree of speciation observed in the Pilbara region is the

extensive morphological variation that is exhibited within some species. Nowhere is this more apparent than in the Mulga woodlands and shrublands that dominate much of the Pilbara landscape. Mulga communities, both in the Pilbara and elsewhere across inland Australia, are characterised by a canopy primarily composed of members of the Mulga species complex (*Acacia aneura* F.Muell. ex Benth. and closely related species). The Mulga species complex is renowned for exhibiting a bewildering spectrum of growth forms, branching patterns and phyllode sizes, shapes and colours, which have been variously classified into a number of distinct species, varieties and informal variants (Miller, Andrew & Maslin 2002, Maslin & Reid 2012). Furthermore, while many species and morphological variants co-occur, the range of variation and number of co-occurring species and variants is purportedly much higher within the woodlands of the Hamersley Ranges than elsewhere across Australia. However, it is unclear if the morphological diversity present in the Mulga complex in the Hamersley Ranges reflects topographic complexity or niche differentiation among sites. Furthermore, it remains unclear if morphological diversity within Mulga is reflected in underlying differences in function that might in-part explain co-occurrence or turnover within the species complex across topographic or environmental gradients.

The Pilbara is also a region of tremendous mineral wealth, which has attracted extensive and rapid development, particularly over the past decade (McKenzie *et al.* 2009, DRDL 2011). Around 410 million tonnes, or 45%, of the global supply of iron ore was exported from the Pilbara in 2011; the combined value of iron ore and offshore petroleum exports have increased more than twenty-fold since 2000 (DRDL 2012). The Pilbara mining industry is expected to continue to expand as evidenced by the forecasted population growth from 63,736 in 2012 to 140,000 by 2035 (DRDL 2012). Consequently, the natural environment of the Pilbara is subject to ever increasing levels of the disturbance. For example, more than 20,000 ha are currently directly disturbed by the iron ore industry in the Pilbara; much of this land is mulga woodland and shrubland (Merritt & Dixon 2011). Additional clearing occurs with mineral exploration surveys and for infrastructure associated with the transport and supply of the mining industry; all of this disturbed land will need to be rehabilitated to meet environmental closure requirements (Merritt & Dixon 2011). While the ecological restoration of mulga communities in arid and semi-arid Australia following mining is of critical importance nationally, the challenges and principles of successfully restoring stable ecosystems that are functionally and genetically diverse are applicable worldwide.

Successful restoration or rehabilitation is predicated on an understanding of the processes and components that both constrain and contribute to fully functioning ecosystems (Aronson *et al.* 1993, Padilla *et al.* 2009). Given that the growth and distribution of mulga woodlands and shrublands are considered to be principally limited by the redistribution and availability of water, the constraints on water capture, storage and utilization by the dominant species are likely of most significance to these systems (Noy-Meir 1973, Morton *et al.* 2011). In arid and semi-arid zones, perennial trees in particular are often growing at their physiological limits, in many cases persisting only where they can access moisture stored at depth to avoid relying on infrequent and unpredictable rainfall. Alternatively, perennial species with shallow root systems must endure long periods of exposure to water stress and dehydration. Consequently, these "drought tolerators" possess a variety of adaptations to maintain cell turgor during prolonged drought or to rapidly recover photosynthetic capacity when positive turgor is re-established. Understanding these adaptations, and in particular the diversity of adaptation mechanisms, is key to resolving the thresholds and limits of drought tolerance in semi-arid and arid ecosystems and thus will underpin our capacity to predict vegetation responses to change or manage them under differing growth conditions in the future, including altered landscapes post mining. For example, how will changing patterns of rainfall in the arid zone (Cullen & Grierson 2007) influence the distribution and abundance of dominant flora? What is the capacity of dominant species to tolerate changes in rainfall timing and intensity whilst at the same time being subject to anthropogenic disturbances associated with development?

Given the urgent need to improve our understanding of the basic habitat requirements of dominant arid and semi-arid flora, the body of research presented in this thesis seeks to increase understanding of the ecophysiological implications of morphological diversity within the Mulga species complex. Below, I provide an overview of how Mulga is currently defined and the distribution and ecology of the Mulga species complex, with a particular focus on *Acacia aneura* F.Muell. ex Benth. I describe the complicated morphological variation present within the Mulga complex and the mechanisms thought to maintain it. I then consider the ecophysiological implications of diversity across different scales; from intra-specific variation in tree and shrub morphology through to landscape scale variation in the spatial patterning of woodlands and shrublands. This background thus provides context for the experimental rationale that is developed in

chapters 2 – 6 of this thesis, including the potential applications of this research to improve management of semi-arid woodlands amidst rapid development of semi-arid and arid Australia.

What is Mulga?

"Mulga" is the common name generally applied to a group of closely related semi-arid tree or shrub species, including *Acacia aneura*, that are the dominant canopy species of the "mulga" woodlands and shrublands that dominate large areas of arid and semi-arid Australia (Bentham 1864, Johnson & Burrows 1994, Miller *et al.* 2002). Until very recently, Mulga more strictly referred to *A. aneura* and a small number of closely related species that formed the 'Mulga complex', including *Acacia ayersiana* Maconochie, *A. minyura* Randell and *A. paraneura* Randell (Miller *et al.* 2002). However, a new treatment of the *A. aneura* "group" in Western Australia defines Mulga as 12 closely related species, five of which were previously described as varieties of *A. aneura* (Pedley 2001), four species not including *A. aneura* that were already part of the complex and two completely new taxa (Table 1.1). Consequently, "Mulga" now refers to a minimum of 12 species of *Acacia* that are all closely related to and morphologically very similar to *A. aneura*. Maslin & Reid (2012) also refer to a further ten species of *Acacia* that they also consider very similar to members of the Mulga complex. Thus, reliably identifying different species or morphological variants of Mulga can be challenging.

One of the challenges in resolving the taxonomy of Mulga has been its tremendous morphological variability (Johnson & Burrows 1994, Miller *et al.* 2002, Maslin *et al.* 2012). The Mulga complex includes species, varieties and informal variants that often co-occur and feature distinctly different growth forms, phyllodes and/or pod characters (Miller *et al.* 2002, Maslin & Reid 2012). For example, vegetative characteristics of Mulga in the Pilbara can vary from a low multi-stemmed shrub of ~ 1-2 m tall, to a tall single stemmed tree of ~ 18 m (Figure 1.1). Phyllodes (the photosynthetic leaf analogue of *Acacia*) can vary from a cylindrical (terete) form ~ 1-2 mm wide and 3–4 cm long to a flat form 8–10 mm wide and 8–10 cm long (Figure 1.2). Phyllodes also vary in colour from grey-blue's to green (Miller *et al.* 2002, Maslin & Reid 2012). Consequently, identification of specimens below the species level can be difficult, especially in the absence of flowers and pods; the *Acacia aneura* group have been revised on multiple

occasions since the species was first described in 1855 (Bentham 1855), to the most recent revision by Maslin & Reid (2012).

Table 1.1 The 12 species of Mulga as described by Maslin & Reid (2012) and their relationship to the earlier classification of Pedley (2001)

Maslin & Reid (2012)	Pedley (2001)
A. aptaneura Maslin & J.E.Reid	(syn. *A. aneura* var. *pilbarana* Pedley and *A. aneura* var. *tenuis* Pedley)
A. macraneura Maslin & J.E.Reid	(syn. *A. aneura* var. *macrocarpa* Randell)
A. aneura F.Muell. ex Benth.	(provisional syn. *A. aneura* var. *intermedia* Pedley)
A. fuscaneura Maslin & J.E.Reid	(syn. *A. aneura* var. *fuliginea* Pedley)
A. caesaneura Maslin & J.E.Reid	(syn. *A. aneura* var. *argentea* Pedley)
A. incurvaneura Maslin & J.E.Reid	(syn. *A. aneura* var. *mirocarpa* Pedley)
A. mulganeura Maslin & J.E.Reid	new taxon
A. pteraneura Maslin & J.E.Reid	new taxon
A. ayersiana Maconochie	retained
A. caspedocarpa F.Muell.	retained
A. minyura Randell	retained
A. paraneura Randell	retained

Only two varieties of *A. aneura* described by Pedley (2001) are not included in this table. *A. aneura* var. *conifera* was not retained by Maslin & Reid (2012) as the growth habit that defined the variety was observed in four of the Mulga species. *A. aneura* var. *major* is deliberately not included here as it is not present in Western Australia and is therefore outside the scope of the most recent revision (Maslin & Reid 2012).

Given the complexity and variable use of common names associated with "Mulga" in the published literature, below I define as clearly as possible the terms used in this thesis. This terminology is based on the most consistent usage in the current literature:

- "Mulga" is used in the broad sense to describe any of the 12 species that currently comprise the "Mulga complex" or "*A. aneura* group", including *Acacia anuera, A. aptaneura* and *A. ayersiana* (Miller *et al.* 2002, Maslin & Reid 2012). This includes any of the species that were previously described by the 10 varieties of *A. aneura* according to Pedley (2001) but are now separate species under the most recent revision (Maslin & Reid 2012). The 12 species that comprise the *A. aneura* group and their relationship to the Pedley (2001) classification are listed in Table 1.1.
- "Morphotypes" is used to describe morphological variants of Mulga that are not captured by the taxonomic keys, and no assumptions are made regarding genetic

or plastic differences. For example, common morphotypes include differences in branching habit or phyllode size and shape, i.e. single or multiple stems, horizontal branching and terete or broad phyllodes. Refer to Chapter 2 for a thorough description.

- "mulga" or "mulga woodland/shrubland" refers to a vegetation community where the dominant canopy is formed by "Mulga".
- When the species name is known, it is referred to explicitly (i.e., *Acacia catenulata* sub. *occidentalis* Maslin)
- When referring to publications that have dealt with Mulga, the species name is used (i.e. *A. aneura*) when the original authors have done so. Wherever possible, I have attempted to clarify precisely which species or variety they were referring to. For example, Everist (1949) was most likely referring to *A. ayersiana* and *A. aneura* but called them both *A. aneura*. However, when authors describe a subspecies of *A. aneura* following Pedley (2001), I have not applied the most recent West Australian classification without seeing the voucher specimens (i.e. Andrew *et al*. 2003), instead retaining the original identification.[1]

[1] Chapters 2 and 6 of this thesis were published in scientific journals before the publication of Maslin & Reid (2012). The species name *A. aneura* was used in the broad sense (*s. lat*.) in these papers.

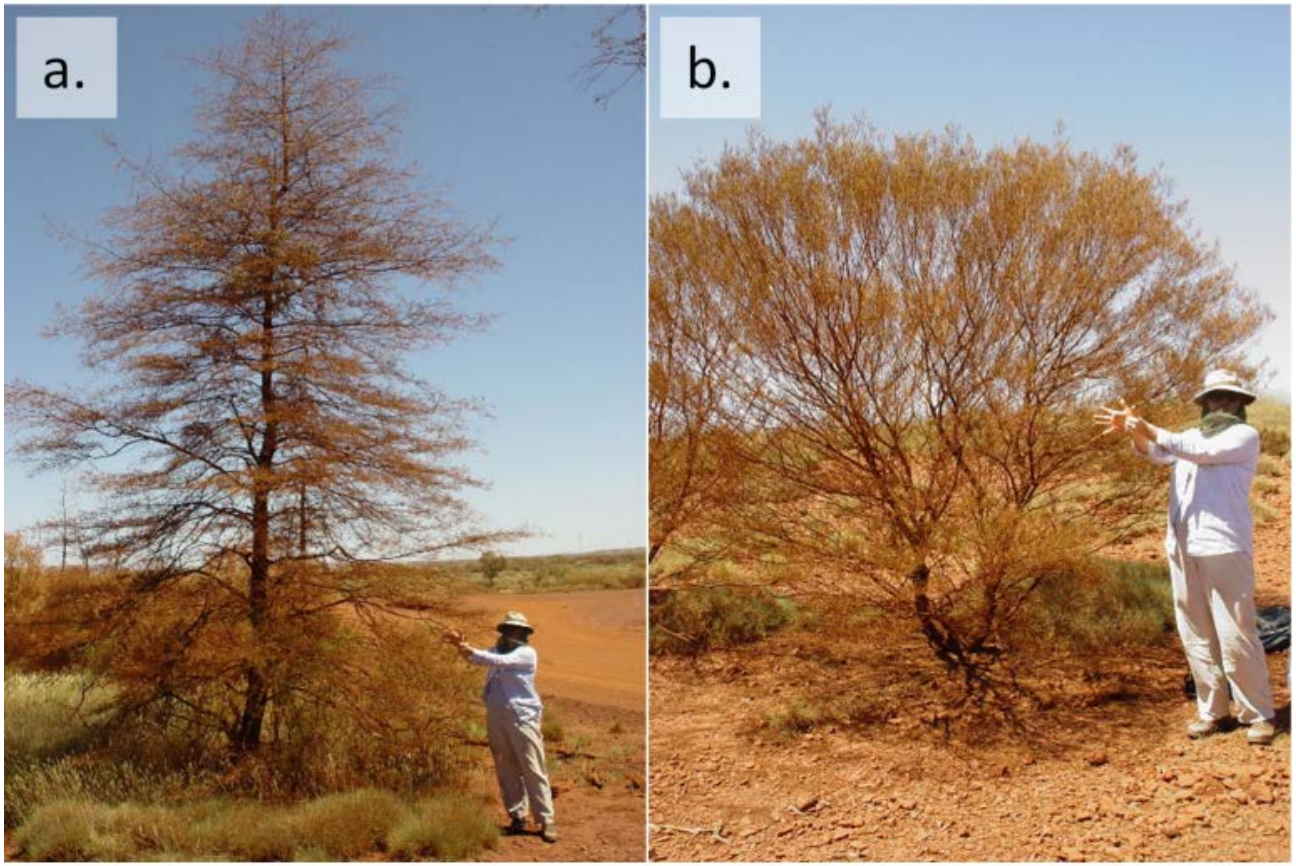

Figure 1.1 Two co-occurring growth forms of *A. aneura* in the Pilbara that are at the extreme ends of the spectrum of variation present within the species (sens. lat.).(a) a “Christmas tree” or coniferous growth habit of Mulga, (b) co-occurring tall rounded shrub growth habit of Mulga.

Figure 1.2 Typical variation in phyllode size and shape of co-occurring *A. aneura* and closely related species in a woodland at West Angelas. T19, T82, T52 & T 105 are most likely *A. aneura*, T104 *A. catenulata* and T2 *A. ayersiana*.[2]

[2]voucher specimens were not collected when this image was taken.

Biotic and abiotic mechanisms that maintain morphological diversity within Mulga

Co-occurrence of different morphotypes of Mulga is very common, with monospecific stands of the same growth form, for example, all tall trees of single stem, being much rarer (Maslin & Reid 2012). It is generally accepted that there is at least some genetic basis to the variation in Mulga, although the exact mechanisms that maintain the variation are not well understood (Fox 1986, Cody 1989, Johnson & Burrows 1994, Miller *et al.* 2002, Andrew *et al.* 2003). Co-occurrence of different morphotypes is indicative of reproductive isolation, a hypothesis supported by the occurrence of triploids of *A. minyura* and *A. aneura* var. *tenuis*, tetraploids of *A. ayersiana*, *A. aneura* var. *intermedia*, *A. minyura* and pentaploids *A. aneura* var. *tenuis* in a single population in the Northern Territory (Andrew *et al.* 2003). It has also been suggested that Mulga is a facultative apomict, allowing the reproduction of sexually sterile polyploids and a small number of hybrids that persist within populations (Miller *et al.* 2002, Andrew *et al.* 2003). Hybridization is also very common among members of the *A. aneura* group further complicating the identification of discrete entities (Maslin & Reid 2012). In addition to these barriers to gene-flow, flowering occurs infrequently depending on episodic rainfall and seed production is even rarer (Preece 1971a, Preece 1971b). Thus, issues related to genetic provenance as well as logistical limitations of seed collection based on seasonal variability present interesting challenges for land managers considering restoring disturbed or cleared mulga communities. For example, how appropriate will seed collection from one particular community be for the restoration of a disturbed site in another location or are different morphotypes suited to particular environments? A better understanding of the functional implications of morphological diversity is fundamental to assessing the contribution of site conditions over and above hybridization and underlying genetic differences to the morphological complexity within Mulga.

Biogeography of mulga with particular reference to the Pilbara region of Western Australia

In Western Australia, mulga woodlands and shrublands dominate not only the southern to central Pilbara, but also large parts of the Murchison and Gascoyne IBRA[3] regions (Figure 1.3). A detailed inventory of the vegetation in Western Australia at a scale of 1:250000 identified 146 out of a total of 819 vegetation associations that contained Mulga, including 34 where they were the principal canopy species and had a total coverage of approximately 46.4 million hectares (Shepherd, Beeston & Hopkins 2001). To put this into an international perspective, the coverage of Mulga in Western Australia is roughly equal in size to the Chihuahuan Desert of North America. The Pilbara region alone is almost 1.5 times the size of the Mojave Desert, and the total coverage of Mulga in Australia (~ 1,500,000 km^2) is almost twice the combined areas of the Chihuahuan, Mojave and Sonoran Deserts (~ 884,000 km^2). Consequently, the Mulga woodlands and shrublands of Australia are comparable with the *Larrea* and *Prosopis* vegetation communities of North America in terms of their dominance and extensive distribution of the arid and semi-arid biome, but have received much less scientific attention.

[3] Interim Biogeographic Regionalisation for Australia (IBRA) classifies Australia's landscapes into 89 large geographically distinct bioregions based on common climate, geology, landform, native vegetation and species information. (http://www.environment.gov.au/parks/nrs/science/bioregion-framework/ibra/index.html)

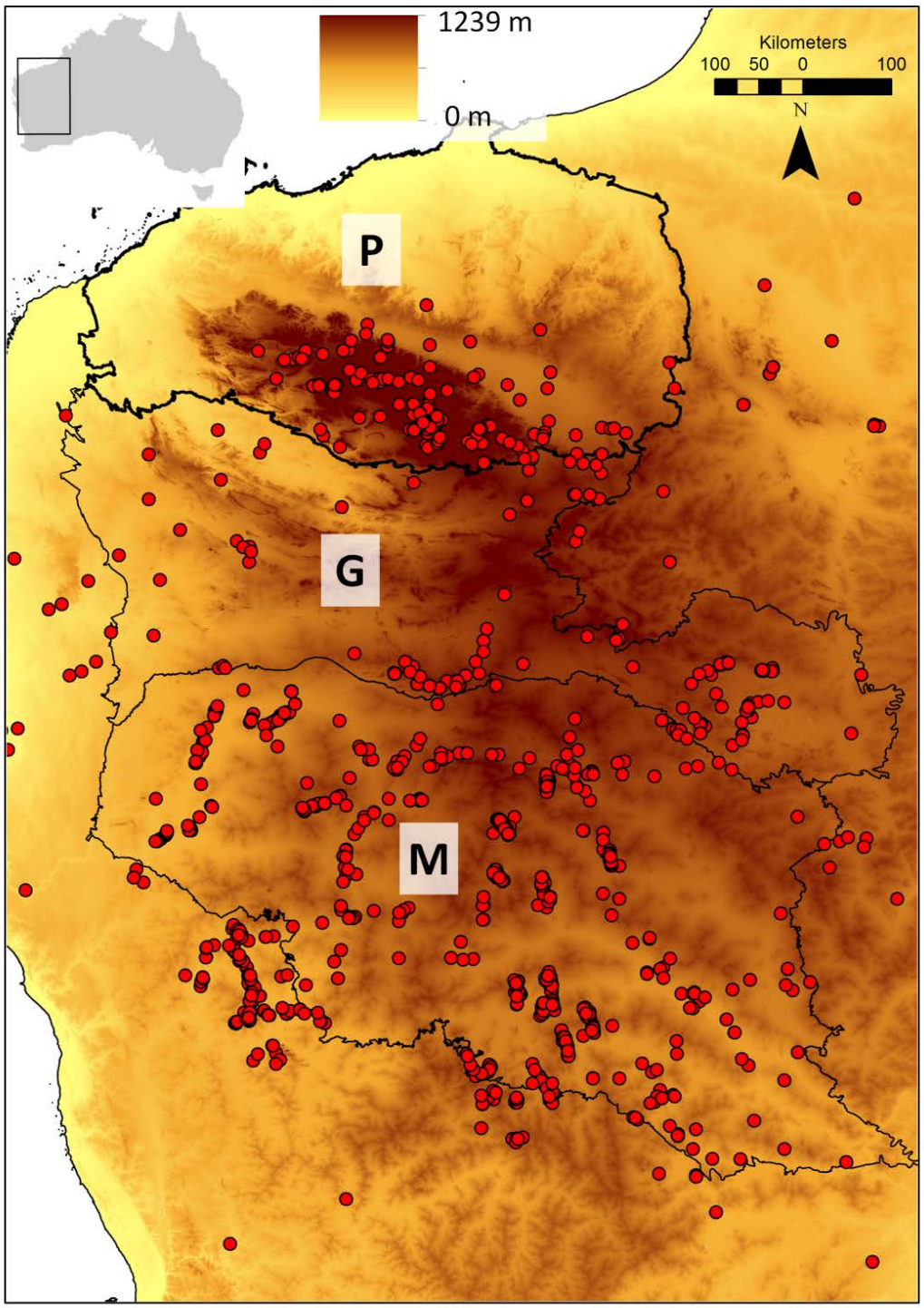

Figure 1.3 Distribution of Mulga (*A. aneura* sens. lat., *A. ayersiana*, *A. minyura* and *A. paraneura* in Western Australia. The Pilbara (P, darker outline), Gascoyne (G) and Murchison (M) IBRA regions are outlined. The shaded digital elevation model (DEM) distinguishes the rugged Hamersley Range in the Pilbara region to the relatively flat topography of the Gascoyne and Murchison regions. Point data were sourced from the Atlas of Living Australia (http://www.ala.org.au) and 90 m SRTM DEM from Geoscience Australia.

The Pilbara region of Western Australia is the north-western most limit of the distribution of Mulga (Figure 1.3). However, while the landscapes of the Pilbara might be considered more marginal habitats for Mulga, the variability in climate and landforms across the region produces large gradients of resource availability that drives complicated patterns of distribution and diversity of species. The Pilbara bioregion is bounded by the Indian Ocean to the northwest, arid inland deserts to the east and extensive rangelands to the south (McKenzie *et al.* 2009). The Pilbara is also a transition zone in the west of Australia between the summer monsoon tropics to the north and the winter-rainfall dominated Mediterranean zone to the south, which results in an arid to semi-arid climate with both summer and winter rainfall possible (Beard 1975, McKenzie *et al.* 2009). The central and southern areas of the Pilbara are also dominated by the rugged Hamersley Ranges with a highly dissected and ancient landscape that is in stark contrast to the more subdued topography of the Gascoyne and Murchison regions to the south and the desert plains to the north and east (Figure 1.3). Therefore, the flora of the Pilbara region is surprisingly diverse considering its climate (McKenzie *et al.* 2009). This high diversity of terrain and soils and a highly dynamic and variable rainfall regime, combined with a high diversity of flora makes the Hamersley Range an ideal location to study the variation in both morphology and physiology within the Mulga complex.

Within the Pilbara region, Mulga occurs across the Chichester, Fortescue Plains and Hamersley sub-regions (Figure 1.4). In the central Pilbara (southern end of the Chichester sub-region), mulga communities occur primarily in valleys and over tussock grasslands on alluvial plains (Beard 1975, Van Vreeswyk *et al.* 2004). The Fortescue Plains consist of extensive salt marsh, mulga-tussock grass, and short grass communities on alluvial plains in the east. In the rugged Hamersley sub-region on the south side of the Fortescue Valley, tree steppe with snappy gum (*Eucalyptus leucophloia* Brooker) is predominant while mulga low woodland occurs in the valleys. Consequently, Mulga grows on a range of different landforms, including rocky hillslopes, at the base of hills and rock outcrops (habitats receiving additional run-off water), and in swales. It has also been speculated that the presence of mulga woodlands as far north as the Fortescue Valley is due to favourable ‘bottomland’ soils and moisture from run-on (Beard 1975, 1990). The low stony hills of the Chichester Range broadly constitute the northernmost extent of Mulga in the Pilbara, which also corresponds to the edge of its climatic range (Beard 1975).

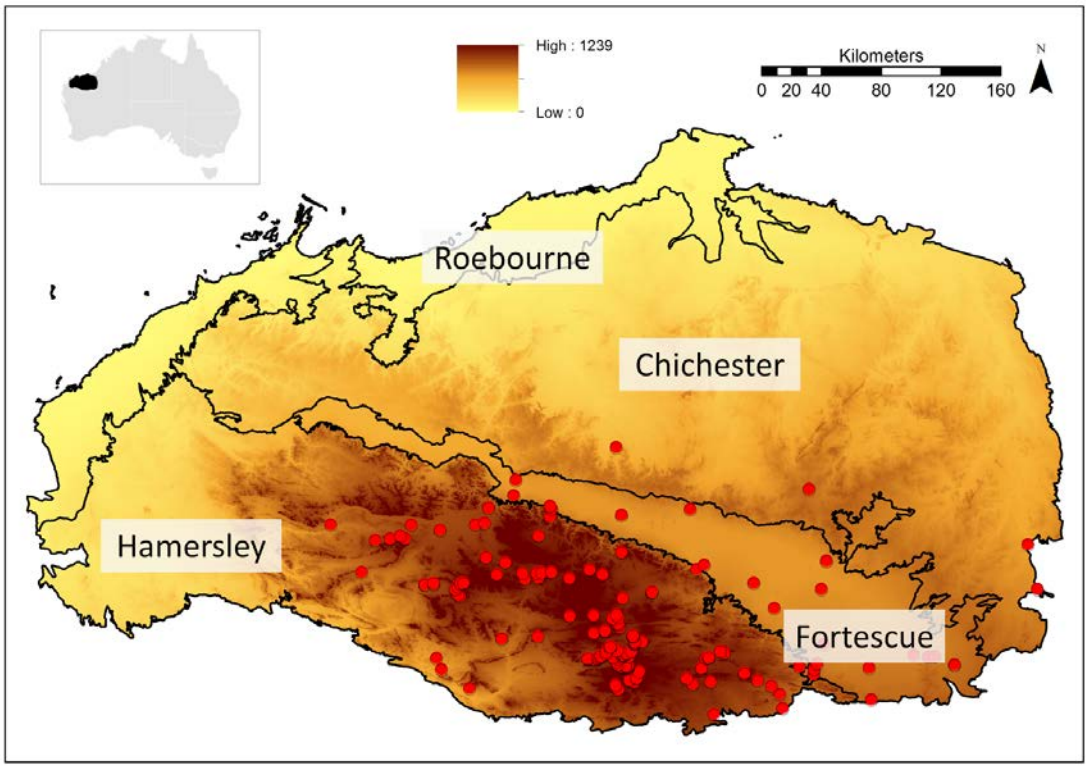

Figure 1.4 The distribution of Mulga in the Pilbara. IBRA sub-regions are outlined and labelled, and a digital elevation model (DEM) is shaded. Mulga is restricted to the southern and central Pilbara in the topographically dissected and rugged Hamersley Ranges. The Fortescue Marsh and Chichester Range immediately north of the Marsh is the northern limit of the distribution. Point data sourced from the Atlas of Living Australia (http://www.ala.org.au) and 90 m SRTM DEM from Geoscience Australia.

The soils of the Pilbara region have developed from some of the oldest erosion surfaces on Earth; exposed Archaean crust (3.6 – 2.7 Ga) in the north and iron rich sedimentary deposits (2.77 – 2.4 Ga) that have been uplifted to form the Hamersley Range in the south (Arndt *et al.* 1991, Kranendonk *et al.* 2002). Consequently, Pilbara soils are heavily weathered like most arid zone soils and show little vertical structure due to a lack of organic matter inputs (Beard 1975, Johnson & Burrows 1994, Van Vreeswyk *et al.* 2004). The soils in the Hamersley and Chichester Plateaus are primarily dissected red-brown sandy loams to loams that are skeletal and rocky on the ridges, and deeper in the valleys. Low woodlands and shrublands on hill slopes have coarser textured soils that are very shallow or skeletal. Most mulga communities occur in valley woodlands that have deep red-brown loams (light textured red earths), that generally have a hard coherent subsoil (Williams 2002). These soils also often have a stony surface cover and are slightly acidic (pH 4 – 7). Mulga is also occasionally found growing on calcrete platforms; however, surface soils at these sites rarely have a pH greater than 7.5. Mulga

is less common on cracking clays and deep sands (Beard 1975). There has previously been some suggestion that growth form variation within Mulga species (and within other *Acacia* species in the Pilbara) may be attributable to differences in substrate (e.g. 'Christmas tree" Mulga on calcrete; Beard 1990); however, relationships between forms and substrates have not been systematically investigated.

Potential impacts of spatial and temporal variability of rainfall and soil moisture in the Pilbara on plant function

Mulga and mulga communities are capable of surviving droughts of unpredictable severity and duration, all the while retaining the capacity to utilize water following a rainfall pulse. Mulga have a shallow root system (<5 m) with a concentration of roots close to the surface making them reliant on rainfall recharge of surface soil (Slatyer 1965, Pressland 1975). These “pulses” of soil moisture associated with major rainfall events drive primary productivity in arid and semi-arid environments (Huxman *et al.* 2004b, Schwinning & Osvaldo 2004), although these rainfall pulses can be rare and unpredictable. For example, mean annual rainfall in the Pilbara town of Newman is 313 mm (1961 – 2010); however, in 1996 the town received their lowest recorded annual total of 36 mm while in 1999, Newman received their highest annual rainfall of 619.2 mm that included 214 mm in one day on the 16th of December 1999 (Bureau of Meteorology 2011a). Most rainfall occurs between December and March from low-pressure systems and cyclones developing off the northwest coast. Cyclonic rainfall events can be large; the highest recorded rainfall total in 24 hours in the Pilbara exceeded 500 mm (Dogramaci *et al.* 2012). Surface water is also scarce and shallow surface soil dries out quickly as evaporative demand is extremely high (average pan evaporation exceeds rainfall by a factor of ten; (Bureau of Meteorology 2011b). Consequently, the supply of water to Mulga and mulga communities is both unreliable and inconsistent.

The supply of water to mulga communities is also strongly influenced by topographic position. For example, a run-on run-off dynamic has been proposed as a controlling mechanism behind banded or grove/inter-grove mulga formations (Slatyer 1961b, Mabbutt & Fanning 1987, Tongway & Ludwig 1990, Greene 1992, Anderson & Hodgkinson 1997, Tongway & Ludwig 1997, Berg & Dunkerley 2004). In this scenario, treeless or less densely vegetated ‘inter-groves’ are slightly more elevated than

groves and have lower infiltration rates, shedding runoff in diffuse surface flows (overland flow; Huggett 2011) to the more densely vegetated ‘groves’. Slatyer (1965) originally proposed that bands were aligned perpendicular to the slope as a mechanism of intercepting surface runoff. However, with modern surveying methods and access to remotely sensed data, it has become apparent that the slope orientation of bands is highly variable. For example, mulga shrublands near Alice Springs once considered perpendicular to the slope direction (Slatyer 1961b, Slatyer 1965), were later discovered to be oblique to the slope (Berg & Dunkerley 2004). Instead of simply intercepting and trapping water runoff from the inter-band, oblique bands may instead create a flow of water along the band down slope, which can in turn provide run-on for woodlands further down the slope and on valley floors. While the hydrology of grove/inter-grove mulga communities has received most attention, the hydrology of other mulga communities is less well understood (Ludwig *et al.* 2005, Moreno-de las Heras *et al.* 2012).

In the Pilbara, mulga woodlands and shrublands grow in a diverse range of habitats and structures, including banded communities, thus encompassing upper slopes through to drainage features in the valley floors (Figure 1.5, Figure 1.6); however, the ecological water requirements of these communities and the way that they may differ among landscape position, is largely unquantified. Most particularly for the key themes of this thesis, it remains unclear whether the morphological variation (growth form or phyllode shape and size) of Mulga reflects underlying environmental conditions influenced by water supply and landscape position. The association between form and function underpins classical plant ecology (Raunkiaer 1934, Kent & Coker 1992). Leaf size and branching habit are key traits used in plant functional type classification as they have been demonstrated to be associated with water and nutrient use and carbon fixation at continental and global scales (Reich, Walters & Ellsworth 1997, Schenk *et al.* 2008). The functional implications (if any) of the variability in phyllode size and shape and growth form of Mulga are unknown.

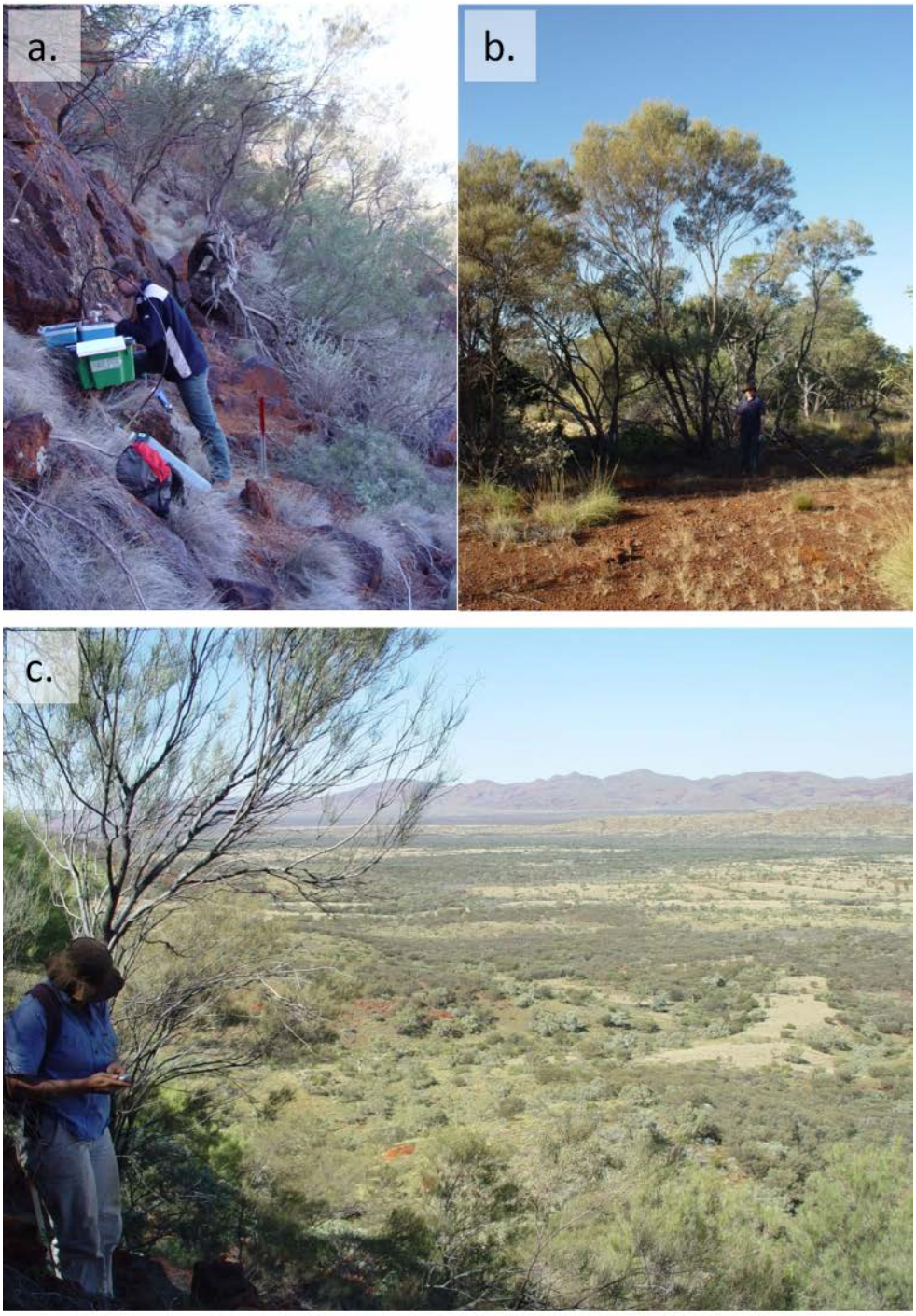
a.
b.
c.

Figure 1.5 Mulga woodlands growing in a variety of habitats in the Pilbara region of Western Australia. (a) Steep upper southern hill slope, (b) tall open woodland in the valleys of West Angelas, (c) a view from a southern hill slope over a typical valley at West Angelas dominated by mulga woodlands in a mosaic with sparse *Eucalyptus* spp. over *Triodia* spp., (d) an inter-grove of tussock grass and termite mounds adjacent to a mulga grove and a southern hill slope covered by mulga woodland in the distance, (e) a drainage line at the bottom of a valley at West Angelas with tall open mulga woodland.

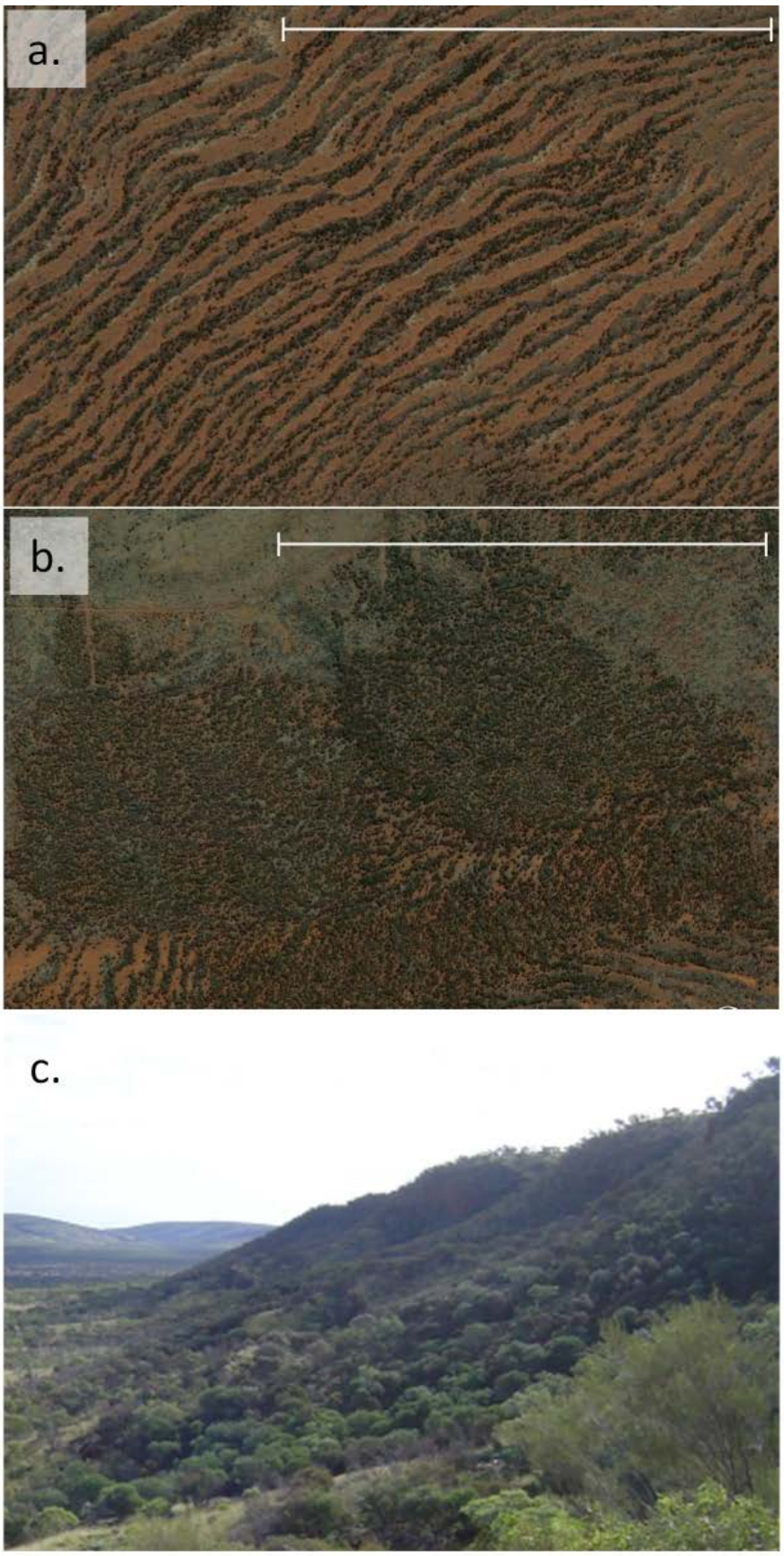

Figure 1.6 Three typical examples of variation in the spatial structure of mulga woodlands in the Pilbara region of Western Australia. (a) Banded woodland, (b) non-banded woodland, and (c) woodland of south facing hill slope. Scale bar in (a) and (b) is 1 km.

Aims and structure of this thesis

The overall objective of this research is to describe and quantify the morphological diversity and ecophysiological attributes within the Mulga complex in the Pilbara region of Western Australia. Specifically, the aims of this thesis are to:

a) determine if there were any identifiable trends or gradients in the morphological diversity within Mulga, particularly across landscape gradients,
b) determine if community patterns in morphological diversity reflected patterns in underlying growth conditions, and
c) investigate whether differences in ecophysiological adaptations among Mulga morphotypes might explain patterns in community composition.

I expected that differences in tree morphology reflect ecophysiological adaptations at the phyllode, branch, whole tree and community level to landscape variation in water availability. Understanding these adaptations, and in particular the diversity of adaptation mechanisms, is key to resolving the thresholds and limits of drought tolerance in semi-arid and arid ecosystems that are subject to increasing levels of anthropogenic disturbance and a changing climate. A better understanding of the traits that allow woody perennials to dominate in the harsh semi-arid climate of the Pilbara will also assist in the design and implementation of restoration and rehabilitation projects.

This research is focused on the greater West Angelas area of the Pilbara region of Western Australia (Figure 1.7). West Angelas is a mining lease managed by Rio Tinto on the south-eastern end of the Hamersley Ranges. West Angelas is also an area of great interest for biodiversity conservation in Western Australia as it is adjacent to Karijini National Park, the second oldest conservation estate in Western Australia. At present, mulga vegetation communities are not well represented in conservation estates in the Pilbara. Furthermore, the greater West Angelas area is characterized by valleys dominated by mulga woodlands that are purported to contain some of the highest intra-specific diversity within the Mulga species complex (Stephen van Leeuwen, pers. com. 2012). The mulga woodlands at West Angelas are also some of the most intact in the region as they have never been grazed by introduced stock.

Chapter 2 quantifies the landscape distribution of growth form and phyllode variants within the Mulga complex across a series of landscape units identified by digital terrain modelling. Further detail of the digital terrain modelling is provided in Appendix A. Chapter 3 tests hypotheses that might explain the influence of landscape position and soil fertility on Mulga distribution that were generated by the results of Chapter 2. Chapters 4 – 6 then examine the ecophysiological diversity within the Mulga complex at a range of scales; from individual phyllodes and branches to broad landscape trends of water-use characteristics within and among woodlands. Chapter 4 quantifies the contribution of stable osmotica to phyllode water potential and turgor maintenance across the landscape gradient. Chapter 5 examines the pulse-response strategy of co-occurring Mulga species and phyllode variants within a single woodland. Chapter 6 then investigates the contribution of three-dimensional xylem architecture for coping with extreme branch water potentials, using branch segments from the trees used in the pulse-response experiment in Chapter 5. Finally, Chapter 7 provides a general discussion of the collective outcomes of this research and its relevance to understanding the diversity of both tree morphology and ecophysiological adaptation in semi-arid regions, and suggests avenues for further research.

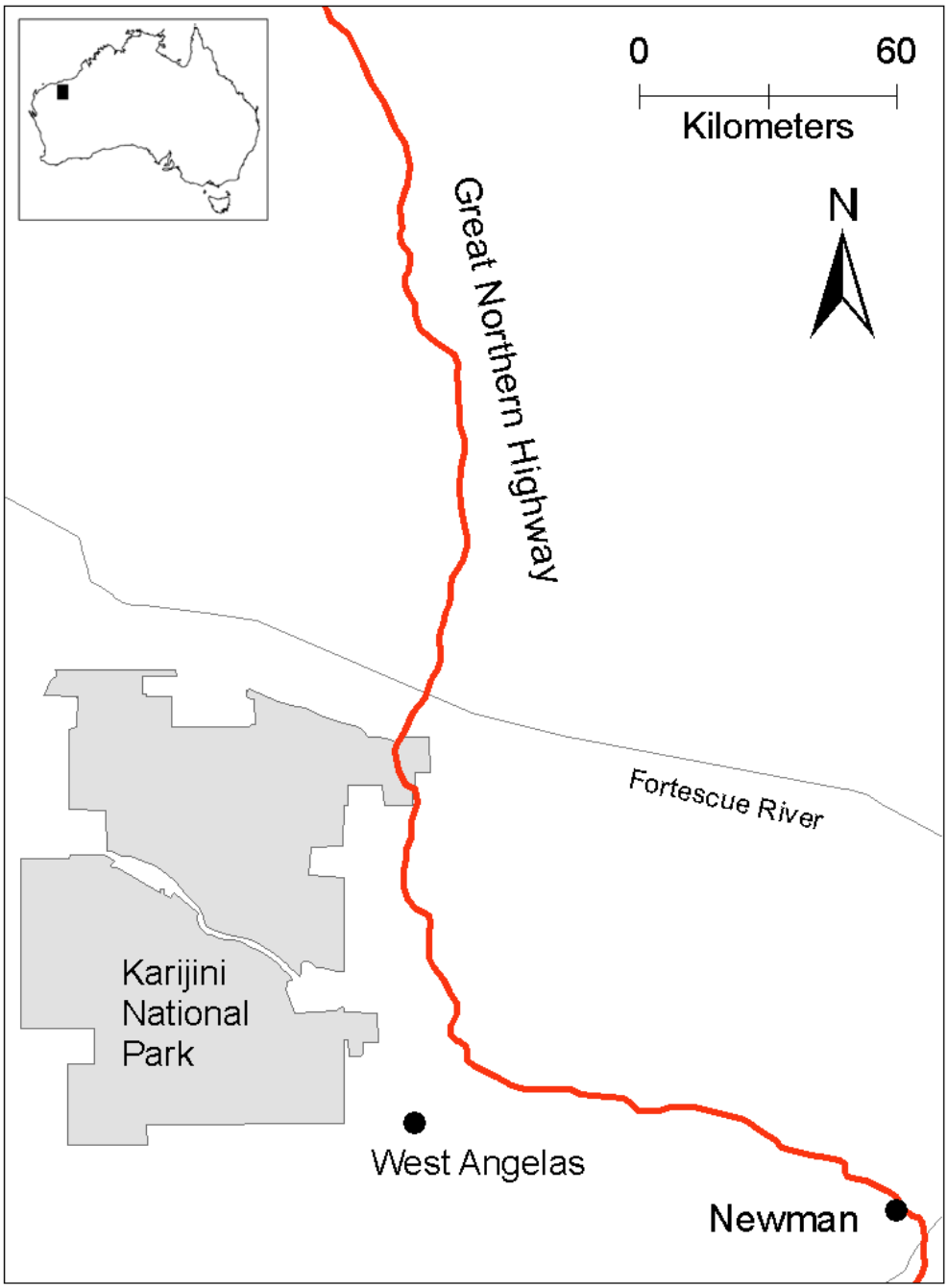

Figure 1.7 Location of West Angelas, the study site for this thesis, in relation to Karijini National Park and major towns and highways in the Pilbara.

Chapter 2: Inter- and intra-specific variation in phyllode size and growth form among closely related Mimosaceae *Acacia* species across a semi-arid landscape gradient[4]

Introduction

Leaf size and growth form are commonly used to identify plant functional types owing to the strong association between plant form and function, particularly carbon fixation and water use (Noble & Slatyer 1980, Díaz & Cabido 1997, Reich *et al.* 1997, Weiher *et al.* 1999). Growth form has also long been a part of structural vegetation classification (Kent & Coker 1992). Differences in leaf size and growth form across communities and ecosystems have been extensively correlated with environmental gradients of resource availability including nutrients and water (McDonald *et al.* 2003, Wright *et al.* 2004b, Schenk *et al.* 2008, Ordoñez *et al.* 2009). However, only a few studies have examined these changes within a single species or species complex (Kalapos & Csontos 2003, Prior, Bowman & Eamus 2005, Beaumont & Burns 2009, Gouveia & Freitas 2009) even though intra-specific studies facilitate a more direct examination of the link between plant form and function because they are less likely to be confounded by phylogenetic adaptation (Prior *et al.* 2005).

The integrated nature of plant traits makes it very difficult to attribute them to only one, or any particular combination of environmental drivers (Shipley 1999, Prior *et al.* 2005, Westoby & Wright 2006). Much of our understanding of plant trait-resource relationships has also been developed from Mediterranean, temperate and tropical ecosystems (Falster & Westoby 2003, McDonald *et al.* 2003, Pickup, Westoby & Basden 2005, Niinemets, Portsmuth & Tobias 2007b, Meier & Leuschner 2008). In such environments, interactions among numerous environmental variables including light, soil nutrients, water and frequent disturbance, result in complex conditions for growth that confound analysis of plant traits. In contrast, ecosystems in semi-arid

[4] Published as: Page G.F.M., Cullen L.E., van Leeuwen S. & Grierson P.F. (2011) Inter- and intra-specific variation in phyllode size and growth form among closely related Mimosaceae *Acacia* species across a semiarid landscape gradient. *Australian Journal of Botany*, **59**, 426-439.
This Chapter has had subsequent minor revisions since publication to incorporate more recent references.

landscapes are principally driven by water availability (Noy-Meir 1973, Williams & Calaby 1985, Stafford Smith & Morton 1990). While other factors are obviously of importance (e.g., nutrients, soil depth, fire regime), semi-arid landscapes provide a relatively simplified system in which to study the relationship between form and function in plant traits.

Mulga woodlands occur across a diverse range of soil types and topographic positions in semi-arid Australia, and their distribution occupies close to 20% of the Australian continent (Everist 1949). Even at a local scale, mulga woodlands can grow across a range of positions in a toposequence, including upper and lower southern hill-slopes, valley floors and drainage lines. The dominant canopy species of mulga woodlands are members of the 'Mulga complex' composed of nine closely related species (Johnson & Burrows 1994, Miller *et al.* 2002). While *Acacia aneura* F. Muell ex Benth (Mulga) is the dominant species in the complex, it also includes *Acacia catenulata* C.T.White subsp. *occidentalis* Maslin (hereafter referred to as *A. catenulata*) and *Acacia ayersiana* Maconochie (Miller *et al.* 2002). *A. aneura*, and to a lesser extent *A. catenulata* and *A. ayersiana*, are renowned for exhibiting a wide range of growth forms and phyllode shapes that often co-occur (Johnson & Burrows 1994). Consequently ten varieties of *A. aneura* are currently described (Pedley 2001), and the Mulga complex has been the focus of several taxonomic revisions (Pedley 1973, Randell 1992, Pedley 2001, Miller *et al.* 2002)[5]. While much of the variation in morphology of *A. aneura* may be genetic (Cody 1989, Andrew *et al.* 2003), it is also likely that a component of the variation is attributable to phenotypic plasticity in response to differences in growing conditions (Fox 1986, Beard 1990). However, little is known about the relationship between morphological diversity within *A. aneura* and closely related species, or habitat attributes of Mulga that are likely related to or determined by topographic position.

The range of both growth forms and phyllode shapes in the Mulga complex and their landscape distribution must be quantified in order to assess the relationship between form and function, including the potential role of morphological plasticity, in contributing to the variation. There have been only a few anecdotal descriptions of habitat preferences by formal varieties of *A. aneura* (Fox 1986, Pedley 2001). *A. aneura*

[5] This chapter was published before the publication of Maslin & Reid (2012). Here, the species name *A. aneura* was used in the broad sense (*s. lat.*). Refer to Table 1.1 for a comparison of Pedley (2001) with Maslin & Reid (2012).

commonly occurs as a range of growth forms between a shrub of less than 2 m in height and a tree up to 15 m tall and can be single- or multi-stemmed. Phyllode shapes range from small cylindrical needles less than 1 mm wide to broader leaf-like shapes that are 10 mm wide and relatively flat (Pedley 2001). Varieties of *A. aneura* are most readily identified by phyllode and seedpod characteristics, but branching architecture is not often considered. Given that that our systematic understanding of Mulga is also still developing (Miller *et al.* 2002), it is unclear to what extent branching architecture can change within varieties, or if phyllode traits and branching architecture are even linked.

The objectives of this study were (i) to describe the variation in branching architecture and phyllode shape for members of the Mulga complex (*A. aneura* and closely related species) around West Angelas in the Pilbara region of Western Australia, and (ii) quantify the landscape distribution of branching architectures and phyllode shapes. I expected that phyllode size and shape would not be independent of growth form (branching architecture and tree size), and that Mulga variants would not occur homogeneously across different landscape positions. For example, I expected communities on valley floors to be dominated by trees with single stems and broader phyllodes while multi-stem trees with more terete phyllodes would dominate communities on upper slopes.

Materials and Methods

Sampling sites

A total of 28 transects were measured across six landscape positions in 60,000 hectares at West Angelas in the Hamersley Ranges of the Pilbara region of Western Australia (-23.175, 118.790). West Angelas has been recognised as one of the richest sites of intra-specific diversity within *A. aneura*, because of its position in a highly dissected landscape that is on the edge of the species' distribution (Pedley 2001, McLeish, Chapman & Schwarz 2007). Valleys at West Angelas are ~ 700 m asl, and relative elevation differences of the hills and ridges is ~ 250 m (Figure 2.1), although the highest local peak is Mount Robinson at 1144 m. I stratified the landscape by terrain analysis and classification using fuzzy *k*-means (Vriend *et al.* 1988, Burrough, van Gaans & MacMillan 2000). Here I briefly describe the method, with more detail provided in Appendix A. Landscape classification used five terrain attributes that are in part

responsible for the redistribution and availability of light and water across the landscape. The following five terrain attributes were derived from a 30 m digital elevation model; elevation, slope angle, cumulative downhill slope length, soil wetness index (Moore *et al.* 1993, Burrough *et al.* 2000) and annual incident solar radiation calculated with the program POTRAD5 for PCRaster by accounting for latitude, season and terrain elevation (van Dam 2000). Further information on the calculation of each of these terrain attributes is provided in Appendix A. Seven terrain units were classified across the site, four of which contained mulga woodlands (upper and lower southern hill slopes, valley floors and drainage lines). Mean values of modelled terrain attributes for the four units that contained mulga woodlands are listed in Appendix B.1. As ~ 90% of the mulga woodlands occurred on valley floors, this terrain unit was further stratified into three mulga woodland types: banded mulga woodland characterised by distinct linear groves separated by bare ground, low mulga woodland characterised by a uniform distribution of Mulga, and low open mulga woodland characterised by a sparse distribution of Mulga separated by bare ground and *Triodia* spp. Consequently, the landscape was stratified into six positions containing mulga woodland going from upper to lower slopes; (1) upper southern hill slope, (2) lower southern hill slope, (3) low mulga woodland, (4) banded or linear mulga woodland, (5) low open mulga woodland, and (6) drainage line mulga woodland (tall woodland) (Figure 2.1). There were no woodlands on north facing slopes (most exposed aspects). I established five transects within each landscape position across the site, except for banded mulga woodland and drainage line mulga woodland. For the banded and drainage line mulga woodlands there were only four sites as a large bushfire burnt most of the study area in October 2006 and limited further sampling. Belt transects were 4 m wide and a minimum of 100 m long, containing a minimum of 20 individuals of *A. aneura* or closely related members of the Mulga complex.

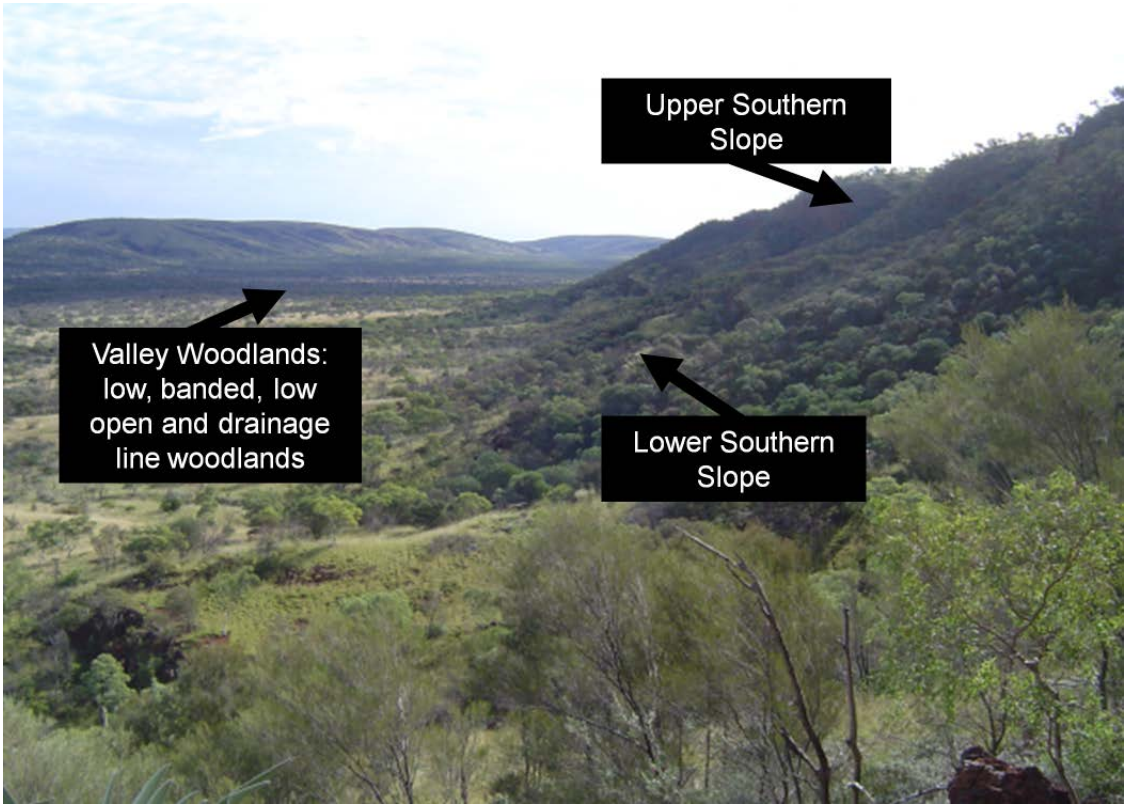

Figure 2.1 Typical landscape profile at West Angelas in the Hamersley Ranges. Relative elevation from valley floor to upper slope is ~ 250 m**.**

Field classification of Mulga growth forms

While growth form has already been included in the classification of some varieties of *A. aneura* (Pedley 1973, Randell 1992, Pedley 2001), the descriptions have been both qualitative and confusing (see Chapter 1). Here, I created a subjective growth form classification, which differentiated between single and multi-stemmed growth habit, and then by tree height, height to stem division and canopy area. I measured a total of 792 Mulga trees and shrubs along 28 belt transects and visually classified them according to a field key of growth forms in the study area (Figure 2.2). Phyllode shapes were classified in a similar way. Phyllodes were subjectively classified as one of six shapes that were prominent in the study area (Figure 2.3). The six phyllode shapes broadly distinguished among three phyllode shape variants of *A. aneura* (terete, narrow and broad) and three other closely related species (*A. ayersiana, A. catenulata*, *A. minyura*). *Acacia paraneura* was also present in the study area but was not captured in the field sampling.

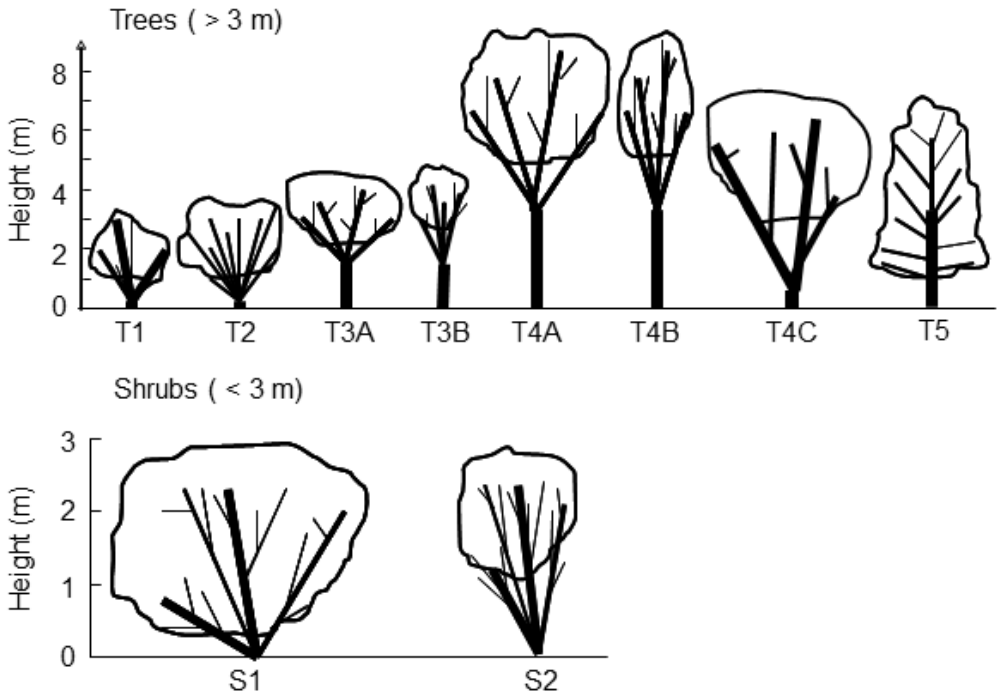

Figure 2.2 Field classification key to growth forms of *Acacia aneura* and close relatives. T1 & T2 are low multi-stemmed trees, where T1 has only two or three main stems and T2 has > three main stems of similar diameters. T3A and T3B are low single-stemmed trees that differ only in the spread of the crown. T4A and T4B are tall single-stemmed trees that differ only in the spread of the crown. T4C is a tall multi-stemmed tree, with a main stem division <50 cm from the ground. T5 is a single-stemmed semi-coniferous looking tree characterised by horizontal branching. S1 and S2 are shrubs <3 m tall, and differ in the spread of the canopy.

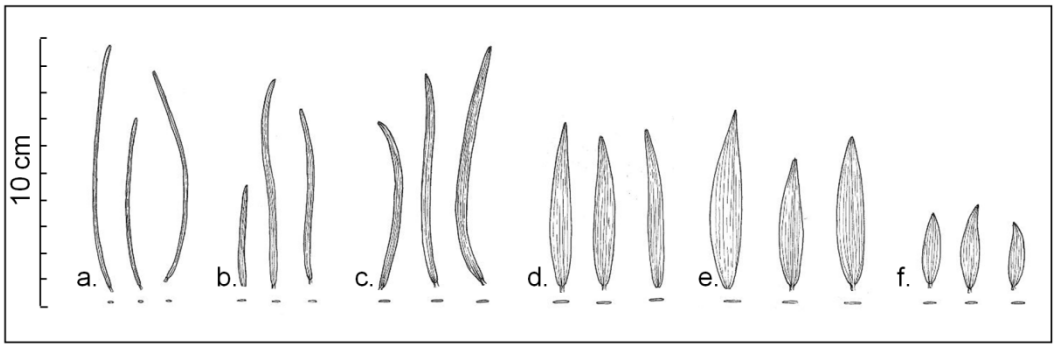

Figure 2.3 Four species of *Acacia* including three phyllode variants of *A. aneura* that were common at West Angelas. (a) *A. aneura* (terete), (b) *A. aneura* (narrow), (c) *A. aneura* (broad), (d) *A. catenulata*, (e) *A. ayersiana*, (f) *A. minyura*. Hand drawn sketches of three typical phyllodes from each type are drawn above stylized transverse sections of each.

Branching architecture, and phyllode size and shape

Measurements of branching architecture and phyllode size were made to quantitatively define growth form, and determine whether the subjective classifications could be substantiated. Six measurements that characterised branching architecture were recorded for all trees in each belt transect: trunk basal diameter, diameter of every stem at 50 cm from the base, height of the first stem division, height to crown break, canopy area (measured at the maximum width and then perpendicular) and total height. Length, width and thickness to the nearest 0.1 mm were measured on 20 phyllodes collected 1-2 m from the ground from four positions spaced equally around the canopy from each of 285 trees and shrubs that spanned all six landscape positions. Approximately five individuals of each phyllode shape were included in the subset of trees and shrubs selected at each transect. Differences in branching architecture will be referred to hereon as differences in 'growth form', and phyllode dimensions as 'phyllode shape'. 'Phyllode variants' will be used only when specifically referring to phyllode shape variants of *A. aneura*.

Data analysis

The experimental design had four factors: landscape position (six levels, fixed), transect (four or five levels nested within each landscape position for a total of 28), growth form (ten levels, random) and phyllode shape (six levels, random). I used permutation multivariate analysis of variance (PERMANOVA, Anderson 2001) and canonical analysis of principal co-ordinates (CAP, Anderson and Willis 2003) to test if mulga variants could be identified from their growth form and phyllode size, and if phyllode size was independent of growth form with a multivariate null hypothesis of no differences among *a priori* groups. The *F-ratio* constructed in PERMANOVA is analogous to Fisher's *F*-ratio and is constructed from the sums of squared distances within and between groups (Anderson 2001). All PERMANOVA tests used 9999 permutations of the raw data from residuals under a reduced model. CAP determines the 'distinctness' of multivariate groups by producing a misclassification error using the 'leave one out allocation of the groups' approach. A higher percentage of correct classifications indicated a more 'distinct' group on the canonical axes (Anderson & Willis 2003). Phyllode data were square root transformed, and growth form attributes were normalized. Bray-Curtis similarity matrices were used in all multivariate analysis. The assumption of homogeneity of dispersions among groups was tested using permutational analysis of multivariate dispersions (PERMDISP, Clarke & Gorley

2006). All multivariate analysis was performed using PRIMER v6 with the PERMANOVA+ add-on (Clarke & Gorley 2006).

I calculated the relative dominance (%) of each growth form and phyllode shape in every landscape position, and tested for differences among landscape positions for every measured attribute with one-way ANOVA models. Pairwise comparisons were made with Tukey's Honest Significant Difference (HSD) post-hoc tests. ANOVA models and post-hoc tests were calculated using R 2.11.0 (R Development Core Team 2010).

Results

General classification of Mulga growth forms and phyllode shapes

Nearly 40% of the trees at West Angelas were tall multi-stemmed trees (T4C), while most others were single-stemmed trees (T3A, T3B, T4A, T4B) and multi-stemmed low trees (T1) (Appendix B.2, also see Figure 2.2 for tree types). The multi-stemmed shrub forms S1 and S2, and the horizontally branched tree form, T5, were only recorded occasionally and constituted less than 4% of the total plants measured (Appendix B.2). Plant height was highly variable (1.7 to 16.4 m), while the number of stems 50 cm from the ground ranged between 1 and 14. Quantitative measurements of branching architecture confirmed the validity of growth form types identified qualitatively (Appendix B.2), as all forms were statistically distinct with the exception of T1 and T5 (PERMANOVA P-values > 0.05, data not shown).

Phyllode shape was also highly variable across all 28 sites for the four co-occurring *Acacia* species, particularly *A. aneura* (Table 2.1). Inter-specific differences in phyllode shape were consistent with current taxonomic descriptions of the species (Pedley 2001), and were the key feature for field identification. Phyllodes were broadest in *A. ayersiana* and decreased in the order *A. catenulata* > *A. minyura* > broad *A. aneura* > narrow *A. aneura* > terete *A. aneura*. *A. minyura* is easily distinguished from the other three species by its short phyllodes (Table 2.1, Figure 2.3; Maslin & Reid 2012). Phyllode width was highly variable for *A. aneura* and varied between 0.46 and 10.3 mm, which is also the total variation described for the species across Australia (Pedley 2001). At the two extremes, terete phyllodes are nearly cylindrical whereas the broadest phyllodes were on average nearly seven times as wide as they were thick. *A. ayersiana*

and *A. catenulata* also showed a large variation in phyllode length and width. Phyllode width varied between 7 and 17 mm in *A. ayersiana* and between 1 and 14 mm in *A. catenulata*. Phyllode length varied from 45 to 90 mm in *A. ayersiana* and 30 to 130 mm in *A. catenulata* (Table 2.1).

Phyllodes of four *Acacia* species, including three subgroups of *A. aneura*, were classified into six shape categories during field data collection based on a visual assessment (Figure 2.3). Broad *A. aneura* were the most common phyllode type (38.5%), followed by terete *A. aneura* (22%), narrow *A. aneura* (19.2%) and then *A. catenulata* (17.4%). Both *A. ayersiana* and *A. minyura* were rarely present (<3%). Of the plants for which phyllode dimensions were measured, 81 were 'terete', 78 were 'narrow", 70 were 'broad', 40 were '*A. catenulata*', 7 were '*A. ayersiana*' and 9 were '*A. minyura*'. All phyllode shapes were significantly different (PERMANOVA $P < 0.001$); however, the assumption of homogeneity of dispersions was not fulfilled ($P = 0.004$ PERMDISP). The standard errors of group dispersions were the same among phyllode shapes, except for '*A. ayersiana*', which had only seven samples and a standard error less than 50% of all other groups. There was significant variation among phyllode shapes at the transect level (PERMANOVA $P < 0.001$), but not among landscape positions (PERMANOVA $P > 0.05$). Estimates of the components of variation indicate that most variation was among phyllode shapes, and that transects, and phyllode shape by transect interactions had estimates comparable with the residuals, which were 20% of the variation among phyllode categories.

Table 2.1 Phyllode size and shape of four *Acacia* species and three phyllode variants of *A. aneura*

		Length (mm)			Width (mm)			Thickness (mm)		
	n	min	mean	max	min	mean	max	min	mean	max
A. ayersiana	*140*	45.5	**65.4 ab** (0.66)	90.5	7.60	**12.3 a** (0.16)	17.8	0.31	**0.48 a** (0.006)	0.72
A. catenulata	*840*	29.7	**80.2 c** (0.55)	133.2	0.97	**6.30 b** (0.07)	14	0.15	**0.41 b** (0.003)	0.87
A. minyura	*220*	8.39	**26.7 d** (1.08)	45.3	2.59	**5.86 c** (0.13)	10.8	0.31	**0.46 ab** (0.006)	0.72
A. aneura (terete)	*1617*	7.40	**62.6 a** (0.34)	115.4	0.46	**1.01 d** (0.01)	2.23	0.25	**0.64 c** (0.004)	1.50
A. aneura (narrow)	*1560*	23.9	**66.3 b** (0.44)	148.9	0.48	**1.62 e** (0.02)	4.99	0.20	**0.56 d** (0.004)	1.18
A. aneura (broad)	*1440*	19.2	**63.5 a** (0.36)	114.6	0.65	**3.18 f** (0.03)	10.3	0.17	**0.47 a** (0.003)	0.99

Mean values are bolded, and standard errors are given in parentheses. Data is untransformed. Lower case letters denote significant groupings from Tukey's HSD post-hoc tests when one way ANOVA $P < 0.05$

There was no clear association between growth forms and phyllode shapes for the 792 trees and shrubs measured in the study, particularly within the population of *A. aneura*. Terete phyllodes were found on seven different growth forms, including both multi- and single-stemmed shrubs and trees, and a similar pattern was observed for the 'narrow' phyllode shape. Seven different growth forms also had broad phyllodes; nevertheless, just under half of individuals with broad phyllodes occurred on multi-stemmed trees (T4C). Similarly 50% of *A. catenulata* were multi-stemmed trees (T4C). *A. minyura* had five distinct growth forms, but mostly (70%) occurred as a multi-stemmed shrub in the category 'S2' (Figure 2.4).

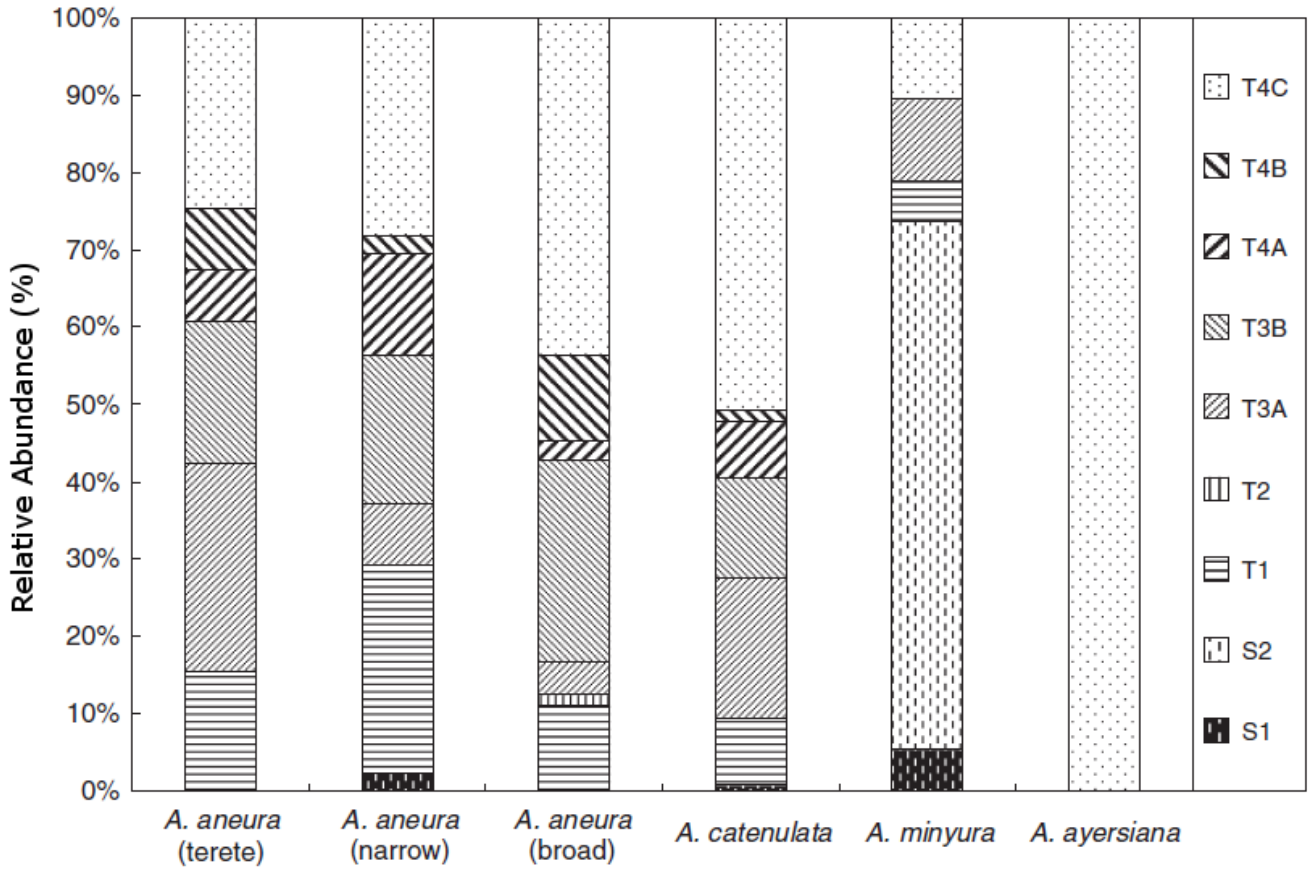

Figure 2.4 The relative abundance of growth forms present in four species of the Mulga complex at West Angelas, including three phyllode variants of *A. aneura*. Horizontal and vertical stripes represent multi-stemmed growth forms, diagonal stripes represent single-stemmed tree forms, and the white dotted fill represents the dominant multi-stemmed tree 'T4C'. While *A. ayersiana* was only present as T4C, only four trees were sampled.

Distribution of growth forms in relation to landscape position

Growth form varied with landscape position (PERMANOVA $P = 0.06$). Drainage lines, banded woodlands and lower hill slopes had the most distinct assemblages of growth forms (40 – 50% allocation success in CAP cross validation), while the three other landscape positions were indistinguishable from each other (0% success rate). Accordingly, drainage line and banded woodlands are clearly separated from the other landscape positions along the first principal co-ordinate axis, which is driven by the abundance of the tree growth forms T4C, T4B and T4A (Figure 2.5).

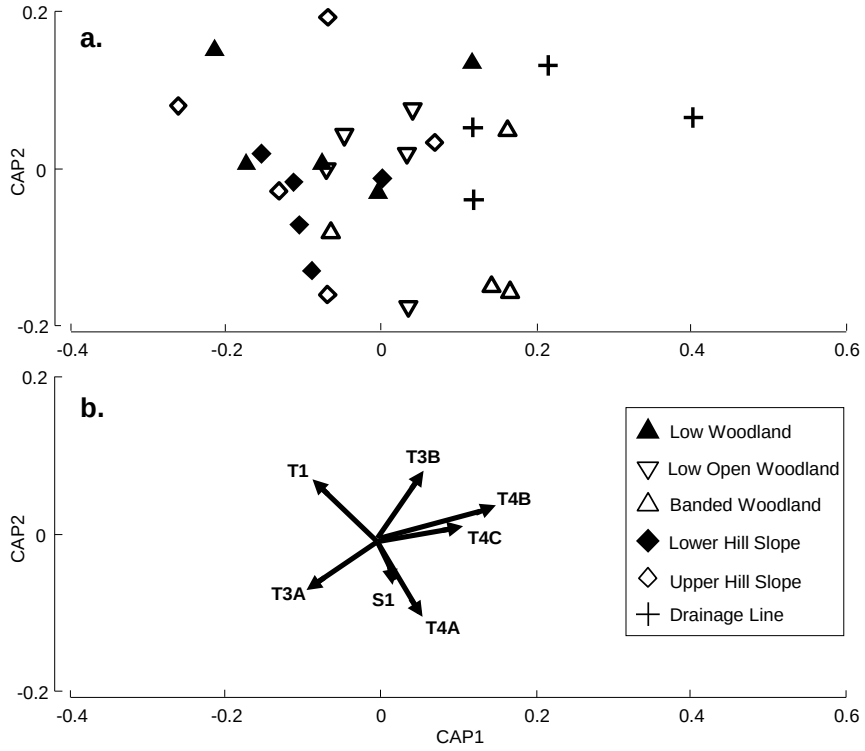

Figure 2.5 Canonical analysis of principal co-ordinates (CAP) of growth form density at each site labelled by landscape position. Hill slopes were separated from drainage lines and banded woodlands on the first axis **(a**), which were the most distinct groups by cross validation. Contribution vectors indicate that multi-stemmed and single-stemmed tall trees were more abundant in drainage lines and banded woodlands, and multi-stemmed shrubs and low trees were more abundant on hill slopes and the remaining valley woodlands (**b**). CAP was generated from a Bray-Curtis similarity matrix derived from square-root transformations of the density of growth forms at each site.

Tall trees with two or three main stems that divide close to the ground (T4C) are the most abundant growth form at West Angelas, and dominate all landscape positions except for the upper hill slopes, which are instead dominated by low single-stemmed

trees with narrow crowns (T3B). On the lower hill slopes low trees with both spreading crowns (T3A) and narrow crowns (T3B) together are equal in abundance to T4C. Taller trees are more dominant in the lower landscape positions, particularly in banded woodlands and the drainage lines. Open woodlands contained a high diversity of tree types: while tall multi-stemmed trees account for half of the growth forms present in open woodlands, the other half is evenly comprised of all other growth forms found at the West Angelas study site. Similarly, approximately 30% of the woodlands are dominated by a range of forms including trees and shrubs with more than three main stems branching at ground level (S1, S2, T1 and T2, Appendix B.3).

Each of the measured growth form attributes also varied with landscape position (Table 2.2). Basal diameters were smallest (generally <120 mm) on the upper hill slopes and largest (>170 mm) in the open and banded woodlands. Trees and shrubs in the woodlands and open woodlands had the most number of stems per induvidual (generally two or more), while trees and shrubs on drainage lines and upper hill slopes generally had only one stem. The height to crown break was uniform across the landscape with the exception of the tall trees in the drainage lines where crown break occurred at 2 m or higher. Nevertheless, there was a trend in average tree height from highest in the valleys (drainage lines, woodlands, open woodlands and banded woodlands) to lowest on hill slopes. Canopy areas were smallest in drainage lines, woodlands and upper hill slopes and largest in the banded woodlands.

Table 2.2 Mean values of branching attributes of Mulga trees by landscape position at West Angelas.

	Landscape Position						
	Drainage Line	Banded Woodland	Low Open Woodland	Low Woodland	Lower Southern Hillslope	Upper Southern Hillslope	***p*-value**
Basal Diameter (mm)	**148 a** (5.59)	**185 b** (7.60)	**175 b** (6.30)	**147 a** (5.83)	**138 a** (6.42)	**112 c** (4.85)	<0.001
Number of Stems	**1.41 a** (0.05)	**1.75 ac** (0.13)	**2.24 bd** (0.14)	**2.35 b** (0.12)	**1.76 cd** (0.09)	**1.33 a** (0.05)	<0.001
Diameter of Stem 50 cm from Ground	**113 a** (4.55)	**138 bc** (6.02)	**115 ac** (4.11)	**100 ad** (4.01)	**111 a** (4.78)	**91 d** (4.50)	<0.001
Height to First Stem Division (m)	**1.71 a** (0.12)	**1.28 ac** (0.13)	**0.86 b** (0.09)	**0.68 b** (0.08)	**0.78 bc** (0.07)	**1.14 ac** (0.08)	<0.001
Height to Crown Break (m)	**5.53 a** (0.15)	**3.60 b** (0.25)	**2.53 b** (0.13)	**2.49 b** (0.11)	**2.04 b** (0.10)	**2.24 b** (0.09)	<0.001
Canopy Area (m^2)	**12.4 a** (0.96)	**18.8 b** (1.34)	**15.8 bc** (0.89)	**12.5 a** (0.82)	**15.3 bc** (0.97)	**12.6 ac** (1.03)	<0.001
Tree Height (m)	**7.97 a** (0.19)	**7.41 a** (0.21)	**5.95 bc** (0.13)	**6.12 b** (0.10)	**5.71 bc** (0.12)	**5.62 c** (0.17)	<0.001

Mean values are bolded and standard errors are in parentheses. *P*-values indicate significance level for one way ANOVA's for each attribute. Lowercase letters denote significant groupings for each attribute according to Tukey's HSD post-hoc tests.

Distribution of phyllode shapes in relation to landscape position

Each landscape position also contained unique assemblages of phyllode shapes (PERMANOVA, $P = 0.04$), particularly when comparing hill slopes to the valley woodlands. Upper hill slopes had the most distinct assemblages (60% cross validation success in CAP), while lower hill slopes (40%), open woodlands (40%) and banded woodland (25%) were slightly less distinct. Woodlands and drainage lines were difficult to classify based on phyllode composition and had a 0% allocation success, meaning that they were indistinguishable from other landscape positions. The low allocation success of drainage lines occurred because of the similarity in phyllode composition to banded woodlands. In contrast, open woodland and the two hill slope woodlands were well separated on the first two principal co-ordinate axes (Figure 2.6). Banded woodlands and drainage lines were scattered with no clear separation, and even though woodlands were not well distinguished by cross validation (0% allocation success) they were well separated by the first two principal co-ordinate axes (Figure 2.6).

Broad phyllodes of *A. aneura* dominated all four of the valley woodland communities, and were most dominant in the drainage lines (Figure 2.7). Indeed, two of the drainage sites were monocultures of broad phyllode mulga (data not shown). In contrast, the two hill slope woodlands had very few broad phyllodes, but a much higher representation of terete phyllodes. The abundance of narrow phyllodes was similar among all landscape positions except drainage lines. *A. minyura* was rare, and *A. catenulata* was not present in large numbers except on upper hill slopes. Of all the landscape positions, the open woodlands had the most even distribution of all the phyllode shapes.

There was no evidence that *A. catenulata* or any of the three phyllode variants of *A. aneura* changed growth form according to landscape position (Appendix B.4). Close to 90% of terete *A. aneura* grew as single-stemmed trees in both upper hill slopes and drainage lines, but the valley woodlands and lower hill slopes had an even composition of single- and multi-stemmed forms. Similarly, 100% of broad *A. aneura* was multi-stemmed on the upper hill slopes, but elsewhere was evenly split between multi- and single-stemmed growth forms. Narrow *A. aneura* and *A. catenulata* were both evenly present as single-stemmed and multi-stemmed growth forms in all landscape positions (Appendix B.4).

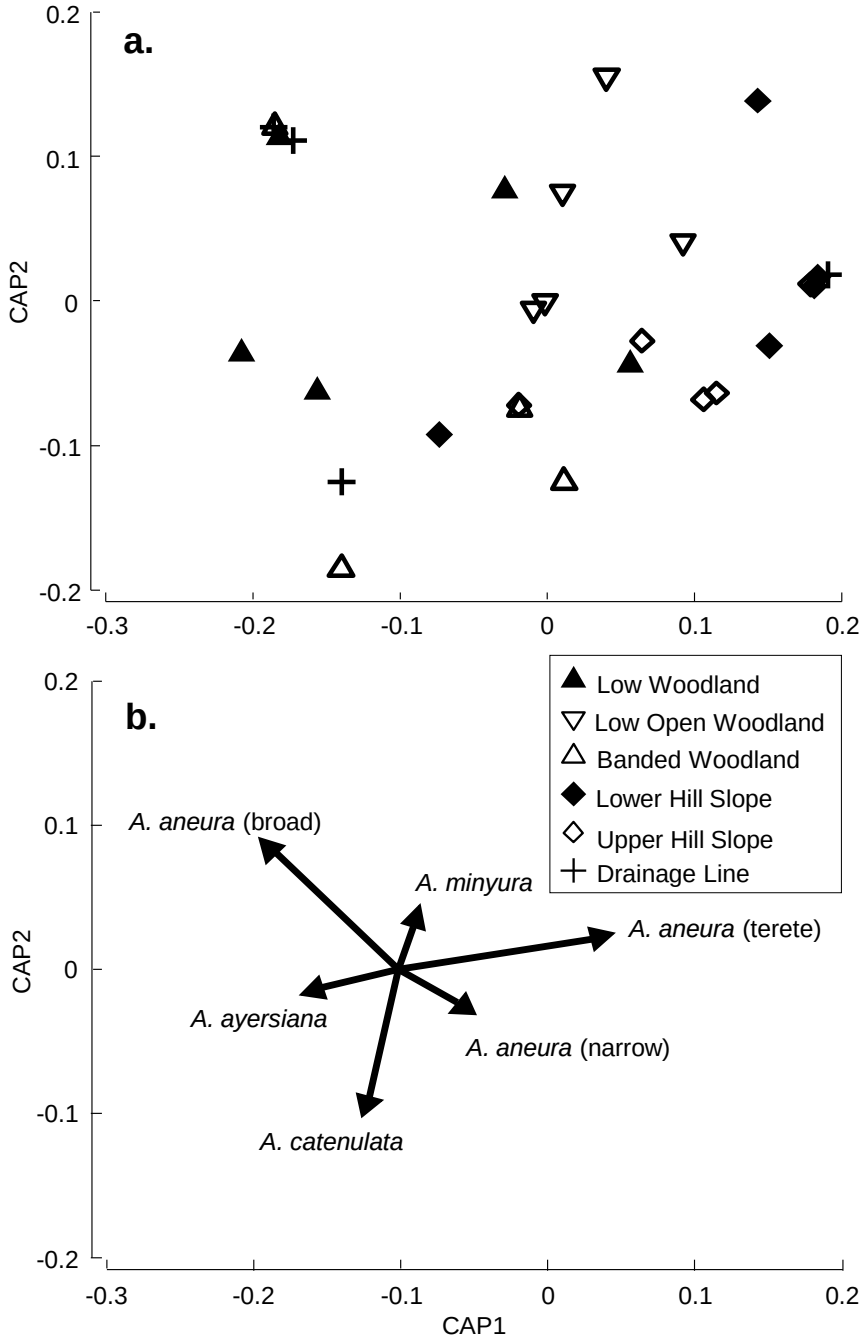

Figure 2.6 Canonical analysis of principal co-ordinates (CAP) of phyllode shape and species density at each site labelled by landscape position. Hill slopes and valleys were well separated by the first two axes (**a**). Upper hill slopes were the most distinct by cross validation (60% allocation success), followed by lower hill slopes, open woodlands (40%) and banded woodlands (25%). Woodlands and drainage lines were indistinguishable by cross validation (0%). Correlations of phyllode shapes with CAP axis indicated that terete and broad *A. aneura* contributed strongly to the first CAP axis, and *A. catenulata* and *A. minyura* to the second (**b**).

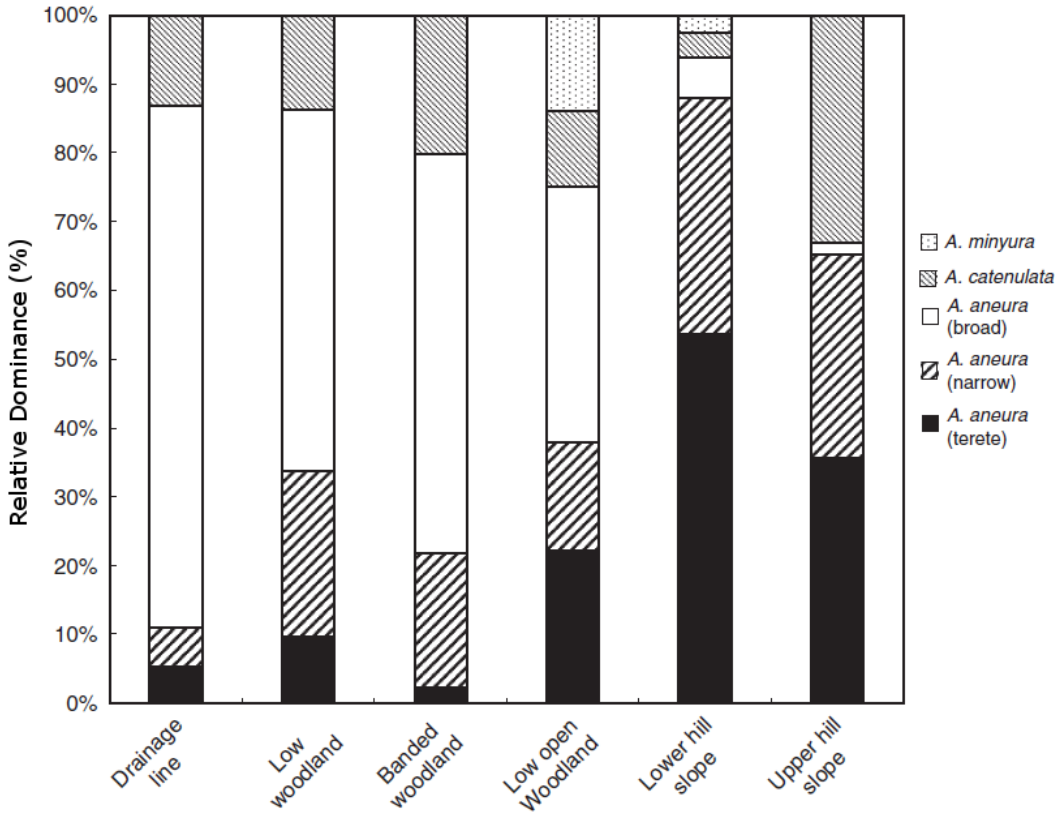

Figure 2.7 Relative dominance (%) of phyllode variants and species by landscape position. Terete and narrow phyllode variants of *A. aneura* were prominent on hill slopes, and broad phyllodes were most common in the open valleys. *Acacia catenulata* was present in all woodlands.

Discussion

Variation in phyllode shape in A. aneura

Phyllode shape of *A. aneura* was strongly influenced by landscape position (Figure 2.6, Figure 2.7) although the relationship between growth form and landscape position was less clear (Figure 2.4, Figure 2.5). Shifts in average leaf size across topographic gradients have previously been reported at the community level. For example, average leaf size in Californian chaparral declines with increasing incident solar radiation, which in turn is determined by topographic position (Ackerly *et al.* 2002). Larger leaved species were present across the landscape, while smaller leaved species were absent from the shadier sites (Ackerly *et al.* 2002). I also observed species with larger phyllodes (i.e., *A. catenulata*) across all landscape positions, but the smallest phyllodes (terete *A. aneura*) were most prominent on the shaded upper southern hill slopes.

Smaller leaf sizes and lower specific leaf area (SLA) are traits often associated with aridity, including high heat and light typical of exposed habitats. Increasing leaf thickness and/or density can be a photo-protective adaptation to high light (Niinemets & Tenhunen 1997, Niinemets, Kull & Tenhunen 1999). Decreasing leaf width increases leaf cooling through higher boundary layer conductance (Givnish 1987, Niinemets *et al.* 1999). The finding that the smallest phyllodes were in the most shaded sites (i.e. south-facing) is unusual given that other semi-arid studies have shown plants with the smallest leaf sizes (or photosynthetic lamina) are on the most exposed sites (Ackerly *et al.* 2002, Cornwell & Ackerly 2009). My results suggest that high light or temperature may not be the most significant factors controlling the distribution of Mulga at West Angelas.

A gradient in water availability controlled by landscape position may be driving the differences in phyllode size of *A. aneura*. Similar shifts in leaf size of perennial vegetation have previously been reported along gradients of water availability at a continental (Wright *et al.* 2004a), community (Prior, Eamus & Bowman 2003, Cornwell & Ackerly 2009), and species level (Farrell & Ashton 1978, Prior *et al.* 2003, Prior *et al.* 2005). While it is often hard to separate the influence of heat, light and water availability in hot dry environments, the prominence of the smallest phyllode sizes in the most shaded environments that occur at high elevations indicates that low water availability may be a significant factor. Smaller leaves (often with higher SLA) may contain a greater investment in leaf structural tissue than photosynthetic tissue (Niinemets *et al.* 2007a), making them more capable of withstanding severe water deficit. Phyllodes have, in themselves, been considered an adaptation to drought owing to their anatomical differences from leaves (Boughton 1986, Warwick & Thukten 2006). Phyllodes of *Acacia melanoxylon* are better able to recover from more negative water potentials, and have higher water use efficiency than leaves from the same species (Brodribb & Hill 1993). Seedlings grown from seeds collected at drier sites switched more quickly from leaves to phyllodes than those from wetter sites when grown under uniform conditions (Farrell & Ashton 1978). Given that most features of phyllode anatomy are considered to be an adaptation to drought and that I have observed the opposite trend in phyllode size than would be expected under reduced light and temperature conditions, I hypothesise that a gradient in water availability is driving a shift in phyllode size among landscape positions at West Angelas. This hypothesis will be investigated more fully in Chapters 4-6.

Co-occurrence of species with different phyllode shapes

Differences in the distribution and relative abundance of *A. aneura* and *A. catenulata* may also reflect different strategies of resource acquisition and use. For example, the dominance of larger phyllode sizes in the lowest parts of the landscape may reflect a competitive advantage over smaller phyllode sizes in conditions of higher resource availability. Competitive exclusion of smaller leaf sizes due to light limitation may also control community assembly of leaf sizes in the Californian chaparral (Ackerly *et al.* 2002). Global trends among plant traits indicate that smaller leaves have a long life-span at the cost of lower rates of mass based photosynthesis and lower rates of dark respiration, all of which result in slower growth rates (Wright *et al.* 2004b, Poorter *et al.* 2009). Trees also grow taller when there is competition for light (King 1990, Koch *et al.* 2004). Average tree height was greatest in landscape positions that had the lowest relative abundance of terete *A. aneura* (Table 2.2, Figure 2.7). If larger phyllode sizes in *A. aneura* translates into faster growth rates, broad *A. aneura* may competitively exclude terete *A. aneura* when water and light availability are high (i.e. drainage lines, mulga groves and valley woodlands). Conversely, when light is low and water run-off potential high (i.e. south facing hill slopes) there is greater diversification in water use strategies and less competition for light resulting in a greater range of phyllode sizes and lower average tree height.

Contrasting patterns in phyllode shape and growth form

In contrast to the trend observed in *A. aneura*, the closely related *A. catenulata* exhibited a constant phyllode size and shape across landscape positions and so is either not subject to the same selection pressures, or has adopted a different strategy in response to these pressures. Heterogeneous soil and light resources within sites can also influence the distribution of these closely related *Acacia* species below the landscape level. Hill slopes have a mixture of rock outcrops, rocky colluvium and small reservoirs of soil. Similarly, shaded slopes produce a variety of exposures to direct light, with trees growing directly beneath vertical rock faces receiving no direct sunlight at any time during the day, while trees further away intercept varying amounts of sunlight depending on season. Similarly, global (Wright *et al.* 2004b, Ordoñez *et al.* 2009) and local leaf trait models (Ackerly *et al.* 2002, Beaumont & Burns 2009) include very high variability and so we would not expect consistency at the community level particularly among species.

The systematic variation of phyllode size across the landscape sequence at West Angelas strongly supports the link between form and function (particularly rates of water use) in morphologically diverse mulga woodlands. It is surprising, however, that the relationship between growth form and landscape was less clear. Plants in arid regions with multiple stems have been associated with increased drought tolerance due to their hydraulically modular design, where segmentation of the xylem pathway ensures that drought damage is not propagated throughout the rest of the plant (Schenk *et al.* 2008, Espino & Schenk 2009). If multiple stems were an adaptation to drought in *A. aneura* I would have expected a relationship between growth form and phyllode shape, or a similar relationship with landscape as for terete *A. aneura*. However, hydraulic modularity may also be evident at the anatomic level and not simply expressed by the number of stems (Schenk *et al.* 2008). So while the number of stems does not infer drought tolerance, hydraulic modularity may still play a role the physiological function of Mulga. Similarly, the capacity for *A. catenulata* to inhabit multiple landscape positions without changing either abundance or phenotype may also indicate plasticity in traits other than phyllode size, i.e. hydraulic architecture including vessel size distributions (Tyree & Ewers 1991, Sperry 2000, Cochard *et al.* 2002, Mokany *et al.* 2003, Cavender-Bares, Kitajima & Bazzaz 2004), or leaf level physiological adaptations, including nitrogen partitioning (Evans 1989, Reich, Ellsworth & Walters 1998), contributions by stable osmotica (Hsiao *et al.* 1976, Merchant *et al.* 2006a, Merchant, Ladiges & Adams 2007), and root architecture (Lynch 1995, North & Nobel 1998).

In summary, this study demonstrates that landscape position strongly influences phyllode shape in *A. aneura*, but not *A. ayersiana* or *A. catenulata*. I determined that growth form was also but less strongly related to landscape position. While it appears that water availability may be responsible for driving differences in phyllode shape further research is required to examine whether differences in phyllode shape among varieties of *A. aneura* are reflected by or contribute to differences in rates and/or timing of water use and drought tolerance.

Chapter 3: Does diversity in soil properties explain the landscape distribution of Mulga 'types'?

Introduction

Landscape-scale variation in vegetation structure and composition often coincides with underlying differences in geology, soil fertility and water availability (e.g., Beard 1990, Scatena & Lugo 1995, Nicolau *et al.* 1996, Perroni-Ventura, Montana & Garcia-Oliva 2006, John *et al.* 2007). Topography in particular has a dominant influence on the distribution of resources across a landscape, including availability of light, as well water and nutrients (Beard 1990, Dyer 2009). However, most studies of soil-vegetation patterns have focussed primarily on shifts in the distribution of major species or community types but with little attention to intra-species patterning. Previously, I showed that mulga woodland composition and growth form variation across the West Angelas Valley was at least partly related to topographic position (Page *et al.*, 2011; Chapter 2) . Consequently, we might expect that part of this patterning would be explained by differences in underlying soil properties.

The relationship between topography and resource availability are exemplified by soil catenas (Milne 1935). A catena is a sequence of soil types arising from the same parent rock, often encompassing a slope, but which are distinct from each other because of variations in drainage, leaching and mass movement arising from differences in topography (Huggett 1975). In Western Australia, some of the best known catenary sequences are those described by Beard (1990) for more temperate southwest Australia, which demonstrate clear relationships between different vegetation units and underlying soil type and depth across quite small scale elevation changes (1-2 m in some cases). A catenary or landscape approach to describing vegetation patterns in relation to underlying soil properties in the more arid northwest of Australia has been less developed, although Beard's mapping of the region in the 1970's (Beard 1975) intuitively accounted for shifts in underlying geology and elevation. Similarly, the detailed mapping of southwest Australian forests undertaken by Mattiske & Havel (1998) included delineation of vegetation types based on underlying soil properties inferred from landscape position.

Landscape scale water availability is the strongest limiting factor in the distribution and productivity of arid and semi-arid zone vegetation (Noy-Meir 1973, Morton *et al.* 2011). However, soil fertility may also significantly influence the distribution of species at the site level (Perroni-Ventura *et al.* 2006). For example, differences in soil fertility and soil structure among sites that are comparable in other characteristics (such as topographic position, light exposure, water availability) may explain differences in species composition either within or between vegetation or community types. In some instances, subtle differences in nutrient availability have major consequences for community composition. For example, the distribution of around 30% of tree species in tropical rainforests in Columbia, Ecuador and Panama were explained by gradients of soil nutrients, even where the sites had very little topographic relief (John *et al.* 2007). However, in areas of high relief it is harder to disentangle the influence of topographic influences from soil resources (John *et al.* 2007).

In arid environments, vegetation patches can increase localised fertility of the soil through biotic and abiotic interactions between plants and soil substrates, including through plant-microbial community associations (Reynolds *et al.* 2003, Maestre *et al.* 2010). For example, concentrations of organic carbon, nitrogen, phosphorus and potassium were higher beneath the canopy of *Prosopis flexuosa* in central Monte desert in Argentina, resulting in spatial variability in community composition in the patchy environment (Rossi & Villagra 2003). Similarly, the hummock grasslands of northwest Australia (Ford *et al.* 2007) exhibit high spatial variability in soil physico-chemical properties, such as nitrogen and phosphorus content or rates of infiltration, owing to patterning beneath vegetation canopies versus adjacent bare soil. It is well-known that interactions between plant age and soil properties relating to water availability can also influence taxonomic species richness and diversity beneath shrub canopies (Pugnaire & Lázaro 2000). However, it is less clear whether shifts in morphological or functional types of closely related species are related to these site-scale variations in soil nutrients. The allocation of biomass to particular plant organs (i.e. leaves, roots and branches) can also change according to resource availability (McConnaughay & Coleman 1999), which may in turn translate into functional differences. For example, higher growth rates and taller trees along a soil nutrient gradient in temperate forest species in North America also correlated to intra-specific differences in leaf nitrogen concentration (Walters & Gerlach 2013). In Chapter 2, I showed that there were large shifts in

dominance of particular species and phyllode variants of Mulga among landscape positions at West Angelas, particularly between the hill slopes and valley floors. The soils and hill-slopes of the Pilbara region of Western Australia are extremely old and tectonically stable (Arndt *et al.* 1991, Kranendonk *et al.* 2002). In the Hamersley Ranges we might expect that patchiness in vegetation distribution will strongly influence the distribution of soil nutrients; however, landscape-scale trends in soil fertility may be greater than within-site variability.

Understanding relationships between the composition of vegetation communities (taxonomically, morphologically and functionally) and underlying soil physico-chemical properties across a landscape gradient is also useful for restoration following disturbance. For example, clearing and excavation associated with open-cut mining projects can change the topography and drainage patterns of a landscape (Cooke & Johnson 2002). Similarly, waste rock and overburden that is translocated and stockpiled can have physical and chemical properties that are very different to the surface soils originally supporting vegetation communities in the area (Lottermoser 2011). Mining companies in Western Australia are required to rehabilitate disturbed land and return it to a self-sustaining native plant community that is as close to the original as possible (EPA 2006). Quantifying the range of soil physico-chemical properties of surface soils before the commencement of mining can assist in designing rehabilitation plans for waste material and modified landscapes following mining. If soil properties of post-mining landscapes can be modified during their creation to more closely resemble natural conditions (e.g. by crushing rocks to a smaller size or by amending with fertilizers or altering the pH), landscape restoration may be more successful. Alternatively, if naturally occurring 'analogues' of post-mining soil can be identified (e.g. particular combinations of soil and physical status), vegetation communities (based on their mix of growth forms and morphological attributes as well as species composition) can be more precisely 'matched' to post-mining landscapes.

The main objective of this Chapter was to assess the distribution of different species and phyllode variants (types) of Mulga at West Angelas (Chapter 2) in relation to a selection of physiographic attributes and soil chemical and physical properties. I hypothesized that local soil characteristics may play an important role in explaining variations in mulga woodland composition and growth across the West Angelas Valley. Therefore, I sought to: (i) quantify the distribution of major nutrients, soil particle size and bulk

density across a landscape gradient at West Angelas, and (ii) evaluate how much of the variance in the density of Mulga types across the landscape gradient identified in Chapter 2 is explained by these substrate properties. My focus for this Chapter is primarily on soil nutrients; later Chapters will discuss adaptations among Mulga types to differing water availability.

Methods

Field sampling design

Soil samples were collected from each of 28 transects that were established for the survey of Mulga phyllode and growth forms variants as described in Chapter 2. These transects encompassed six discrete landscape positions: (i) upper southern hill slope, (ii) lower southern hill slope, (iii) low mulga woodland, (iv) banded mulga woodland, (v) low open mulga woodland, and (vi) drainage line mulga woodland. Five replicate transects were established in each landscape position except for drainage line and banded woodlands where there were four transects. Belt transects were 4 m wide and a minimum of 100 m long, containing a minimum of 20 individuals of *A. aneura* or closely related members of the Mulga complex.

I collected ten soil samples (0-5 cm depth) along each transect. Of the ten samples, five were collected from within 'patches' of Mulga (within 0.5 m of the base of a tree *A. aneura*) and five were collected from the barely vegetated 'inter-patch' (areas outside the canopy of Mulga and with little/no ground cover of litter or grass). Difficulties associated with access to rugged terrain and the rockiness of many sites restricted sampling to greater depth; however, I acknowledge that other soil attributes such as depth to hardpan would be highly informative. Nevertheless, previous studies in the region have repeatedly shown that the 0-5 cm soil layer contains the most of the plant-available soil nutrients (Bennett & Adams 1999, Bentley *et al.* 1999). Samples were sieved to <2 mm in the field then kept cool for transport back to The University of Western Australia (Perth, WA). I also attempted to collect bulk density samples from one 'patch' and one 'interpatch' on three replicate transects within each landscape position (16 sites in total); however, samples were unobtainable from some sites owing to the rockiness of the ground surface, which made it almost impossible to collect an accurate volume of soil. Consequently, no bulk density samples were collected from the

upper southern hill slopes, and only one transect was sampled from the lower southern hill slopes.

Soil chemical analyses

Soil pH was measured in 1:1 mix with milliQ water (Thomas 1996). Hydroxide-extractable phosphorus (OH-P) was measured by shaking 10 g of soil for 16 h in 50 mL 0.1 M NaOH (Bowman & Cole 1978). Extractions were immediately filtered and an aliquot was digested (H_2SO_4/H_2O_2) and analysed for total phosphorus (OH-Pt). Phosphorus concentrations were determined colorimetrically using an Auto Analyzer 3 (SEAL Analytical, Germany). Labile inorganic N as NO_3^--N and NH_4^+-N were extracted by shaking 1 g of soil in 1 M KCl for one hour, filtered (Whatman #40). Extracts were then analysed colorimetrically using an Auto Analyzer 3 (SEAL Analytical, Germany). Extractable Fe concentration was determined from DTPA extracts analysed by atomic absorption spectrophotometry following Loeppert and Inskeep (1996). Soil samples were also analysed for total N and C content (%) with an Automated Nitrogen Carbon Analyser-Mass Spectrometer consisting of a Roboprep connected with a Tracermass isotope ratio spectromer (Europa Scientific Ltd., Crew, UK). Soils were determined to contain negligible concentrations of carbonates and so no pre-treatment was required for C analysis. Samples were weighed to 0.1 mg accuracy and analytical precision was determined by repeated analysis of a laboratory standard that had been calibrated against international standards IAEA-N1, IAEA-N2, NBS-22 and IAEA-CH6. Precision for C% and N% was better than 1 standard deviation of 0.20.

Soil physical properties

Particle size analysis (PSA) was measured on one patch and one interpatch sample from a subset of sites using the pipette method after being pre-treated for the removal of carbonates with 1 *M* NaOAC at pH 5 (Gee & Bauder 1986). Bulk density was measured for cores taken from one patch and one interpatch at a subset of sites using the method described by Blake and Hartge (1986). Field observations of the soil surface, including rockiness and estimates of gravel size, were also made to complement the quantitative soil data.

Statistical analysis

Differences in soil chemical and physical attributes among landscape positions and patches (i.e. patch or interpatch within each transect) were determined using two-way

analysis of variance (ANOVA) with R 2.14.1 (R Development Core Team 2010). ANOVA models were fitted to average values of patch and interpatch locations on each transect for each chemical attribute (i.e., n = 28). Standard assumptions of data normality and equality of variance among groups were tested with a Shapiro-Wilk normality test and Levene's test for homogeneity of variance. Soil attributes were log-transformed when these assumptions were violated and outliers removed when anomalous data were unexplained by either sampling or methodological variations. Pair-wise comparisons were made using Tukey's Honestly Significant Difference post-hoc tests.

I tested a multivariate hypothesis of no differences among landscape positions and patch/interpatch locations for soil chemical attributes using permutation multivariate analysis of variance (PERMANOVA, Anderson 2001) and canonical analysis of principal coordinates (CAP, Anderson and Willis 2003) with the PERMANOVA+ add-on for Primer version 6 (Anderson, Gorley & Clarke 2008). The *F*-ratio constructed in PERMANOVA is analogous to Fisher's *F*-ratio and is constructed from the sums of squared distances within and between groups (Anderson 2001). A two-factor PERMANOVA model was fitted with fixed effects for "landscape position" and "patch/interpatch", with 9999 permutations of the raw data from residuals under a reduced model. CAP determines the "distinctness" of multivariate groups by producing a misclassification error using the 'leave one out allocation of the groups' approach, where a higher percentage of correct classifications indicates a more distinct group on the canonical axes (Anderson & Willis 2003). Soil data were averaged for each transect (i.e. pooled patch and interpatch data) and a one-factor CAP analysis with a fixed effect for "landscape position" was used, as the effect size of landscape position was larger than for patch/interpatch in the PERMANOVA model. All soil data were square-root transformed and normalized, and Bray-Curtis similarity matrices were used in both analyses.

The proportion of the variance in density of Mulga variants among all 28 sites (irrespective of landscape position) explained by soil chemical and physical attributes was determined using nonparametric multivariate multiple regression (DISTLM) (McArdle & Anderson 2001). A Bray-Curtis similarity matrix was calculated from square-root transformed phyllode density data for calculations with DISTLM using the transect data from Chapter 2. Each soil attribute was analysed separately for their

relationship with multivariate species density data and then subjected to a 'step-wise' model selection routine using an adjusted R^2 selection criterion from 9999 permutations. The 'step-wise' model selection routine is similar to forward selection but also attempts to improve the selection criterion by removing a term at each step (Anderson *et al.* 2008). The explanatory power of soil chemical attributes over and above the influence of 'landscape position' was also determined by running a DISTLM analysis that partitioned the variance into two sets of variables: landscape position (upper hill slope etc.), and soil chemical attributes. A separate DISTLM analysis was conducted for soil particle size as these data were only available for a subset of 16 sites. A distance-based redundancy analysis (dbRDA) was used to visualize the results of DISTLM by performing a constrained ordination using the soil attributes included in the optimal model identified with DISTLM.

Results

Soil physico-chemical properties across the landscape gradient

The most consistent differences in soil nutrients were between the south facing hill slopes and the valley woodlands (banded, low and low open woodlands), although there were some subtle differences in soil nutrients present among most landscape positions. South facing hill slopes had approximately twice the total hydroxide extractable P (OH-Pt; 105.6 ± 7.59 mg/kg), DTPA-Fe (33.9 ± 3.41 mg/kg), N (0.18 ± 0.01%) and C (2.64 ± 0.16%) than the valley woodlands ($P < 0.001$, Table 3.1). Drainage lines had similar concentrations of total N (0.14 ± 0.02%), total C (1.90 ± 0.28%) and OH-Pt (85.0 ± 6.45 mg/g) to lower south facing hill slopes ($P > 0.05$, Table 3.1). NH_4^+-N concentrations were consistently low among all landscape positions (3.57 ± 0.24 mk/kg); while NO_3^--N concentrations were also very low (<10 mg/kg), lower southern hill slopes and drainage lines (5.92 ± 0.53 mg/kg) had twice the NO_3^--N of the low open woodlands (2.65 ± 0.60 mg/kg; $P < 0.001$, Table 3.1). Soils were acidic in all landscape positions (average pH 4.80). Soil beneath the canopy of Mulga ('patches') had consistently greater concentrations of NH_4^+-N, NO_3^--N, DTPA-Fe, N (%) and C (%) in all landscape positions ($P < 0.01$, Table 3.1). OH-Pt and pH were similar in patches and interpatches.

Table 3.1 Soil chemistry of each landscape position.

Landscape Position - Patch/Interpatch		NH4-N (mg/kg)	NO3-N (mg/kg)	Soil OH-Pt (mg/kg)	DTPA-Fe (mg/kg)	pH (1:1)	Total N (%)	Total C (%)	n
Drainage line	IP	3.96 (1.37)	5.80 (1.44)a	82.3 (12.3)ab	13.1 (1.50)b	5.29 a	0.11 (0.03)b	1.52 (0.37)bc	4
	P	4.70 (0.74)	6.92 (0.86)	87.8 (6.13)	20.7 (4.43)	5.12	0.17 (0.02)	2.27 (0.37)	4
Low woodland	IP	3.80 (1.72)	2.97 (1.14)ab	57.1 (11.8)b	11.8 (1.53)b	4.52 ab	0.07 (0.02)c	1.09 (0.26)cd	5
	P	3.80 (0.56)	4.68 (1.10)	60.4 (10.4)	17.6 (1.54)	4.96	0.10 (0.02)	1.55 (0.15)	5
Low open woodland	IP	3.47 (1.29)	2.66 (1.11)b	60.8 (4.51)b	12.7 (3.02)b	4.81 ab	0.04 (0.01)c	0.82 (0.15)d	4
	P	3.01 (0.32)	2.64 (0.65)	63.9 (6.06)	23.2 (8.47)	5.13	0.10 (0.00)	1.59 (0.17)	5
Banded woodland	IP	2.15 (0.32)	4.55 (1.58)ab	91.5 (13.9)ab	10.0 (1.04)b	4.70 b	0.06 (0.01)c	0.74 (0.14)d	4
	P	3.66 (0.45)	5.13 (1.77)	93.9 (9.97)	14.5 (1.32)	4.68	0.11 (0.01)	1.31 (0.13)	4
Lower hill slope	IP	2.45 (0.15)	3.94 (0.66)a	108.1 (17.3)a	23.9 (3.78)a	4.71 ab	0.11 (0.00)ab	2.05 (0.35)ab	5
	P	4.39 (0.49)	7.23 (0.75)	103.2 (10.2)	41.5 (5.50)	4.81	0.20 (0.01)	3.11 (0.15)	5
Upper hill slope	IP	3.25 (0.52)	4.44 (0.58)ab	106.4 (22.0)a	35.2 (9.15)a	4.68 ab	0.15 (0.02)a	2.23 (0.18)a	5
	P	4.26 (0.56)	6.42 (0.42)	104.7 (14.2)	34.9 (7.27)	4.90	0.24 (0.02)	3.17 (0.22)	5
F-values	Landscape	ns	4.17**	5.47***	8.98***	2.50*	20.1***	19.2***	
	Patch/Interpatch	13.0***	8.68**	ns	11.8**	ns	53.9***	34.6***	
	Interaction	ns	ns	ns	ns	ns	ns	ns	

Mean values with one standard error in parentheses of untransformed data. pH means were calculated from $[H^+]$ and then converted to pH, and standard errors are not given because the $-\log_{10}([H^+])$ transformation gives asymmetric values. Letters denote significant groups determined using Tukey's Honest Significant Difference test when ANOVA tests were significant ($P < 0.05$).

Soil physical attributes were similar among landscape positions. Soil profiles on the hill slopes are best described as ‘skeletal’ (Beard 1975) and as rudosols in the valleys (Isbell 1996). Soils were mostly a mixture of sandy loams and light sandy clay loams (Uc1.43; Northcote 1971). Soils in banded woodlands had less sand, more silt and more clay than all other landscape positions ($P < 0.01$, Table 3.2), and were sandy clay loams (Um1.43; Northcote 1971). Particle size distribution was similar in patches and interpatches in all landscape positions ($P > 0.05$, Table 3.2). Bulk density reflected the high clay contents at all sites and was also similar across landscape positions (1.21 ± 0.05; $P > 0.05$, Table 3.2).

Table 3.2 Soil physical attributes of each landscape position

Landscape Position - Patch/Interpatch		Sand (%)	Silt (%)	Clay (%)	*n* (PSA)	Bulk Density (g/cm3)	*n* (BD)
Drainage line	IP	66.5 (5.87)a	10.2 (2.36)a	23.3 (3.69)a	4	1.15 (0.20)	4
	P	80.1 (6.74)	5.63 (3.16)	14.3 (3.58)	2	1.11 (0.25)	4
Low woodland	IP	76.5 (7.41)a	7.12 (7.12)a	16.4 (0.29)a	2	1.44 (0.17)	4
	P	75.3 (10.6)	7.94 (7.94)	16.7 (2.64)	2	1.26 (0.17)	5
Low open woodland	IP	80.4 (3.96)a	1.92 (0.55)a	17.7 (3.41)a	2	1.02 (0.12)	2
	P	86.6 (0.27)	3.56 (0.55)	9.87 (0.28)	2	1.43 (0.47)	4
Banded woodland	IP	50.5 (3.27)b	20.1 (2.31)b	29.4 (1.06)b	3	1.38 (0.47)	4
	P	51.1 (2.8)	16.5 (1.82)	32.4 (1.47)	3	0.99 (0.24)	5
Lower hill slope	IP	61.4 (28.2)a	25.4 (23.5)a	13.2 (4.93)a	3	1.06	1
	P	75.1 (1.47)	8.50 (2.75)	16.4 (1.49)	4	0.86	1
Upper hill slope	IP	69.8 (4.35)a	9.44 (1.63)a	20.8 (3.80)a	3	^	
	P	72.3 (3.65)	7.70 (2.19)	20.1 (1.65)	5	^	
F values	Landscape	13.4***	5.62**	11.7***		ns	
	Patch/Interpatch	ns	ns	ns		ns	
	Interaction	ns	ns	ns		ns	

Mean values with one standard error in parentheses. [#]no standard error for bulk density of lower hill slope samples as *n* limited to 1. ^no data as ground was too rocky to obtain a sample from upper hill slopes.

Multivariate analysis of soil chemical attributes determined that the clearest distinction was between the hill slopes (lower and upper) and the valley woodlands (banded, low open and low woodland) (PERMANOVA pair-wise tests $P < 0.001$, Figure 3.1). Lower and upper southern hill slopes had similar soil chemical profiles. Likewise, the three valley woodlands were similar (PERMANOVA $P > 0.05$). While 'patch' and 'interpatch' were also significant multivariate groups (PERMANOVA $P = 0.002$), variance component estimates from the two-factor PERMANOVA model indicated that differences in landscape position (σ^2 2.54) accounted for more than twice the model variance than if soil was collected from a 'patch' or an 'interpatch' (σ^2 0.99). Upper southern hill slopes, lower southern hill slopes and drainage lines had the most distinct soil chemical profiles (50, 60, 50% CAP allocation success, Figure 3.1). Of those, the hill slopes were the most distinct, with 100 % allocation success if the upper and lower hill slope groups were pooled. Similarly, while the three valley woodlands had lower allocation success (low woodland 20%, low open woodland 40% and banded woodlands 0%), overall classification success was 87% if pooled together (i.e., 12 of 14 sites classified as "valley woodland").

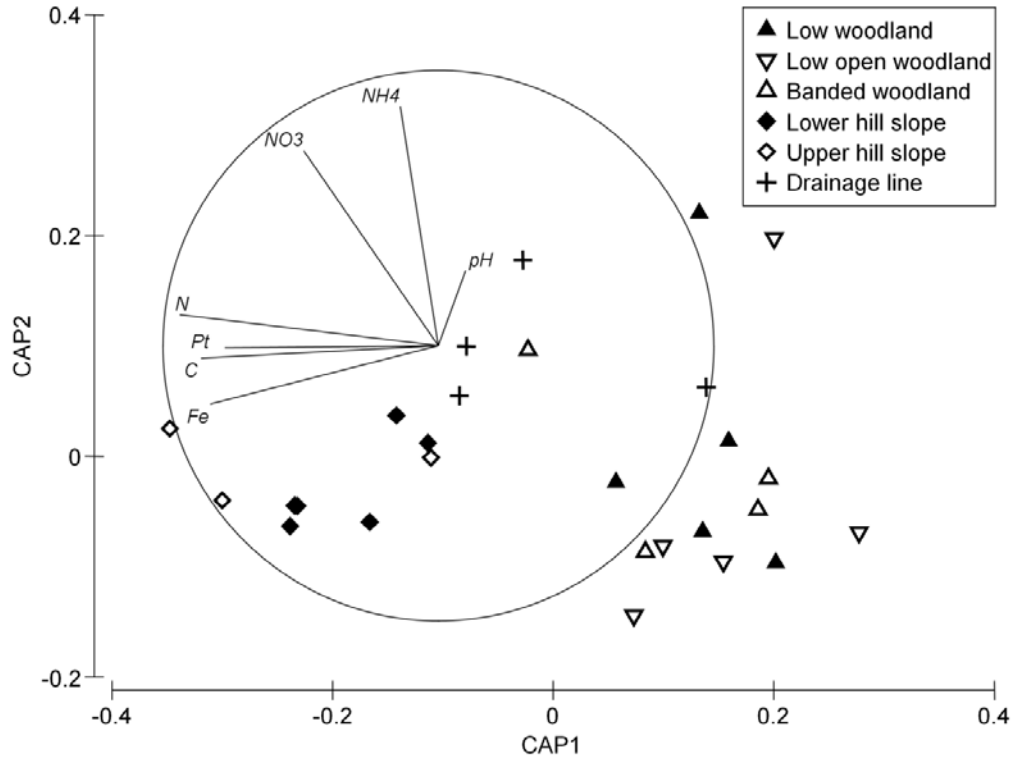

Figure 3.1 Canonical analysis of principal coordinates (CAP) of mean soil chemical attributes at each site at West Angelas, labelled by landscape position. Hill slopes were distinguished from valley woodlands, whereas drainage lines were less clearly distinguished from either group. Vectors indicate the strength of the relationship between soil chemical attributes and each principle coordinate axis.

Relationship between soil physico-chemical attributes and Mulga 'type' distributions

Soil chemical attributes explained 38.2% of the variance in the density of Mulga 'types' at 28 sites in the greater West Angelas area (Table 3.3). The best model to explain the variance in the density of Mulga 'types' used five of the seven attributes measured in this study (Table 3.3). Of those, DTPA-Fe concentration explained the highest fraction of the variance (13.4%), and in the conditional model pH, NO_3-N, NH_4-N and total carbon (%) all explained 5 – 7% of the variance. DTPA-Fe and C (%) contributed most strongly to the first RDA axis that explained 24.6% of the variance in Mulga 'type' density, separating the hill slopes from the valley woodlands (Figure 3.2). pH and NH_4-N contributed more strongly to the second RDA axis which less clearly distinguished landscape positions, and explained only 10.4% of the variance in Mulga 'type' density (Figure 3.2). Inclusion of soil particle size data or a categorical explanatory variable for "landscape position" did not explain any more of the variance in the distribution of Mulga 'types' (DISTLM $P > 0.05$, data not shown).

Table 3.3 Individual and cumulative proportion of the variance in density of Mulga 'types' across 28 sites explained by soil chemical attributes, determined by nonparametric multivariate multiple regression (DISTLM).

Variable	Adj R^2	SS (trace)	Pseudo-F	P	Proportion R^2	Cumulative R^2
+Fe (mg/kg)	0.10	8195	4.03	0.009	0.13	0.13
+pH	0.15	4767	2.48	0.06	0.08	0.21
+NO_3-N (mg/kg soil)	0.17	3286	1.76	0.16	0.05	0.27
+C (%)	0.21	3560	1.99	0.12	0.06	0.32
+NH_4-N (mg/kg soil)	0.24	3482	2.03	0.12	0.06	0.38

The five chemical attributes listed here were included in the best model to describe the variance in Mulga 'type' density across 28 sites based on an adjusted R^2 criterion. N (%) and OH-Pt were dropped from the model.

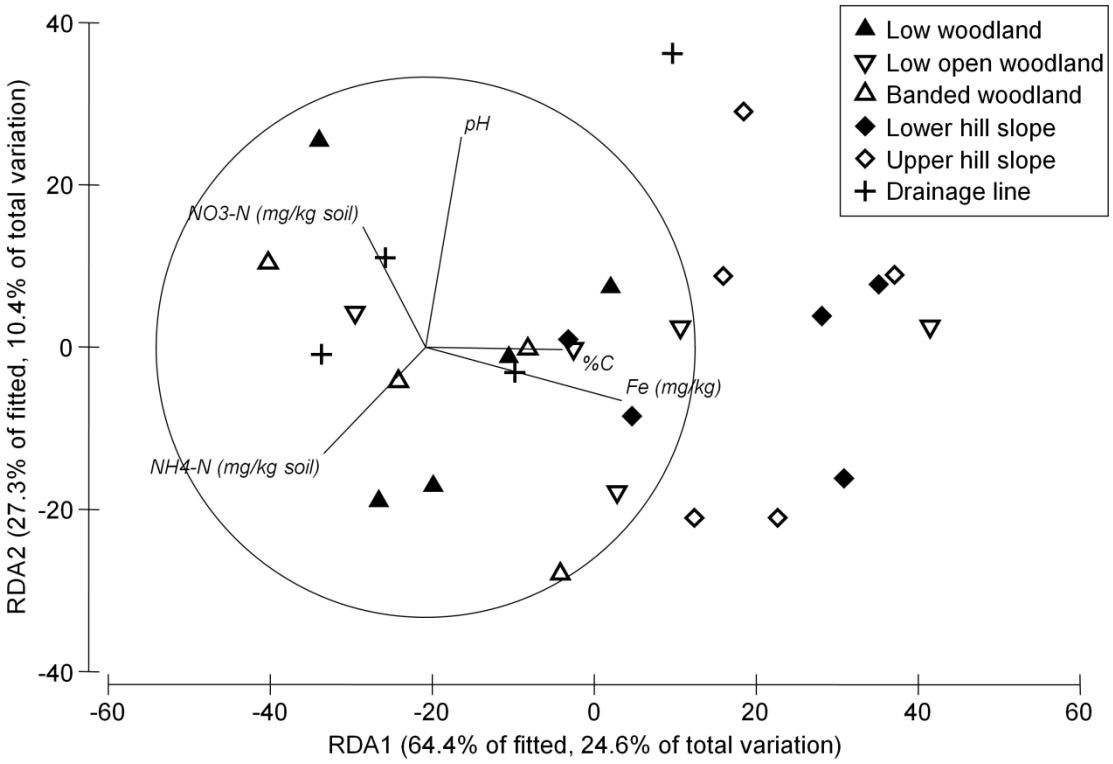

Figure 3.2 Distance-based redundancy analysis (dbRDA) ordination displaying the first two axes relating soil chemical attributes to the density of Mulga species and phyllode variants at 28 sites across a landscape gradient at West Angelas. A Bray-Curtis dissimilarity matrix was generated from Mulga 'type' density data at each site. Vectors indicate the strength of the relationship between soil chemical attributes and each dbRDA axis.

Discussion

The soil chemical and physical attributes measured here are surprisingly similar across the landscape gradient at West Angelas, which is partly the reason why these soil attributes did not explain much of the valley-scale variations in Mulga woodland composition and growth. Nevertheless, NH_4-N and NO_3-N concentration explained a small amount of the variance in the landscape distribution of Mulga 'types', mostly labile inorganic nitrogen was consistently low across the landscape gradient (Table 3.1). However, gravimetric soil moisture was less than 10% in all samples at the time of sampling. Previous biogeochemical studies from the Pilbara have demonstrated that inorganic nitrogen concentrations are low when soils are dry, but increase as short-term pulses following rainfall events (Ford *et al.* 2007). Therefore, the explanatory power of NH_4-N and NO_3-N in this study may be limited by an underestimation of plant available nitrogen following rainfall. Alternately, total nitrogen concentration did not explain a significant proportion of the variance in this analysis. If total nitrogen concentration is used as an estimate of substrate availability and thus mineralization potential (Ford *et al.* 2007), nitrogen availability is unlikely to further explain variance in the distribution of Mulga 'types' at West Angelas.

Additional information on soil profiles across landscape position would help clarify the findings of this study. While particle size and bulk density are important soil properties relating to water holding capacity and soil water potential, they do not account for other factors that can influence water availability, including soil depth and storage capacity, and surface properties (such as crust integrity) that control infiltration capacity. Even though soils collected from the hill slopes had textures similar to the valley woodlands, the volume of soil is vastly different between skeletal soil profiles on hills and deeper soils in the valleys. Likewise, soil surface features that influence the capacity of water to infiltrate or run off were very variable across the range of Mulga woodlands at West Angelas. For example, some sites had clay surface crusts with or without a stony mantle and others had stony mantles with or without subsurface vesicles. Therefore, even though the soil chemical and physical properties were very similar across the landscape gradient at West Angelas, other physical properties of the soil relating to the ability of water to infiltrate, and the volume of soil to store water may have a large influence on the structure and composition of Mulga woodlands at West Angelas. I did attempt to record detailed measurements of infiltration rates across sites but owing to logistic constraints, these measurements were inconclusive and insufficient to report here.

However, qualitatively, infiltration appeared equally fast at upslope sites compared to downslope, largely owing to irregular distribution of large boulders and rocks just beneath the surface at upslope sites that create preferential pathways for water flow. Elsewhere in the Pilbara, infiltration rates have been measured ~ 200 – 300 mm/h in a range of patch and inter-patch soils in banded mulga woodlands (Heyting 2011). However, these rates are hard to compare with other published data as correction methods and infiltration methods differ among studies. For example, the correction for lateral water flow from infiltration rings can reduce estimates of infiltration by ~ 75% (Dunkerley 2002). Generally, infiltration rates are highly variable within both groves and intergroves (or patches and inter-patches), and rates tend to be higher under the canopies of individual trees, consistent with observations of mulga woodlands and shrublands elsewhere (Slatyer 1961b, Pressland 1973, Pressland 1976, Dunkerley 2002).

One of the original motivations for this study was to determine the specific soil chemical and structural requirements of particular Mulga 'types' so that they could be used to "site match" particular varieties to available substrates for restoration purposes following mining. While the consistency of soil chemical and physical attributes among the variety of Mulga woodlands at West Angelas did not explain the diversity of Mulga types observed within an among communities, these data do provide a "target" range of soil properties that can be used in post-mining landscape rehabilitation planning of mulga woodlands in the region. In the following Chapters, I examine features of tree ecophysiological function that are indirectly related to measures of water availability, including pre-dawn branch water potential. Water availability is highly dynamic in semi-arid environments, and the supply of water may provide an alternative explanation for the diversification of mulga communities that is independent of soil nutrient status.

Chapter 4: Physiological traits that facilitate a rapid response of Mulga to a simulated rainfall pulse

Introduction

Survival of plants in arid environments requires both an ability to persist through prolonged drought and a capacity to respond to strongly episodic patterns of water availability (Noy-Meir 1973, Morton *et al.* 2011). A rapid increase in soil moisture associated with major rainfall events can stimulate an almost instantaneous response in both photosynthesis and plant respiration (Huxman *et al.* 2004b, Schwinning & Osvaldo 2004). The majority of studies of the physiology of plant species in arid environments have tended to focus on the traits that facilitate plant survival during drought periods, i.e. desiccation tolerance or drought avoidance. However, the linkages between physiological traits that facilitate a rapid response to rainfall pulse events and traits that facilitate persistence through prolonged drought are not well understood.

Most studies of desiccation tolerance and pulse response have focused on grasses (Huxman *et al.* 2004a, Xu, Zhou & Shimizu 2009), the classic examples of 'resurrection plants' (Scott 2000, Liu *et al.* 2007) or drought deciduous shrubs (Xu *et al.* 2010, Yazaki *et al.* 2010). In contrast, there have been few observations of long-lived and evergreen woody perennials (Resco *et al.* 2008, Resco *et al.* 2009, Grigg, Lambers & Veneklaas 2010, Pockman & Small 2010). Individual plant species also vary considerably in their responses to rainfall pulses. Resurrection plants, including many ferns in the genus *Cheilanthes* and grasses in Australia (Gaff & Latz 1978), are at the extreme end of pulse response strategies; resurrection plants can survive drought periods with apoplastic water content below 10% and then resume physiological function within hours of a rainfall event (Scott 2000, Vicré, Farrant & Driouich 2004). Differences in the rate and timing of water uptake can also partly explain the co-occurrence of particular species. For example, woody perennials from a cold desert shrubland on the Colarado Plateau without access to deep soil moisture were the slowest to respond of all life forms to a simulated rainfall pulse of 25 mm (Gebauer & Ehleringer 2000). Some species like the evergreen gymnosperm *Ephedra viridis*, were still increasing in the usage of pulse water five days later. In contrast, some species

either didn't directly use rainfall at all (the evergreen perennial forb *Cryptantha flava*), or supplemented uptake from rainfall with uptake from deep soil moisture (Gebauer & Ehleringer 2000). In environments where rainfall is highly episodic, knowing something of the timing and rate of water use by individual plants is critical for contrasting strategies of desiccation tolerance and pulse-response among co-occurring species.

Numerous approaches have been used to follow the responses of individual plants through to communities and ecosystems to rainfall pulses. At the scale of individual plants, instantaneous measures of photosynthesis and respiration have been used to assess the immediate status of plant growth and physiological activity (Resco *et al.* 2009). Other studies have used labelled water isotopes to follow the pathways of water in ecosystems and to trace water uptake by individual plants (Gebauer & Ehleringer 2000, Fravolini *et al.* 2005). The eddy covariance method is increasingly utilised to provide an integrated measure of whole ecosystem pulse-response by quantifying net CO_2 exchange and evapotranspiration (Wohlfahrt, Fenstermaker & Arnone 2008, Williams *et al.* 2009, Barron-Gafford *et al.* 2012). However, this whole of system approach does not elucidate the physiological mechanisms by which different species may vary in their rate or magnitude of response via water uptake or the resumption of carbon fixation. Where individual plants or populations are a focus, analysis of foliar $\delta^{13}C$ coupled with measurements of foliage hydration, stomatal conductance (g_s) and branch water potential (Ψ), both prior to and following a rainfall event, are some of the most useful measures for simultaneous determination of both short-term pulse response dynamics as well as long-term water use. Foliar $\delta^{13}C$ (the ratio of $^{13}C/^{12}C$ isotopes against a standard), when coupled with measurements of transpiration and carbon fixation, is considered a proxy for long-term water use efficiency (WUE) in C3 plants owing to the controlling influence of g_s on the ratio of carbon dioxide concentration inside and outside the leaf (c_i/c_a), which in turn influences the carbon isotope discrimination ($\Delta^{13}C$) (Farquhar, Ehleringer & Hubick 1989, Cernusak *et al.* 2008). Reduced g_s associated with water stress increases the proportion of the heavy isotope (^{13}C) fixed relative to the light isotope (^{12}C) owing to slower exchange of CO_2 with the atmosphere. However, measures of whole-leaf $\delta^{13}C$ may not reveal short-term responses to a rainfall pulse as new photoassimilates will only constitute a small fraction of the overall leaf carbon (Brugnoli *et al.* 1988, Gessler *et al.* 2009). Therefore, analysis of $\delta^{13}C$ of new photoassimilates should provide a better indication of short-term changes in

$\Delta^{13}C$ as a result of the prevailing environmental conditions i.e. a sudden rainfall event (Brugnoli *et al.* 1988, Gessler *et al.* 2009).

Mulga (*Acacia aneura* F.Muell. ex Benth. and associated species; see Chapter 1; also Maslin & Reid 2012) is a woody Australian perennial shrub or tree that dominates much of the arid and semi-arid zones of Australia and can withstand months to years of extended drought (Winkworth 1973). Branch water potentials of Mulga are routinely measured as more negative than -10 MPa (Slatyer 1961a). These extremes of water potential are indicative of severe water deficit that lasts for months - sometimes years - at a time between rainfall pulses; these species have a shallow root system with little or no access to groundwater (Slatyer 1965, Pressland 1975). Previously, I showed that mulga communities with more terete to sub-terete phyllodes were predominant on the shaded hill slopes compared to a dominance of broader phyllode shapes in the valley woodlands (Chapter 2). As explained in Chapter 3, lower slopes and valley floors would likely have greater water availability and storage capacity than upper slopes due to accumulation of run-off from the slopes and deeper soil profiles. Consequently, we might expect growth forms with terete type phyllodes to be more drought tolerant/resistant and able to respond to pulse events more quickly than broader phyllode forms.

In this experiment I simulated a large rainfall event to investigate the pulse-response of *A. ayersiana* and two phyllode variants of *A. aneura* (terete versus broad) that formed the canopy of a low mulga valley woodland (see Chapter 2) at West Angelas. All trees had similar growth forms (multi-stemmed growth form 'T4C'; Chapter 2). I hypothesized that trees with different phyllode shapes would exhibit differences in tolerance of minimum water potential and in their capacity to respond to a simulated rainfall pulse. These differences in pulse-response capacity related to timing and rates of water use could explain the larger patterns in landscape scale distribution and abundance of the variants described in Chapter 2. I expected that Mulga with terete phyllodes were more suited to dry conditions owing to their predominance in the more elevated and potentially drier parts of the landscape at West Angelas. Therefore, I expected that trees with terete phyllodes would have more negative water potentials and would respond more quickly to a rainfall pulse than trees with broader phyllodes, reflecting adaptation to drier conditions.

Materials and Methods

Study site

I simulated an 80 mm rainfall pulse by irrigating nine trees over 24 hours on the 14th of June 2008 within a mulga woodland at West Angelas (-23.045932S, 118.827095E), in the Hamersley Ranges, 135 km northwest of the town of Newman in the Pilbara region of Western Australia. Episodic rainfall pulses of 80 mm are not uncommon (Figure 4.1). Mean annual minimum temperature at Newman is 16.1 ^{o}C and mean maximum temperature is 31.9 ^{o}C. On average there are 218 days of the year where the maximum temperature is above 30 ^{o}C (Bureau of Meteorology 2011a). A more thorough description of the climate of the region is provided in Chapter 1. Monthly rainfall totals and monthly average air temperature and vapour pressure deficit data for West Angelas are provided in Figure 4.1.

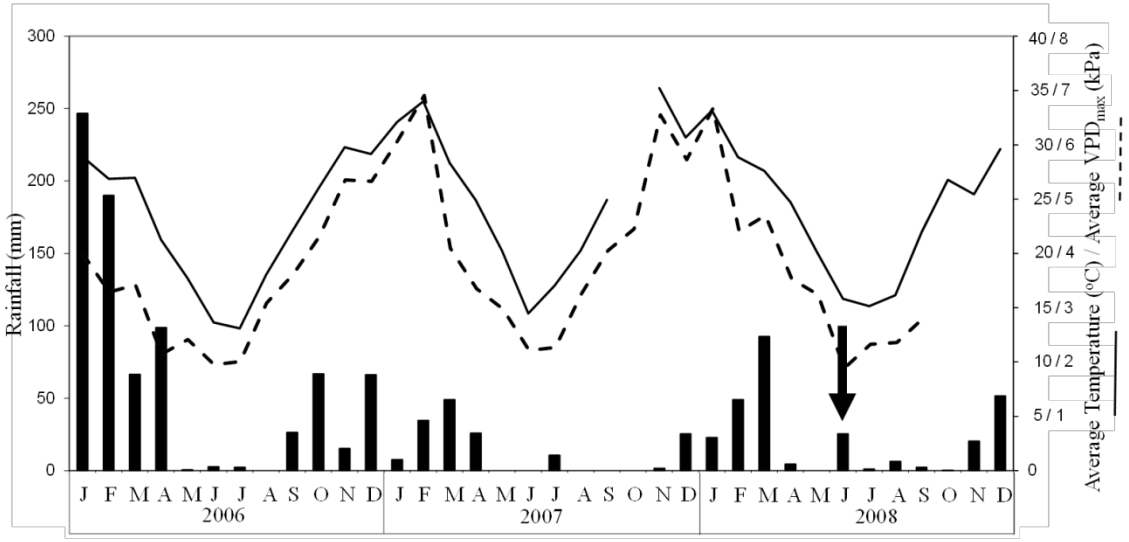

Figure 4.1 Monthly rainfall, average air temperature and average daily maximum vapour pressure deficit (VPD_{max}) at West Angelas 2006 – 2008. Precipitation is greatest in the summer months December - March, although there is the chance of rainfall in all seasons. Arrow indicates when a ~ 80 mm rainfall pulse was simulated in June 2008, 2 days after a natural 20 mm rainfall pulse.

Daily rainfall data were collected at the West Angelas airstrip, 16.5 km southwest of the study site, between January 2005 and December 2008. Total rainfall in 2005 was 237 mm, 2006 was 781.8 mm and in 2007 was 154.6 mm. In 2008, there was 165 mm of rain between January and March and a further 25 mm in June; 21 mm on the 10th of

June 2008 (4 days before irrigation), and 4 mm two days before irrigation on the 12th of June 2008 (Figure 4.1).

The soils at the site are predominantly light sandy clay loams (Uc1.43; Northcote 1971). Soil particle size fractions for the study woodland were silt 15%, clay 20% and sand 65%. Moisture release curves from similar Pilbara soils have an inflection point at ~ 15% gravimetric soil moisture and -100 kPa, and a soil matric potential far exceeding -1500 kPa when gravimetric soil moisture is below 10% (Ford *et al.* 2007, McIntyre, Adams & Grierson 2009).

Design of irrigation experiment

Water was applied to three replicate trees each of *A. aneura* (terete phyllodes), *A. aneura* (broad phyllodes) and *A. ayersiana*. The nine trees encompassed a range of specific leaf area (SLA) between 1.8 and 3.8 mm^2 mg^{-1} (these data are described more fully in Chapter 6). The two phyllode variants of *A. aneura* targeted in this study are common in the mulga woodlands of the Pilbara (Chapter 2, Maslin & Reid 2012). Both phyllode types are typically less than 10 cm long but differ in cross section. 'Terete' *A. aneura* has almost cylindrical phyllodes, roughly 1 x 1 mm (SLA ~ 1.5 m^2 kg^{-1}), whereas 'broad' *A. aneura* are about 1 x 3 mm (SLA ~ 2 m^2 kg^{-1}). *A. ayersiana* typically have much broader phyllodes and are 0.5 x 12 mm in cross section (SLA ~ 3 m^2 kg^{-1}). All trees were approximately the same height (4 – 5 m) and were selected for consistency in growth habit (Figure 4.2).

A 20 cm deep earth trench lined with plastic was installed at a 2 m radius from the base of the tree to prevent surface water runoff. Approximately 1000 L of water was applied via irrigation to the base of each tree on the 14th of June 2008. The nine study trees therefore received the equivalent of 105 mm rainfall between the 10th and 14th of June. Foliage samples and measurements of soil moisture content, branch water potential and stomatal conductance were collected 16 days prior to irrigation, one day prior to irrigation, and then one, three, five and seven days after irrigation. No measurements were made on "control trees", i.e. trees with no irrigation water applied, owing to time limitations. Instead, a before/after irrigation "pulse" design was used.

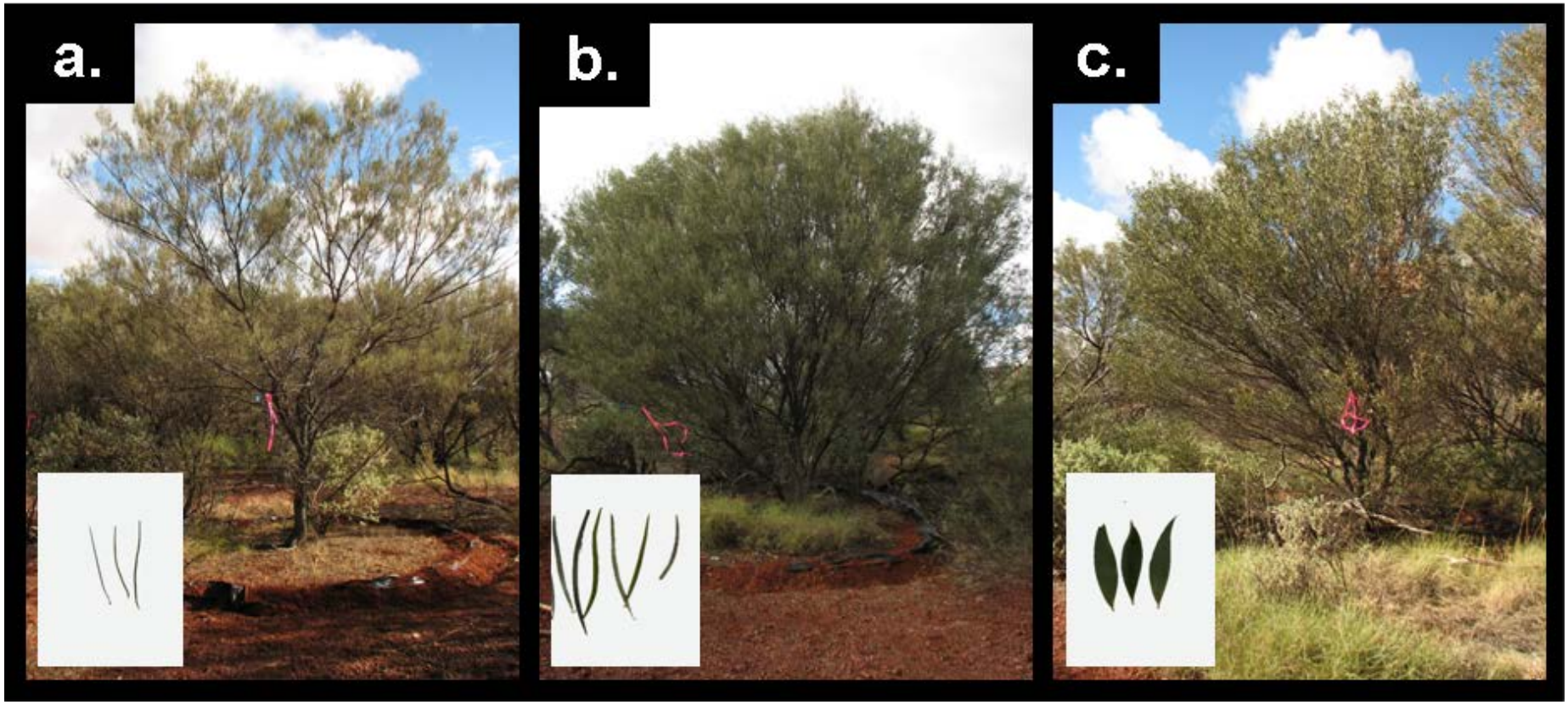

Figure 4.2 Trees and corresponding phyllode shapes selected for experimental irrigation treatment. (a) terete *A. aneura*, (b) broad *A. aneura*, and (c) *A. ayersiana*. Each of these three phyllode groups had three replicate trees, one of which is pictured here. Phyllode sizes in picture inserts are relative. All three trees are of similar height (4-5 m).

In order to check the consistency of irrigation treatment among all nine trees, at midday on each day of measurement, volumetric soil moisture content (v/v) was measured using a Trase 1 TDR (Time Domain Reflectrometry) system (Soil Moisture Equipment Corp., Santa Barbara, CA). Uncoated probes (15 cm) were inserted into the soil at three equally spaced locations that were 1 m from the base of each tree. The permittivity of the soil was converted to volumetric moisture content using a calibration against gravimetric moisture content of a soil sample collected from the site and transported back to the laboratory (Whalley 1993). Volumetric soil moisture content was the same among all trees over the course of the experiment and showed the same pattern of wetting up and drying down. Soil moisture content was 6.5% (v/v) on day -16 (Table 4.1), increased to 20% (v/v) on the day of irrigation and declined to 15% (v/v) by day 7 (Table 4.2). Maximum daily air temperature and vapour pressure deficit (VPD_{max}) were relatively high prior to irrigation (day -16: VPD_{max} 3.05 kPa, maximum air temperature 26.8 °C). The daily maximum air temperature and VPD_{max} had decreased following the rainfall on day -2 (VPD_{max} 1.40 kPa, average daily temperature maximum 19.6 °C days -1 to 7); these conditions closely resemble the monthly average (Figure 4.1).

Tree water relations

Three replicates of branch water potential were measured on each tree one hour before dawn and at midday on days -16, -1, 1, 3, 5, and 7 using a Scholander type pressure chamber (PMS Instrument Co., Albany, OR). Branches of ~ 50 cm length were cut from the outer canopy at 2 m above the ground using tree pruners. Terminal branchlets (approximately 10 cm in length) were then cut with a razor blade and branch water potential measured immediately. Relative water content (RWC) was determined from measurements of five phyllodes removed from each branch both at predawn and midday. After total fresh weight (FW) was determined for all five phyllodes they were transferred to a zip-lock bag and kept cool until transported back to the laboratory at the University of Western Australia (UWA) in Perth. All five phyllodes were then submerged in deionised water in the dark overnight, gently blotted on absorbent paper and weighed to determine turgid weight (TW). Submerging foliar material may over-estimate TW because of infiltration of water into air-spaces. Therefore, an alternative method of attaining TW by rehydrating phyllodes through the cut petiole was also attempted but proved unsuccessful. Dry weight (DW) was then determined after phyllodes were dried at 80^{o}C for 48 hours. RWC was determined using Equation 4.1.

$$RWC(\%) = \frac{FW - DW}{TW - DW} \times 100 \quad \text{(eq. 4.1)}$$

Stomatal conductance (g_s) was measured on five randomly selected fully expanded phyllodes on each tree every two hours between 7am and 5pm on the same day as water potential measurements using a SC-1 steady state porometer (Decagon Devices Inc., Pullman, WA).

Specific leaf area (SLA) and the sapwood area/one sided leaf area ratio (Huber value, H_v) were measured for all nine trees during this experiment. I sampled one branch at 2 m height from each tree; each branch was within a range of 70-100 cm long and 5-8 mm in diameter at the cut end. All phyllodes were collected from each branch for measurement with a leaf area meter (LI-3100, LI-COR inc., Lincoln, NE). SLA was calculated as the one-sided leaf area divided by the oven dry weight of foliage after being dried at 80^{o}C for 48 hours. The Huber value, H_v, was calculated by dividing the branch cross sectional area by the one-sided leaf area.

Foliar $\delta^{13}C$ analysis

The water-soluble carbon fraction was used as an estimate of recent photoassimilates (sugars) following a simplified version of the method of Brugnoli *et al.* (1988). Each measurement of $\delta^{13}C$ of the water-soluble carbon fraction ($\delta^{13}C_{soluble}$) and total phyllode ($\delta^{13}C_{total}$) used material from one bulk sample of 20 phyllodes per tree that had been sampled from the three branches used to measure water potential at midday on each day of sampling (n = 3). Phyllodes were stored in paper seed envelopes and kept cool until transported to UWA. Phyllodes were then oven dried at 60 ^{o}C for 48 hours and ground to a fine powder in a ball mill. Subsamples ~ 5 mg were weighed into 6 x 4 mm tin capsules (SerCon Ltd., Crewe, UK) for analysis of $\delta^{13}C_{total}$. The water-soluble carbon fraction was extracted by adding 50 mg of powder to 1mL of milliQ water and vortexed then incubated at 70^{o}C for 1 hour. Samples were centrifuged at 13 000 g for 10 minutes and 300 µL of the supernatant was dried down at 70 ^{o}C in an 11 x 4 mm tin capsule and then analysed.

I also tested whether a delay between collection and sample preparation influenced the $\delta^{13}C$ values of both total phyllode ($\delta^{13}C_{total}$) and water soluble carbon ($\delta^{13}C_{soluble}$).

Foliage from five *A. aneura* trees were collected into paper bags and transported back to the laboratory at UWA by air on the same day of sampling. Foliage from each tree was stored in three different ways; (1) frozen at -80 ^{o}C and then freeze-dried, (2) microwaved on high in a 1000W microwave oven for 30 seconds to denature any enzymes and oven dried at 60^{o}C for 48 hours and (3) left untreated at 25 ^{o}C for 14 days and then dried at 60^{o}C for 48 hours. All phyllode samples were then oven dried at 60 ^{o}C for 48 hours, ground to a fine powder in a ball mill and prepared for analysis of the water-soluble C ($\delta^{13}C_{soluble}$) and total phyllode C ($\delta^{13}C_{total}$) as above.

All phyllode samples were analyzed for stable carbon isotope composition (δ^{13}C, VPDB ‰) and carbon concentration (% by weight) using a 20/20 isotope ratio mass spectrometer (IRMS) connected with an ANCA-S1 preparation system (Europa Scientific Ltd., Crewe, UK), at the West Australian Biogeochemistry Centre at The University of Western Australia (http://www.wabc.uwa.edu.au). Samples were quantitatively combusted in the ANCA-S1 Elemental Analyser at 1700-1800°C (Skrzypek & Paul 2006). Yielded gases are carried in a stream of He through water traps and a GC column before CO_2 is introduced into the IRMS as transient peaks. The stable carbon isotope composition is reported in the standard δ-notation in permil [‰] after normalization of raw isotopic data to VPDB scale using multi-point normalization based on four standards (USGS24, NBS22, USGS41, USGS40) each replicated twice (Paul, Skrzypek & Fórizs 2007). Values for δ^{13}C standards were as calibrated by the Commission on Isotopic Abundances and Atomic Weights (Coplen *et al.* 2006). The uncertainty associated with stable isotope analyses (1σ - standard deviation) was not more that 0.20‰.

Data analysis

Differences in physiological parameters among *A. ayersiana* and the two variants of *A. aneura* (types) before irrigation (day -16) were tested using one-way ANOVA models in R 2.11.0 (R Development Core Team 2010). When $P \leq 0.05$, post-hoc tests were performed using Fisher's Honest Significant Difference test from the 'multcomp' package (Hothorn, Bretz & Westfall 2008).

Repeated measures analysis was used to test for differences in soil moisture, Ψ_{pd}, Ψ_{md}, $\Delta\Psi$, $g_{s\ max}$, RWC, $\delta^{13}C_{total}$ and $\delta^{13}C_{soluble}$ among the three groups of trees following irrigation. Specifically, linear mixed effects models (LMM) were fitted to the

longitudinal data (data for days 1-7) in R using the 'lme4' package. A null model (equation 4.2), an additive model (equation 4.3) and an interaction model (equation 4.4) were fitted, where '*day*' is a continuous variable defined by $N(0, \sigma_j^2)$, '*type*' is a factor with the three levels 'terete *A. aneura*', 'broad *A. aneura*', and '*A. ayersiana*', $\mu_i \sim N(0, \sigma_\mu^2)$ is a random intercept term for each tree and $\varepsilon_{ij} \sim N(0, \sigma_\varepsilon)$ are the within group errors for each tree *i* at each value of *day*. A quadratic term and a cubic term for 'day' were also included if they improved the model fit.

$$y = day + \mu_i + \varepsilon_{ij} \quad \text{(eq. 4.2)}$$

$$y = day + type + \mu_i + \varepsilon_{ij} \quad \text{(eq. 4.3)}$$

$$y = day + type + (day \times type) + \mu_i + \varepsilon_{ij} \quad \text{(eq. 4.4)}$$

Models were compared using both a pair-wise chi-squared likelihood ratio test and a comparison of Akaike's Information Criterion (AIC). When the chi-squared $P \leq 0.05$ and AIC values for the models differed by >10 the model with the smallest AIC value was chosen as the best fit, otherwise the most parsimonious model was preferred (Bolker *et al.* 2009). Differences among the three 'types' were determined as a $P \leq 0.05$ produced for the parameter estimates using Markov chain Monte Carlo sampling from the posterior distribution of the parameters with the pvals.fnc function in the 'languageR' package (Baayen, Davidson & Bates 2008).

Results

Ψ and phyllode relative water content

At day -16, terete *A. aneura* was significantly less negative in both Ψ_{pd} (-6.91 ± 0.51 MPa) and Ψ_{md} (-8.13 ± 0.41 MPa) compared to the other two (more broad) phyllode types, which were generally ~ -9.2 MPa at pre-dawn and <-10 MPa at midday (one-way ANOVA $P < 0.001$, Table 4.1). All trees had begun to rehydrate following a 20.6 mm rainfall event on day -2. Trees continued to hydrate the following day owing to the greater surface soil moisture coupled with lower evaporation losses due to heavy cloud cover. Consequently, branch water potential was the same among all trees ($P > 0.05$) and was similar between pre-dawn (-3.07 ± 0.25 MPa) and midday (-2.46 ± 0.27 MPa) on day -1 ($P > 0.05$).

Ψ_{pd} was the same among all trees for the 7 days following irrigation (Table 4.2). All trees were ~ -1 MPa at pre-dawn one day after irrigation and became progressively less negative over the course of the week (Table 4.2, Figure 4.3a). However, branch water potential at midday (Ψ_{md}) was consistently less negative in terete *A. aneura* following irrigation (-1.8 MPa) compared to the broad phyllode *A. aneura* and *A. ayersiana* (~ -2.5 MPa) (Table 4.2, Figure 4.3b). The decrease in water potential between pre-dawn and midday was significant in all three phyllode types for the 7 days following irrigation ($\Delta\Psi$, Table 4.2). Terete *A. aneura* had the smallest change (0.85 MPa) compared to broad *A. aneura* (1.11 MPa) and *A. ayersiana* (1.39 MPa). $\Delta\Psi$ values were larger than 1.10 MP before irrigation in broad *A. aneura* and *A. ayersiana*, although absolute values are unknown as Ψ_{md} was <-10 MPa and beyond the measurement limits of my equipment (PMS Model 1000 pressure chamber). $\Delta\Psi$ of terete *A. aneura* before irrigation was 1.22 MPa.

Phyllode relative water content pre-dawn was less than 55% at day -16 for all phyllode types. However, terete *A. aneura* were significantly more hydrated (54.4 ± 2.55%) than *A. ayersiana* (42.7 ± 1.69%) or broad *A. aneura* (47.1 ± 1.50%) (Table 4.1). By mid-day all phyllodes had dehydrated further and RWC was the same among all three phyllode variants (43.4%, $P > 0.05$, Table 4.1). Following irrigation, foliage in all three phyllode variants had completely rehydrated at pre-dawn every day (96.7%), and did not change over the 7 days of measurement (Table 4.2). RWC dropped to ~ 90% at midday each day, but was completely rehydrated again the following morning (Table 4.2). The almost complete rehydration of phyllodes following irrigation indicates that TW was not over-estimated by submerging phyllodes in water (refer to methods). Nevertheless, if these data are still underestimating RWC, it is by a maximum of approximately 3%.

Table 4.1 Soil moisture content and ecophysiological parameters of *A. ayersiana* and two phyllode variants of *A. aneura* 16 days (day-16) before water was applied.

	Terete *A. aneura*	Broad *A. aneura*	*A. ayersiana*	F-value	P-value
Soil Moisture (%)	6.40 (0.22)	6.14 (0.37)	6.72 (0.21)	1.11	0.39
Pre-dawn RWC (%)	54.4 [a] (2.55)	47.1 [ab] (1.50)	42.7 [b] (1.69)	8.98	0.02
Mid-day RWC (%)	46.6 (2.55)	41.7 (1.35)	41.9 (2.24)	1.70	0.26
$\delta^{13}C$ (‰)	-26.9 (0.62)	-28.0 (0.46)	-26.6 (0.46)	1.85	0.24
$\delta^{13}C_{soluble}$ (‰)	-26.5 (0.50)	-27.8 (0.36)	-27.3 (0.31)	2.52	0.16
Ψ_{pd} (MPa)	-6.91 [a] (0.51)	-8.93 [b] (0.14)	-9.42 [b] (0.4)	12.1	<0.001
Ψ_{md} (MPa)	-8.13 [a] (0.41)	<-10 [b] (na)[#]	<-10 [b] (na)[#]	48.9	<0.001
$g_{s\ max.}$ (mmol m^{-2} s^{-1})	25.6 (5.85)	12.5 (4.82)	26.5 (1.33)	3.13	0.12
SLA (m^2 kg^{-1})	1.45 [a] (0.06)	1.81 [a] (0.21)	2.86 [b] (0.08)	30.3	0.001
Hv **(m^2 m^{-2} x10^{-4})**	27.7 [a] (8.36)	12.8 [ab] (1.77)	7.33 [b] (0.36)	4.54	0.06

Mean values given with 1 standard error in parentheses. n = 9 for Ψ_{pd} and Ψ_{md}, and n = 3 for all other measurements. F-values and P-values are results of one-way ANOVA models. When P-values were ≤ 0.05, Fishers Honest Significant Difference post-hoc tests were applied and significant groupings indicated by superscript letters. [#] All measurements exceeded the 10 MPa limit of the PMS Model 1000 pressure chamber and so were assigned the value of -11 MPa thus no standard error could be calculated.

Table 4.2 Parameter estimates of linear mixed effects models (LMM) fitted to ecophysiological measurements made over a seven day period following irrigation with water equivalent to ~ 80 mm of rainfall.

Response Variable	Model Term	Estimate	S.E.	p-value
Soil Moisture (%)	Intercept	26.0	1.02	<0.001
	Day	-1.53	0.19	<0.001
Ψ_{pd} (MPa)	Intercept	-1.19	0.07	<0.001
	Day	0.07	0.007	<0.001
Ψ_{md} (MPa)	Intercept (Broad *A. aneura*)	-2.96	0.2	<0.001
	Terete *A. aneura*	1.075	0.28	<0.001
	A. ayersiana	-0.26	0.28	0.4
	Day (x Broad *A. aneura*)	0.38	0.09	<0.001
	Day^2 (x Broad *A. aneura*)	-0.04	0.01	<0.001
	Day x Terete	-0.28	0.12	0.03
	Day x *A. ayersiana*	0.08	0.12	0.54
	Day^2 x Terete	0.03	0.02	0.06
	Day^2 x *A. ayersiana*	-0.01	0.02	0.5
$\Delta\Psi$	Intercept (Broad *A. aneura*)	-1.11	0.09	0.00
	Terete *A. aneura*	0.26	0.10	0.01
	A. ayersiana	-0.28	0.10	0.01
	Day	-0.03	0.01	0.04
g_s (mmol m^{-2} s^{-1})	Intercept (Broad *A. aneura*)	65.3	14.1	<0.001
	Terete *A. aneura*	4.93	15.6	0.75
	A. ayersiana	57.5	15.6	<0.001
	Day	16.7	5.5	0.004
	Day^2	-2.03	0.67	0.005
$\delta^{13}C$ (‰)	Intercept	-26.7	0.3	<0.001
	Day	-0.19	0.03	<0.001
$\delta^{13}C_{soluble}$ (‰)	Intercept	-27.0	0.23	<0.001
	Day	-0.06	0.03	0.05
pre-dawn RWC (%)	Intercept	96.7	0.49	<0.001
	Day	0.007	0.01	0.54
mid-day RWC (%)	Intercept	90.1	0.39	<0.001
	Day	0.01	0.008	0.13

Slope and intercept parameters are listed for the best-fit LMM determined by a chi-squared likelihood ratio test. Models with only one intercept and slope are for the null model and were not improved by the inclusion of a 'type' parameter indicating that all three phyllode types exhibited similar responses to the simulated rainfall pulse. P-values derived from a Markov chain Monte Carlo sampling procedure, where $P \leq 0.05$ indicates a significant estimate. Parameter estimates in multi-level models (g_s and Ψ_{md}) are interpreted by adding estimates together. For example, the g_s intercept parameter for broad *A. aneura* is 65.3, and terete *A. aneura* is 65.3 + 4.93 = 70.2

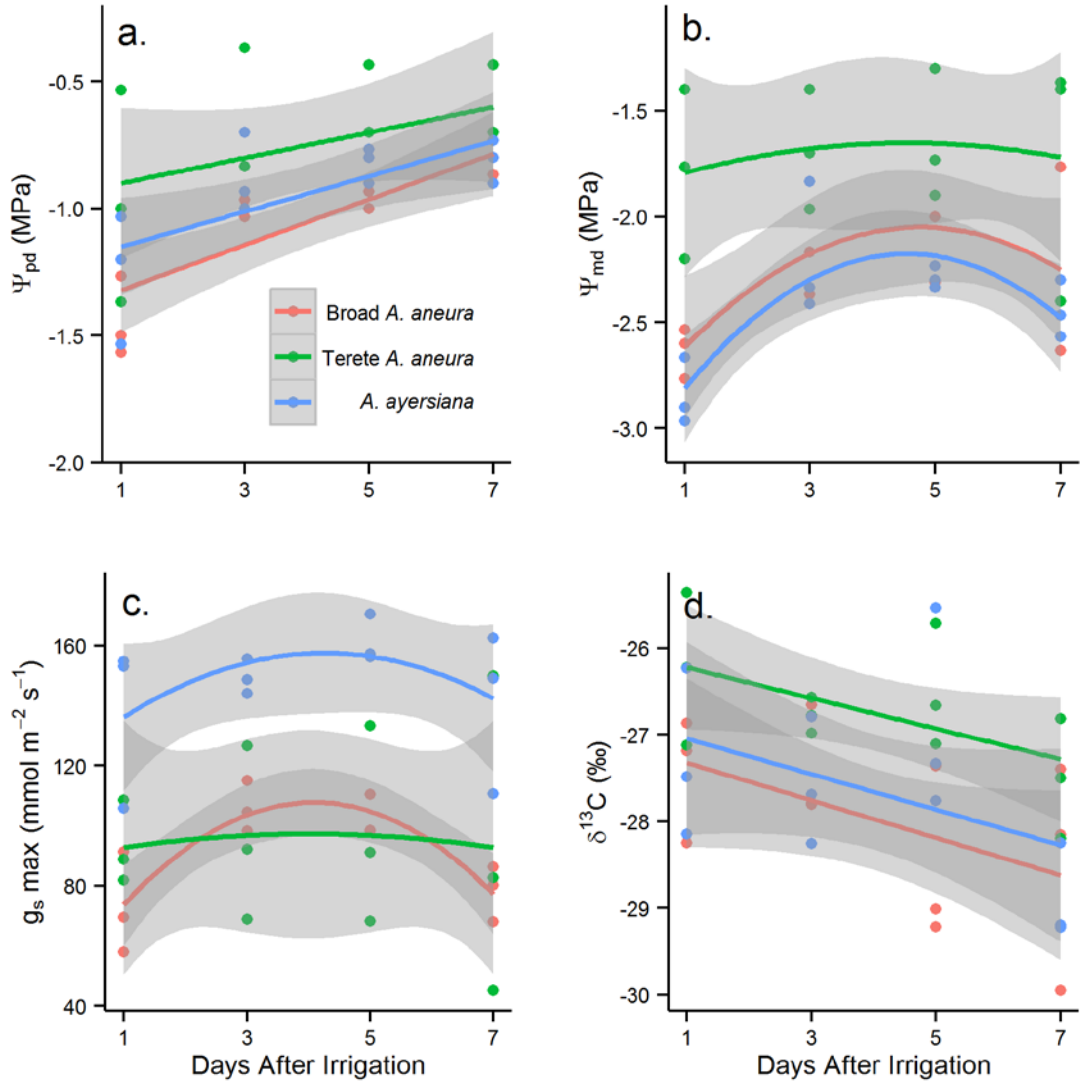

Figure 4.3 Physiological response of *A. ayersiana* and two phyllode variants of *A. aneura* to precipitation and irrigation with water equivalent to ~ 105 mm of rainfall. (a) pre-dawn water potential Ψ_{pd}, (b) midday water potential Ψ_{md}, (c) Daily maximum stomatal conductance, and (d) total phyllode $\delta^{13}C$. Raw data is plotted and fitted linear models with 95% confidence intervals shaded in grey using the ggplot2 package for R.

Daily maximum stomatal conductance, $g_{s\ max}$.

Two weeks before irrigation (day -16), all trees had consistently low stomatal conductance (mean $g_{s\ max}$= 21.5 mmol m^{-2} s^{-1}, P = 0.12; Table 4.1). Immediately following irrigation at day 0, $g_{s\ max}$ increased sharply in all trees. Stomatal conductance of *A. ayersiana* (~ 150 mmol m^{-2} s^{-1}) was greater than either phyllode type of *A. aneura* (~ 100 mmol m^{-2} s^{-1}) for the 7 days following irrigation (Figure 4.3c, Table 4.2). Stomatal conductance was the same in broad and terete *A. aneura* (Figure 4.3c, Table 4.2). Stomatal conductance continued to increase until reaching a peak at approximately 4 days after irrigation before beginning to gradually decline in all trees (Figure 4.3c, Table 4.2).

Patterns of water soluble and total phyllode $\delta^{13}C$

The $\delta^{13}C_{total}$ values were similar among all three phyllode types at day -16 (-27.2 ± 0.33 ‰, Table 4.1). Total foliage $\delta^{13}C$ did not change significantly during the following two weeks (-26.7 ± 0.38 ‰ on day -1). The total leaf pool of $\delta^{13}C_{total}$ was rapidly diluted by ~ 0.2 ‰ per day over a period of 7 days following irrigation, reaching -28.3 ± 0.33 ‰ on day 7 (Table 4.2, Figure 4.3d). A similar trend was not evident for $\delta^{13}C_{soluble}$, which was consistent both before and after irrigation (~ -27.0 ± 0.13 ‰, Table 4.1, Table 4.2). The $\delta^{13}C_{total}$ was significantly less negative in terete *A. aneura* compared to either either broad *A. aneura* or *A. ayersiana* for the seven days following irrigation when analysed with a linear model without random effects. However, inclusion of random effects using a linear mixed model accounted for the variation among phyllode variants, indicating that all three were the same. Neither $\delta^{13}C_{total}$ nor $\delta^{13}C_{soluble}$ were correlated with any of the other measured physiological parameters, including g_s ($P > 0.05$).

Discussion

My results demonstrate that the magnitude and rate of response of Mulga to an ~ 80 mm rainfall pulse is large and rapid (i.e., within1 - 3 days; branch water potential increasing from ~ -8 MPa at pre-dawn to >-1 MPa), irrespective of species or phyllode shape. This rapid rehydration coupled with increases in g_s illustrates the central role that pulsed water availability has at these sites, and likely mulga communities more generally. These findings are consistent with studies of woody species in semi-arid and arid environments elsewhere. For example, *Prosopis velutina* recovered fully from

dehydration within one to three days of a pulse application of water in an Arizonan desert, USA (Fravolini *et al.* 2005, Resco *et al.* 2009).

My results are also consistent with observations of ecosystem scale pulse-response in a wide variety of semi-arid regions. At the ecosystem scale, carbon fixation (indicated by net ecosystem CO_2 exchange) generally resumes within three to five days after a rainfall pulse among a range of environments, including in a Mongolian Steppe (Wohlfahrt *et al.* 2008), a Mojave Desert shrubland, USA (Wohlfahrt *et al.* 2008) and semi-arid grasslands in Arizona, USA (Potts *et al.* 2006). However, whilst whole ecosystem results are qualitatively informative, it is likely that the response magnitude of vegetation to a rainfall pulse depends on both the severity of the preceding drought and the size of the rainfall pulse. While I found that all trees responded within 3 days of rainfall, the preceding drought period (no rain) had been relatively short for this region (2 months). There had been ~100 mm of rainfall three months before the experiment and a further ~ 25 mm in the four days before the irrigation for this experiment (Figure 4.1). In cases of severe drought preceding a pulse, the resumption of carbon fixation may take as long as two weeks (Resco *et al.* 2009, Shim *et al.* 2009). Similarly rainfall pulses below a threshold value of around 10 – 25 mm may also fail to rehydrate vegetation sufficiently enough to restore photosynthesis (Chen *et al.* 2009, Pockman & Small 2010). Here, a rainfall pulse of 20 mm four days prior to the irrigation experiment did cause an increase in water potential, but did not significantly change the values of $\delta^{13}C_{total}$. These data suggest that the 20 mm rainfall may not have been sufficient to restore photosynthesis. However, to confirm this result instantaneous measurements of photosynthesis are required; regrettably not here owing to a breakdown of gas exchange equipment during the field experiment

Foliar $\delta^{13}C_{total}$ also responded rapidly to the irrigation pulse confirming that this may be a useful surrogate measure of physiological activity in these species. There was a significant trend of 0.2 ‰ day^{-1} depletion of ^{13}C in leaf tissue among all trees from the day before irrigation until seven days following (Table 4.2), consistent with a dilution of the ^{13}C pool by new photoassimilate with more negative $\delta^{13}C$ as a consequence of higher g_s and higher C_i/C_a (Brugnoli *et al.* 1988, Farquhar *et al.* 1989). However, measures of $\delta^{13}C_{soluble}$ as an approximation of new photoassimilate did not explain the depletion of ^{13}C in foliage following irrigation. $\delta^{13}C_{soluble}$ did not significantly fluctuate post irrigation and was more enriched in ^{13}C than total leaf material in all three phyllode

variants from one day after irrigation (~ 27.0 ‰ Table 4.2, Figure 4.3d). This is a surprising result, as previously experimental data from *Eucalyptus globulus* Labill. has demonstrated the sensitivity of $\delta^{13}C_{soluble}$ to drought stress (Merchant *et al.* 2010). Alternatively, $\delta^{13}C_{soluble}$ was not sensitive to changes in C_i/C_a when assessed simultaneously with leaf level gas exchange measurements in *Eucalyptus delegatensis* R.T.Baker. (Gessler *et al.* 2007). Therefore, the decrease of $\delta^{13}C_{total}$ following irrigation was either not attributable to new photoassimilate, or $\delta^{13}C_{soluble}$ was not a reliable estimate of new photoassimilate.

A second explanation for the observed depletion of ^{13}C in leaf tissue and stable $\delta^{13}C_{soluble}$ may be high rates of respiration. Dark respiration in C3 plants has been shown to discriminate against ^{13}C resulting in the evolution of enriched CO_2 and a dilution of ^{13}C in the remaining plant material (Duranceau *et al.* 1999, Ghashghaie *et al.* 2003). High rates of respiration undoubtedly play a role in the growth and productivity of plants in extreme hot and arid environments. Whilst not possible in the current study, quantifying the rates of respiration and discriminatory effects on ^{13}C and subsequent effects on heterotrophic tissues (Ghashghaie *et al.* 2003, Cernusak *et al.* 2009, Gessler *et al.* 2009), would help disentangle the relative contributions of carbon fixation and dark respiration to the pulse-response strategy of these species.

Analysis of the size and $\delta^{13}C$ of carbohydrate pools in the foliage of these trees would help resolve the physiological process driving the ^{13}C depletion/dilution. These results may be explained by a large proportion of the soluble carbon fraction not participating in core plant metabolism. For example, $\delta^{13}C_{soluble}$ may be strongly influenced by amino compounds and organic acids which have a different isotopic composition to starch (Gessler *et al.* 2007). Consequently, the $\delta^{13}C$ of a smaller soluble carbon pool with higher flux rates which make a disproportionate contribution to bulk leaf tissue is lost in a background of the much larger soluble carbon pool. Characterizing such a system relies on the measure of flux (Schwender, Ohlrogge & Shachar-Hill 2004) or of compound specific measures of ^{13}C distributions (e.g. Wild *et al.* 2010) well beyond the scope of my study. Nevertheless, previous studies highlight notable candidates for large pools of soluble carbon known to accumulate in *A. aneura* (Seigler 2003, Merchant *et al.* 2006b, Warwick & Thukten 2006, Liu *et al.* 2008), to buffer against dehydration (Erskine *et al.* 1996). These results highlight a need to consider temporal (and spatial)

variation in plant metabolic activity and the importance of understanding pool sizes within the soluble fraction of plants.

Several quantitative aspects of physiology observed in my study suggest that *A. aneura* and *A. ayersiana* possess survival and growth strategies adapted to the pulse availability of resources not unlike the function of 'resurrection plants'. I measured foliage RWC of ~ 42% before irrigation, and while more hydrated than true resurrection plants (which commonly reach <10%), are not the lowest values recorded for *A. aneura*. Previous studies on water relations of *A. aneura* have measured RWC as low as 35%, which can rehydrate to ~ 100% within three to four days of a rainfall pulse (Slatyer 1961a). Resurrection plants are able to tolerate extreme cellular dehydration by concentrating highly reduced soluble compounds to stabilize cellular components (Scott 2000, Andersen *et al.* 2011). Similarly, the accumulation of 'compatible solutes' likely plays a key role in the ability of *A. aneura* and *A. ayersiana* to rapidly rehydrate and resume physiological activity after withstanding prolonged periods of cellular dehydration. Consequently, further investigation of the temporal variation in metabolic activity and the size of soluble pools will further elucidate the role of compatible solutes in the growth and survival of arid *Acacia* spp.

While the response to rehydration was uniform and rapid among all trees, differences in the rates of water use were reflected by the size of $\Delta\Psi$. Terete *A. aneura* had consistently less negative Ψ_{md} than either of the other two phyllode variants (Table 4.2), most likely as a consequence of a larger *Hv* and lower g_s (Table 4.1) that translated into lower overall rates of water use. However, differences in $\Delta\Psi$ following irrigation were not reflected by differences in $\delta^{13}C$ (either total or soluble fractions), although $\delta^{13}C_{total}$ was significantly less negative in terete *A. aneura* when analysed with a linear model without including random effects. These results demonstrate a pulse response strategy in *A. aneura* and *A. ayersiana* that includes rapid rehydration and the resumption of photosynthesis. Larger phyllodes transpire more water, which generates a larger $\Delta\Psi$. Once soil water reserves are low (i.e. 2 months of drought), trees are unable to fully rehydrate overnight causing Ψ_{pd} to decrease. This response demonstrates that gas exchange in *A. aneura* and *A. ayersiana* is tightly controlled by soil water availability and g_s. However, it is unknown how these species respond to longer drought that is common in the semi-arid deserts of Australia.

In conclusion, in this experiment, I demonstrated that the two dominant canopy *Acacia* spp. of the study woodland have a capacity to persist during drought periods with extreme levels of cellular dehydration (~ 40% RWC), while retaining an ability to respond to a rainfall pulse within one to three days. I also demonstrated that variation in SLA among *A. ayersiana* and two phyllode variants of *A. aneura* translated into differences in rates of water use, which in turn resulted in differences in Ψ_{md} both during drought and for the seven days following a rainfall pulse. The rapid hydraulic response to the rainfall pulse was also detected as a significant daily depletion of foliar ^{13}C of 0.2 ‰ day^{-1}; however, further analysis of the size and temporal variation of pool sizes within the soluble carbon fraction of plants is required to elucidate the role of compatible solutes and metabolic processes in facilitating the drought response capacity of these *Acacia* spp. These aspects are the focus of the next Chapter (Chapter 5).

Chapter 5: The contribution of osmolytes to drought tolerance in the Mulga species complex

Introduction

Plants exposed to drought often increase their cellular osmolality through the accumulation and concentration of compatible (i.e. non-toxic) solutes (osmolytes) to maintain turgor (Turner & Jones 1980). In arid and semi-arid environments, the dehydration of plant tissues and loss of turgor is an unavoidable scenario for many plant species, particularly those that are shallow-rooted and where conditions are typified by prolonged drought periods, high irradiance and high vapour pressure deficit (VPD). Consequently, the accumulation of osmolytes can play important roles in cellular water relations (Hare, Cress & Van Staden 1998, Bartlett, Scoffoni & Sack 2012), as well as contribute to the protection of subcellular structures and processes through the maintenance of tertiary protein structure (Orthen, Popp & Smirnoff 1994, Orthen & Popp 2000) and to maintaining metabolic processes at low cellular water content (Paul & Foyer 2001, Jaindl & Popp 2006, Conde, Chaves & Gerós 2011). Osmolytes also play important roles in homeostatic regulation of cellular conditions by scavenging free radicals (Orthen *et al.* 1994), or provide a metabolic pathway to dissipate excess photochemical energy, regenerating NAPDH for continued photosynthesis. (Hare *et al.* 1998). As shown previously, Mulga tolerate extreme cellular dehydration during drought (~ 43%) yet rapidly rehydrate and resume gas exchange following a rainfall pulse (Chapter 4). Osmolytes are thus likely to be integral to the ecophysiological functioning of the Mulga species complex.

Plants accumulate a wide range of solutes that contribute to osmotic potential. However, the synthesis of particular osmolytes depends on the availability of pre-cursor substrates, as well as the type of stress that induces a response (Hare *et al.* 1998). Inorganic ion pairs (i.e., K^+ Cl^-) make a large contribution to the osmotic balance of cells but are toxic at high concentrations (Maathuis & Amtmann 1999). Instead, plants may actively regulate the concentration of osmolytes to cope with environmental stress without the toxic metabolic side-effects (Hare *et al.* 1998). Simple sugars that are involved in primary metabolism (i.e., sucrose, glucose and fructose) also contribute to

the osmotic balance of cells in the short-term, but pool sizes can fluctuate rapidly depending upon metabolic demand (Hummel *et al.* 2010). Thus, organic compounds with slower rates of turnover, i.e., secondary metabolites (carbohydrates), may make a longer-term impact on cellular osmotic balance and play an integral part in acclimation to environmental stress (Hare *et al.* 1998, Merchant *et al.* 2006b). For example, photorespiration can increase under conditions of drought stress as reduced stomatal conductance decreases intercellular CO_2 levels within leaves that in turn facilitates photorespiration (Warren, Aranda & Cano 2011, Voss *et al.* 2013). Polyols (e.g., glycerol) including cyclitols (e.g., pinitol, ononitol) are highly stable organic compounds that function as osmolytes and can be accumulated in leaves exposed to high heat and light stress (Merchant *et al.* 2006b). Amino acids (e.g., glycine, proline) and methylamines (e.g., glycine-betaine) are also common osmolytes in plant cells involved in mitigating photo-oxidative damage (Hare *et al.* 1998, Yancey 2005). Therefore, identification and quantification on the pools of osmolytes present in plants provides further information on the type and duration of stress, particularly in relation to drought.

The osmolytes of *Eucalyptus* and *Acacia* have only recently received detailed attention, which is somewhat surprising considering these are both the largest and most dominant plant genera in Australia. The elegant work of Merchant and colleagues has demonstrated that both *Eucalyptus* and *Acacia* have clear quantitative and qualitative patterns in both the concentration and composition of osmolytes found in leaves and phyllodes, that correspond to evolutionary divergence along aridity gradients (Merchant *et al.* 2007). In particular, cyclitols including quercitol have been identified as significant osmolytes that increase in concentration under drought stress in arid zone species of *Eucalyptus* and *Acacia* (Merchant *et al.* 2006a, Arndt *et al.* 2008, Liu *et al.* 2008). For the genus *Acacia*, the cyclitol D-Pinitol may contribute up to 4% of the leaf (phyllode) dry weight from various species (Merchant *et al.* 2006a). Similarly, pinotol and its pre-cursor ononitol comprised 10-15% of the organic solutes in two more mesic *Acacia* species *(A. mangium* Willd. and *A. maidenii* F.Muell.) that were exposed to drought stress under glasshouse conditions (Warren *et al.* 2011). The accumulation of cyclitols, as well as methyl amines, including glycine-betaine, in semi-arid *Acacia* (Erskine *et al.* 1996) and *Eucalyptus* species (Warren *et al.* 2011) is unsurprising considering the regular exposure to moisture and light stress in these species. However, while cyclitols and amino acids are significant osmolytes in many species, they may not

make the largest osmotic contribution in *Acacia* growing in dry environments. For example, *Acacia auriculiformis* A.Cunn. ex Benth. are trees common across northern Australia that regulate osmotic potential of foliage through large increases of sucrose during seasonal drought stress (Liu *et al.* 2008). However, while our understanding of the role of osmolytes in dominant Australian genera is increasing, much of these data are obtained from glass house experiments using tropical and temperate species.

Overall, it remains unclear how the accumulation of osmolytes by long-lived species in arid environments may contribute to the persistence of those species during long periods of drought. My objective for this Chapter was to investigate the contribution of osmolytes to the maintenance of phyllode water potential in a suite of co-occurring *Acacia* species during drought in a semi-arid environment. In the previous Chapters I showed that more broad phyllode forms of *A. aneura* and *A. ayersiana* had significantly lower (i.e., more negative) minimum branch water potentials during drought than co-occurring terete phyllode *A. aneura*. Furthermore, all trees were exposed to very low cellular water content (~ 43%). However, all trees featured an identical capacity to respond to a rainfall pulse regardless of the magnitude of the preceding drought stress (Chapter 4). Therefore, I would expect that osmolytes make a larger contribution to osmotic potential in the foliage of trees that tolerate more negative water potentials during drought. In this study I thus sought to: (i) determine the contribution of soluble carbohydrates and inorganic cations to osmotic potential in a suite of co-occurring *Acacia* species, (ii) determine whether the osmotic profile was conserved among the phyllode variants and species, and (iii) determine whether any differences in osmotic profiles were associated with the severity of water stress (minimum branch water potential and cellular hydration) experienced during an extended drought period.

Materials and Methods

Site description

Branch water potential was measured and foliage collections made from *Acacia aneura* F.Muell. ex Benth. and *Acacia catenulata* C.T.White at West Angelas in the Hamersley Ranges of the Pilbara region of Western Australia (–23.175 S, 118.790 E) in August 2007. Daily rainfall and temperature data were collected at the West Angelas airstrip (-23.135 S, 118.705 E) between January 2005 and December 2008, and climate data is

presented relative to the sampling period (Figure 5.1). A more detailed description of the climate is provided in Chapter 1.

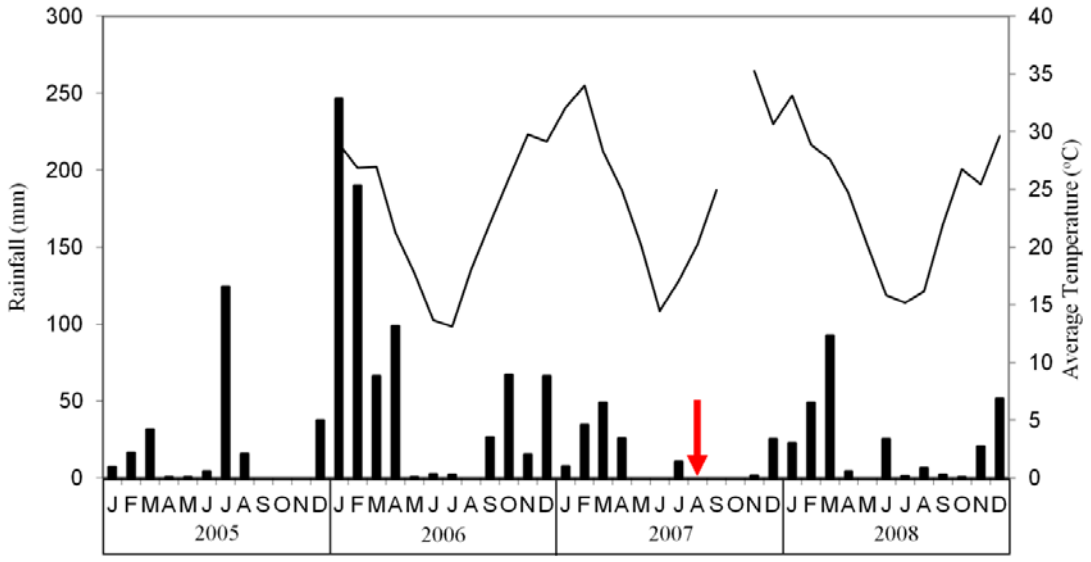

Figure 5.1 Monthly average temperature and rainfall at West Angelas 2005 – 2008. Red arrow indicates sampling period.

Six transects were sampled for branch water potential and foliage collections for carbohydrate and inorganic cation analysis. The transects were a subset of the 28 surveyed in Chapter 2 and were selected to represent all six landscape positions: (i) upper southern hill slope, (ii) lower southern hill slope, (iii) low mulga woodland, (iv) banded or linear mulga woodland, (v) low open mulga woodland, and (vi) drainage line mulga woodland (tall woodland) (Chapter 2). There were no woodlands on north-facing slopes (most exposed aspects). Belt transects were 4 m wide and a minimum of 100 m long, containing a minimum of 20 individuals of *A. aneura* or closely related members of the Mulga complex (*Acacia aneura* F.Muell. ex Benth., *Acacia catenulata* C.T.White, *Acacia ayersiana* Maconochie and *Acacia minyura* Randell). My objective was to capture the diversity of osmolyte accumulation across the Mulga complex and at the landscape scale. Therefore, I sampled from all trees previously measured (Chapter 2) along one transect in each landscape position (i.e., without replication). Data from

transects were subsequently pooled into three main landscape positions: hill slope, valley floor and drainage line.

Branch water potential

Three replicates of branch water potential were measured on each tree that was sampled for osmolyte analysis one hour before dawn and at midday using a Scholander type pressure chamber (PMS Instrument Co., Albany, OR). Branches of ~ 50 cm length were cut from the outer canopy at 2 m height using tree pruners. Terminal branchlets (approximately 10 cm in length) were then cut with a razor blade and branch water potential measured immediately.

Foliage collection

Between 10 and 20 young and fully expanded phyllodes were sampled from each tree between 10 am - 12 pm, stored in air-tight bags and kept cool to avoid dehydration. It was not possible to snap-freeze foliar material owing to the remoteness of the field sites. Therefore, to denature enzymes in the foliage and stop metabolic transformations of carbohydrates, a subset of foliage from each tree was microwaved at full power for 20 seconds in an 800W microwave oven between 5pm and 6pm on the day of collection following the method of Popp *et al.* (1996) and Merchant *et al*. (2007). Relative water content (RWC, %) was determined for each tree at the same time as foliage was collected for carbohydrate analysis. Five young and fully expanded phyllodes were sampled from each tree and placed in zip-lock bags with the air squeezed out and stored on ice. Fresh weight (FW) was then measured on the five phyllodes in the evening on the day of collection. Phyllodes were returned to the zip-lock bag and kept refrigerated and transported back to the University of Western Australia in Perth. All five phyllodes were then submerged in deionised water and kept in the dark overnight, gently blotted on absorbent paper and weighed to determine turgid weight (TW). Dry weight (DW) was determined after phyllodes were dried at 80^{o}C for 48 hours. RWC was determined using equation 5.1.

$$RWC(\%) = \frac{FW - DW}{TW - DW} \times 100 \qquad \text{(eq. 5.1)}$$

Carbohydrate extraction and analysis

Soluble carbohydrates were extracted following the procedure described by Merchant & Adams (2005). First, the samples were de-ionised. Phyllodes were dried at 80 °C and then ground to a fine powder using a ball mill. Then 40 mg of the ground sample was weighed into a 2-mL screw-cap microtube before adding 1 mL of hot (75°C) methanol-chloroform-water mixture (MCW, 12:5:3). The water fraction of the MCW mixture also included an internal standard of 0.4% penta-erythritol. Samples were shaken by hand for 10 seconds to ensure mixing and then incubated at 75°C for 30 minutes. Samples were then centrifuged (11 400 *g*) for 3 minutes. A 800 µL aliquot of clear supernatant was transferred from the centrifuged sample to a new round-bottom microtube with 200 µL chloroform and 500 µL milliQ water to facilitate phase separation; the sample was then agitated on a vortexer and again centrifuged (11 400 *g*) for 3 minutes. An aliquot of 800 µl of clear supernatant was then transferred to a clean 1.5 mL microtube with 300 µL of mixed-bed resin (MBR). The MBR consisted of 1 part Dowex 1 x 8 (anion exchange, Cl^- form) and 1 part Dowex 50W (cation exchange, formate form). Samples were shaken at room temperature for one hour and then pulse centrifuged. Finally, 400 µL of clear supernatant was transferred to a clean microtube and stored at -80°C.

The de-ionised MCW extracts (60 µL) were dried and re-suspended in 400 µL anhydrous pyridine to which 50 µL of trimethylchlorosilane (TMCS)/bis-trimethylsilyl-trifluoroacetamide (BSTFA) mix (1:10, Sigma Aldrich, St Louis, MO) was added. Samples were incubated at 75°C for one hour and then analysed for carbohydrates within 12 hours. Separation of organic compounds in the extracts was performed with a Shimadzu 17A series gas chromatograph (Shimadzu Corporation, Columbia, MD) using a DBl (30 m) column. Split injection was made at 300°C with an initial oven temperature program of 60°C for 2 minutes increasing to 300°C at 10°C min^{-1} and maintained for 10 minutes. Column flow rate was maintained at 1.5 mL min^{-1}. Peak integration was made with Class VP analysis software (Shimadzu Corporation Ltd.).

Cation extraction and analysis

The concentration of inorganic cations in phyllodes was determined after extraction in hot water. First, 1 mL of 80°C milliQ water was added to 40 mg of the dried and ball-milled phyllode material, which was then vortexed and incubated at 80°C for 30 minutes. Samples were then centrifuged at 13 000 *g* for 10 minutes. A 400 µL aliquot of clear supernatant was then transferred to a 10 mL vial and made up to 6 mL with milliQ

water prior to analysis. Extracts were analysed on a PerkinElmer Optima 5300DV simultaneous inductively coupled plasma optical emission spectrometer (PerkinElmer Inc., Waltham, MA). Samples were run in batches of 40 with four internal standards (ASPAC 142) and two blanks for drift correction. I assumed a similar accumulation of inorganic anions existed in the solution to balance the electrochemical charge of the cations ('Anion Estimate', Table 5.1).

Pressure-volume analysis

Pressure-volume analysis was used to determine the contribution of total osmotic potential and cell wall elasticity to phyllode water potential and turgor maintenance in a small sub-sample of trees at one transect in the "low mulga woodland" landscape position. *Acacia ayersiana* was sampled in the place of *A. catenulata* for pressure-volume analysis owing to the availability of trees at the field site. Likewise, only terete and broad phyllode variants of *A. aneura* were present so pressure-volume data for narrow *A. aneura* is not presented. Branch samples were collected in June 2008, six days after the trees had received approximately 80 mm of simulated rainfall, and measurements made using the bench top dehydration method (Tyree & Hammel 1972, Sack, Pasquet-Kok & PrometheusWiki contributors 2011) and as described briefly below.

One branch ~ 30 cm in length was cut from three replicates each of *A. ayersiana*, *A. aneura* (broad phyllodes) and *A. aneura* (terete phyllodes) and then re-cut underwater. Branches were left standing with the cut end in water and covered with a plastic bag overnight to allow rehydration. Samples were considered rehydrated when phyllode water potential (Ψ) was >-0.05 MPa. All water potentials were measured using a Scholander pressure chamber fitted with a digital pressure gauge and recorded to within 0.01 MPa (PMS Instrument Co., Albany, OR, USA).

Pressure-volume measurements were made on a ~ 10 cm section cut from the terminal end of each branch. Branch water potential was measured and then the weight of the branch immediately recorded to within 0.10 mg. Each sample was then re-measured for water potential and weight when it was estimated that the branch water potential had declined by ~ 0.10 MPa. Measurements continued until Ψ reached ~ - 6.00 MPa in most branches. Between 28 and 35 measurements were made on each sample. Samples were then dried at 80°C for 48 hours and weighed for dry weight (DW).

Sample weights were converted to relative water content (RWC %) where turgid weight (TW) was the initial weight of the sample, fresh weight (FW) was the weight at measurement and dry weight (DW) was the oven dry weight at the end of the experiment. The reciprocal of Ψ was then plotted against the RWC and used to determine four parameters: the bulk modulus of elasticity of the cell wall (ε), osmotic potential at full turgor (π_{100}), osmotic potential at turgor loss point (π_0) and relative water content at turgor loss point (RWC_0) (Tyree & Hammel 1972, Sack *et al.* 2011).

Data analysis

Differences in branch water potential, relative water content and osmolyte concentration among species and phyllode variants of members of the Mulga complex and among landscape positions were tested using one- and two-way ANOVA models in R 2.11.0 (R Development Core Team 2010). When $P \leq 0.05$, post-hoc tests were performed using Fisher's Honest Significant Difference test from the 'multcomp' package (Hothorn *et al.* 2008).

Permutation multivariate analysis of variance (PERMANOVA, Anderson 2001) and canonical analysis of principal co-ordinates (CAP, Anderson & Willis 2003) were used to test the null hypothesis of no differences in the osmotic profile among phyllode variants and species. All PERMANOVA tests used 9999 unrestricted permutations of the raw data. Multivariate analysis was performed using a Euclidean distance similarity matrix that had been calculated from a logarithmic transformation of the original matrix of carbohydrate and cation data.

Correlations among physiological parameters and osmolyte concentrations were tested using linear models in R 2.11.0. Concentration of osmolytes per unit dry weight was used for comparison with RWC, as the standard measurement of concentration in mmol L^{-1} of phyllode water is derived from the measurement of RWC. Only 45 observations were included in linear models using branch water potential data, as 40 trees had Ψ_{pd} <-10 MPa and beyond the range of the pressure chamber (limit of -10 MPa).

Results

Composition and concentrations of osmolytes

The concentration of osmotically active carbohydrates and inorganic cations ranked in order of highest to lowest and pooled across all species and phyllode variants was the following: K > Mg > Pinitol > Ca > Ononitol > S > Sucrose > Fructose > P > Glucose > Mn > Na. Potassium contributed the largest proportion of osmolarity among all variants and species (56.1%, $P > 0.05$; Table 5.1). The relative concentrations of less abundant osmolytes differed among *A. catenulata* and the three phyllode variants of *A. aneura* (Table 5.1, Figure 5.2). *Acacia catenulata* (a broad phyllode species) was distinguished from the three phyllode variants of *A. aneura* by lower concentrations of most carbohydrates and inorganic cations (Table 5.1, Figure 5.2), with the largest difference in osmolarity attributable to concentrations of Ca (1.38 mM *A. catenulata*, 23.1 mM for *A. aneura* pooled).

Acacia catenulata and all three phyllode variants of *A. aneura* had distinct carbohydrate and cation profiles (PERMANOVA $P < 0.05$, Figure 5.2). *Acacia catenulata* had the most distinct osmolyte profile (100% CAP allocation success), followed by broad *A. aneura* (82.1%), terete *A. aneura* (66.7%) and narrow *A. aneura* (63.4%). However, carbohydrate and cation profiles were similar among landscape positions (PERMANOVA $P > 0.05$).

Estimates of total osmolarity were low in all phyllode variants and species. Osmolarity was lowest in *A. catenulata* (360 mM) and highest in narrow (467 mM) and broad *A. aneura* (487 mM, $P < 0.01$, Table 5.1). The low total osmolarity was also reflected by small osmotic potentials estimated with the van‘t Hoff equation (*A. catenuata* 0.88 MPa, terete *A. aneura* 1.03 MPa, narrow *A. aneura* 1.14 MPa and broad *A. aneura* 1.19 MPa).

Table 5.1 Osmolarity of metabolites and inorganic cations in the foliage of *A. catenulata* and three phyllode variants of *A. aneura*.

Osmolyte (mM)	***A. aneura* (terete)**	***A. aneura* (narrow)**	***A. aneura* (broad)**	***A. catenulata***	***F-value***
Ononitol	17.6 (1.86)^{ab}	18.4 (3.25)^{a}	18.8 (1.99)^{a}	8.80 (0.83)^{b}	4.96**
Pinitol	24.7 (2.52)^{ab}	20.5 (3.28)^{ab}	27.7 (2.94)^{a}	13.0 (1.39)^{b}	5.91**
Sucrose	12.5 (1.25)^{a}	9.03 (0.83)^{a}	9.76 (0.89)^{a}	3.52 (0.33)^{b}	19.1***
Glucose	3.96 (0.61)^{a}	3.01 (0.52)^{a}	2.20 (0.19)^{a}	0.95 (0.08)^{b}	11.0***
Fructose	9.85 (0.74)^{a}	6.04 (0.75)^{bc}	6.58 (0.61)^{ac}	2.27 (0.18)^{b}	19.9***
Mg	16.4 (1.11)	25.5 (2.74)	24.8 (1.85)	19.1 (1.67)	3.21*^
P	3.33 (0.47)^{ab}	3.17 (0.34)^{a}	4.79 (0.41)^{b}	2.35 (0.14)^{a}	10.3***
S	9.67 (1.94)	7.16 (0.83)	8.50 (0.60)	8.40 (0.67)	NS
K	137.0 (7.62)	140.0 (12.25)	142.7 (7.90)	130.7 (8.96)	NS
Ca	12.96 (1.15)^{a}	26.4 (2.36)^{b}	30.0 (1.43)^{b}	1.38 (0.16)^{c}	77.0***
Mn	0.74 (0.19)^{a}	1.72 (0.42)^{ab}	0.88 (0.09)^{a}	2.51 (0.26)^{b}	8.03***
Anion Estimate	181 (9.08)^{ab}	205 (16.7)^{ab}	212 (8.19)^{a}	165 (10.2)^{b}	3.51**
Total Osmolarity	423 (21.2)^{ab}	467 (40.1)^{a}	487 (18.9)^{a}	360 (20.0)^{b}	4.84**
n	9	23	28	25	

Osmolarity corrected for foliage relative water content at the time of sampling. Mean values are listed with 1 standard error of the mean in parentheses. Where a one-way ANOVA returned a significant result ($P \leq 0.05$) the *F-value* is listed and *P*-value indicated (* P 0.05 – 0.01, ** P 0.01 – 0.001, *** P < 0.001). Significant groupings determined by Tukey's Honest Significant Difference post-hoc test are denoted by bolded and superscript letters. ^ One-way ANOVA result was significant but no post-hoc significant differences were detected by Tukey's HSD test. Total anion concentration estimated to be equal to the concentration of cations in solution.

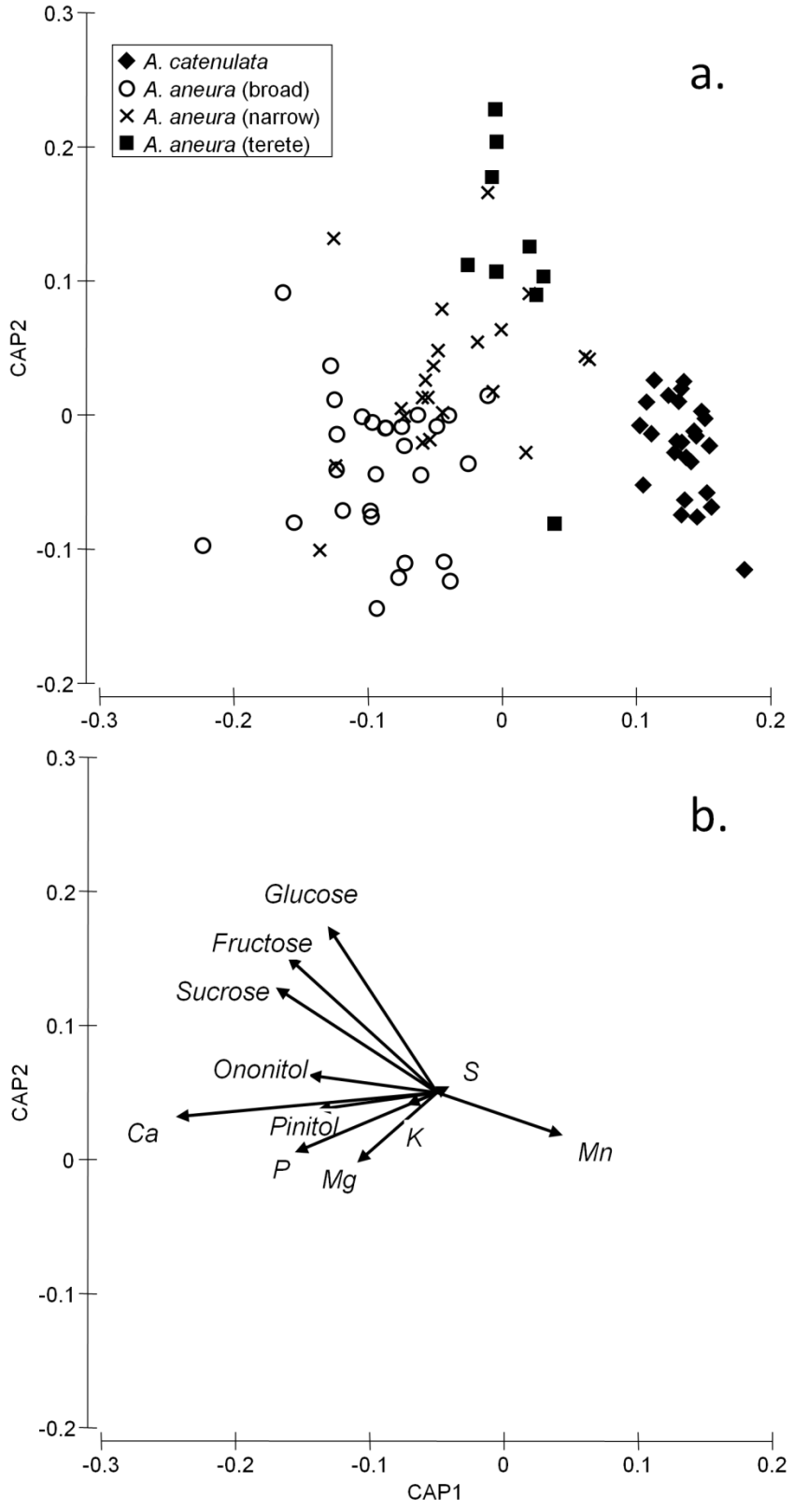

Figure 5.2 Canonical analysis of principal co-ordinates (CAP) of carbohydrate and cation profiles in the foliage of *A. catenulata* and three phyllode variants of *A. aneura*. (a.) *A. catenulata* (♦) was well separated from broad (○), narrow (**X**) and terete (■) *A. aneura*. (b.) Vectors indicate the strength of the correlation between each measured carbohydrate and cation and the CAP axes. *A. catenulata* were distinguished by higher concentrations of manganese (Mn) in foliage and lower concentrations of most other osmolytes, particularly glucose, fructose and sucrose.

Relative water content and water potentials

RWC was the same for all trees (44.1 ± 0.75%, $P > 0.05$). Branch water potential (Ψ) was variable among species and phyllode varieties at both pre-dawn and midday (Table 5.2). Ψ_{pd} was less negative for terete and narrow phyllode variants of *A. aneura* (combined mean -7.67 ± 0.42 MPa) compared to broad *A. aneura* or *A. catenulata* (combined mean -10.8 ± 0.25 MPa, $P < 0.001$, Table 5.2). Ψ_{md} was least negative in terete *A. aneura* on hill-slopes (-7.33 ± 0.44 MPa) and narrow *A. aneura* on the valley floor (-8.73 ± 0.62 MPa; Table 5.2). Ψ_{md} was the same among all other phyllode variants and species across the landscape (Table 5.2), although this result may be confounded by the limitations of the PMS Model 1000 pressure chamber. Many measurements were <-10 MPa and were estimated to be -12 MPa for data analysis, thus mean values <-10 MPa presented in Table 5.2 must be interpreted with caution. $\Delta\Psi$ was the same among all landscape positions and species/phyllode variants (1.14 ± 0.43 MPa, $P > 0.05$). There was no relationship between either Ψ_{pd} or Ψ_{md} and total osmolarity of phyllode water ($P > 0.05$).

Table 5.2 Pre-dawn and midday water potential of *A. catenulata* and three phyllode variants of *A. aneura* in three different landscape positions.

Landscape Position	**Species**	**Ψ_{pd} (MPa)**	**Ψ_{md} (MPa)**	**n**
Drainage Line	*A. aneura* (broad)	-12.0 (0.00)^{bc}	-12.0 (0.00)^{a}	10
Valley Woodland	*A. aneura* (terete)	-9.63 (0.86)^{a}	-11.2 (0.86)^{ab}	4
	A. aneura (narrow)	-7.90 (0.77)^{a}	-8.73 (0.62)^{bc}	12
	A. aneura (broad)	-11.0 (0.50)^{bc}	-11.3 (0.40)^{ab}	17
	A. catenulata	-10.3 (0.46)^{c}	-11.4 (0.30)^{ab}	13
Hill Slope Woodland	*A. aneura* (terete)	-6.21 (0.56)^{a}	-7.33 (0.44)^{c}	5
	A. aneura (narrow)	-7.33 (0.67)^{a}	-12.0 (0.00)^{a}	11
	A. aneura (broad)	-9.4 (0.00)^{bc}	-12.0 (0.00)^{a}	1
	A. catenulata	-9.96 (0.56)^{c}	-10.3 (0.38)^{ab}	12
Species F-Value		18.4***	9.33***	
Landscape F-value		NS	NS	
PT:Landscape F-value		NS	18.6***	

Mean values are listed with 1 standard error of the mean in parentheses. Two-way ANOVA F-values are provided and significance (*** $P < 0.001$) indicated by asterisks. Significant groupings determined by Tukey's Honest Significant Difference post-hoc test are denoted by superscript letters. Values below -10 MPa were beyond the range of The PMS Model 1000 pressure chamber and values were approximated as -12 MPa for data analysis. Therefore, mean values <-10 MPa should be interpreted with caution.

Relative water content was positively correlated with Ψ_{pd} ($P < 0.001$, $R^2 = 0.40$, Figure 5.3). There were fewer trees with Ψ_{md} >-10 MPa, and so the correlation with RWC was weaker ($P = 0.01$, $R^2 = 0.18$, data not shown). RWC was therefore selected for comparison with osmotic data because of the greater number of observations and the strong correlation with Ψ_{pd}. Total concentration of carbohydrates and inorganic cations (mmol g^{-1} phyllode dry weight) were not significantly correlated with RWC ($P > 0.05$, data not shown).

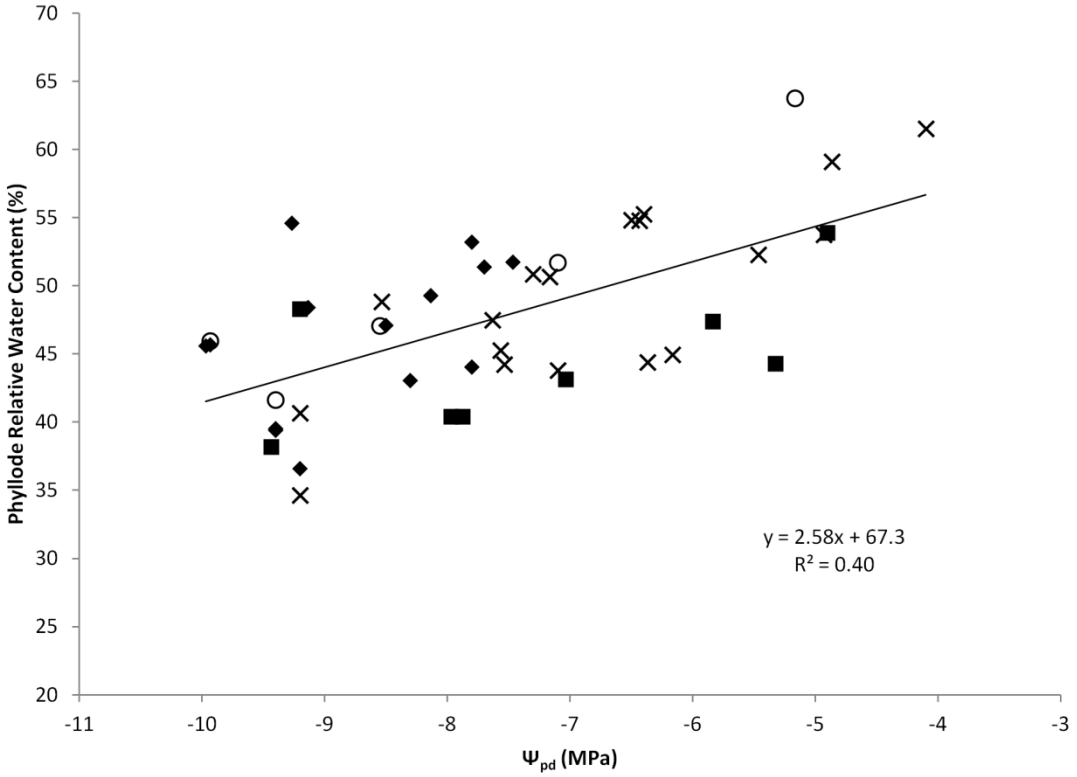

Figure 5.3 Correlation between phyllode relative water content (%) and Ψ_{pd} (MPa). RWC is positively correlated with Ψ_{pd} ($P < 0.001$, $R^2 = 0.40$). A subset of 45 observations are plotted out of a total of 85 samples, as 40 trees had Ψ_{pd} <-10 MPa. One outlier with a RWC of 22.2% was removed. *Acacia catenulata* (♦), broad *Acacia aneura* (○), narrow *A. aneura* (**X**) and terete *A. aneura* (■).

All four parameters estimated by pressure-volume analysis were similar among *A. ayersiana* and two co-occurring phyllode variants of *A. aneura* ($P > 0.05$, Table 5.3). However, the relative water content at the turgor loss point (RWC_0) was variable among the nine branches with a minimum of 92.6% and a maximum of 97.8%. RWC_0 was also strongly and positively correlated with the bulk modulus of elasticity (ε) ($P = 0.002$, Figure 5.4). Neither π_0 or π_{100} were correlated with either ε or RWC_0 ($P > 0.05$).

Table 5.3 Pressure-volume analysis parameters from one population of *A. ayersiana* and two co-occurring phyllode variants of *A. aneura*.

	ε (MPa)	**π_{100} (MPa)**	**π_0 (MPa)**	**RWC_0 (%)**
A. aneura (broad)	11.7 (1.11)	-2.90 (0.04)	-3.93 (0.15)	95.3 (0.28)
A. aneura (terete)	8.23 (1.12)	-2.49 (0.28)	-3.53 (0.29)	94.0 (0.99)
A. ayersiana	14.7 (3.88)	-2.56 (0.15)	-3.30 (0.23)	96.2 (0.89)

All data are means with standard error of the mean in parentheses, n = 3. One-way analysis of variance determined that mean values were among the three *Acacia* spp. for all pressure-volume parameters (P > 0.05).

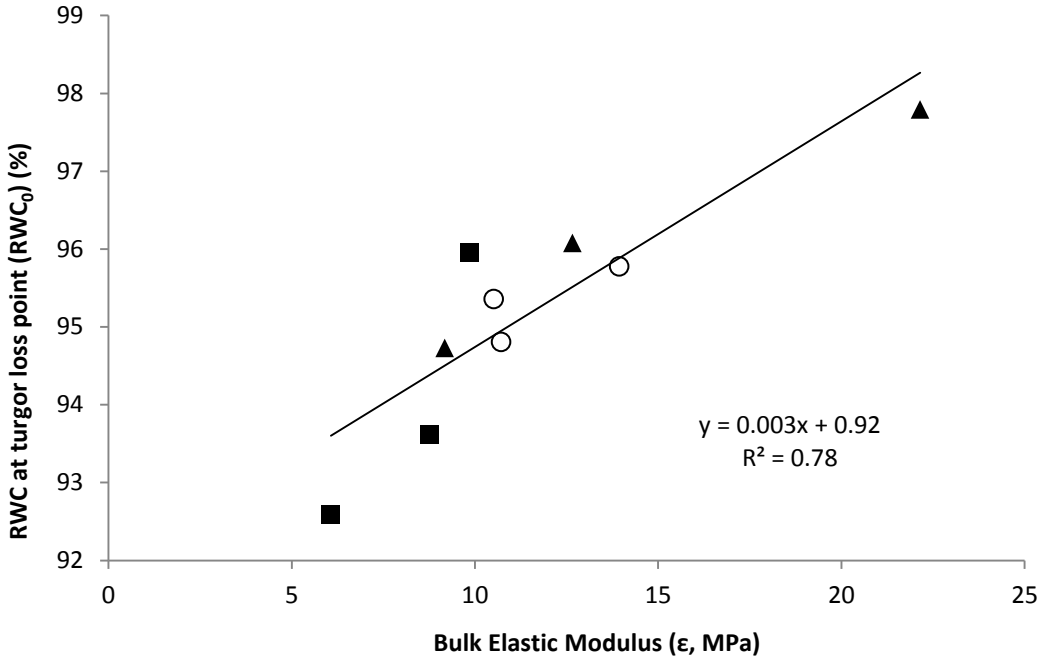

Figure 5.4 Relationship between cell wall flexibility and relative water content at the turgor loss point of *Acacia ayersiana* (▲), broad *Acacia aneura* (○) and terete *A. aneura* (■).

Discussion

The contribution of soluble carbohydrates and inorganic cations to osmotic potential in the Mulga complex at West Angelas

The contribution of soluble carbohydrates and inorganic ions to cellular osmolarity was relatively small (~ -1 MPa) in *A. catenulata* and the three phyllode variants of *A. aneura*. This was a surprising result given the extreme degree of cellular dehydration (44% relative water content) and branch water potential (Ψ_{md} <- 10 MPa in many trees) at the time of sampling. Furthermore, the contribution of soluble carbohydrates and inorganic ions to cellular osmolarity fell well short of the osmotic potential at full turgor determined on a small number of trees using pressure-volume analysis (mean π_{100} = -2.65 MPa, Table 5.3). The degree of water stress during drought recorded in this study is consistent with the seminal publications on arid zone water relations featuring *A. aneura*, where branch water potentials of -11.2 MPa and phyllode relative water contents of ~ 40% were recorded (Slatyer 1961a). The estimates of π_{100} and π_0 generated by pressure-volume analysis (Table 5.3) are also consistent with data collected in related experiments by Slatyer, when osmotic potentials of *A. aneura* foliage were -2.3 MPa at full turgor (π_{100}) and -2.89 MPa at zero turgor (π_0) (Slatyer 1960). Similar values have also been reported in other semi-arid *Acacia* species. For example, the foliage of *Acacia craspedocarpa* F.Muell. had an osmotic potential that ranged from ~ -2 MPa in early winter to ~ -4.66 MPa in late summer (Hellmuth 1969). *Acacia harpophylla* F.Muell. also had maximum and minimum phyllode osmotic potentials of -2.7 MPa and -5.5 MPa over a 2.5 year period (Tunstall & Connor 1975). Therefore, it appears that total cellular osmolality in *A. aneura* was well estimated by these pressure-volume data but my quantitative determination of soluble carbohydrates and inorganic ions may significantly underestimate total cellular osmolarity. However, while the carbohydrates and inorganic ions were quantified during a dry period, these pressure-volume data were collected 6 days following a “rainfall pulse”, and it is unclear to what extent osmotic adjustment may have modified the osmotic potential of the foliage. An increase in photosynthesis following the rainfall pulse may have caused a large increase in primary metabolites (i.e. photoassimilates) with a concomitant decrease in osmotic potential. However, without quantification of the osmolytes present in the trees sampled for pressure-volume analysis, it remains unclear whether osmotic

adjustment could account for the discrepancy between my estimates of osmolarity and the pressure-volume data.

Previous analysis of osmolytes in *Acacia* species have determined that amino acids and quaternary-ammonium compounds may contribute an osmotic potential approaching that of soluble carbohydrates during periods of drought-stress. For example, free amino acids accounted for ~ 20% of the total soluble sugars and amino acids in the foliage of drought hardened *Acacia saligna* (Labill.) H.L. Wendl. (syn. *Acacia cyanophylla* Lindl.) at the end of a prolonged drought treatment when phyllode osmotic potential was -4.5 MPa (Albouchi, Ghrir & El Aouni 1997). Similarly, two amino/imino acids that are structurally similar to proline (pipecolic acid and trans-4-hydroxypipecolic acid) accounted for ~ 15-30% of osmotic adjustment two *Acacia* species exposed to a drought treatment, and concentrations of proline increased 15 to 17 fold (Warren *et al.* 2011). However, while one published study has determined concentrations of proline and glycine-betaine in *A. aneura*, these data were from assays of phloem sap and so it is not possible to determine the contribution these compounds may have made to osmotic potential in foliage (Erskine *et al.* 1996). Similarly, the study of Erskine *et al.* (1996) did not analyse inorganic ions or carbohydrates and so I am unable to make a comparison of the relative contribution of each fraction. Amino acids were not quantified in my analysis, and may explain the shortfall in my estimates of cellular osmolarity. However, as soluble carbohydrates contributed <20% of the estimated osmolarity in my samples and assuming that amino acids contributed roughly the same amount, then the overall estimate of cellular osmolarity would fall well short of the <-3 MPa range that we might expect.

While inorganic ions provide a large osmotic contribution to plant cells, it is assumed they are mostly restricted to the vacuole to reduce interference with cytosolic enzymes (Hare *et al.* 1998). Consequently, it is assumed the bulk of organic solutes occur in the cytoplasm to balance the osmotic potential across the tonoplast membrane. For example, one study of organic solutes and inorganic ions in *Eucalyptus spathulata* Hook. determined inorganic ions contributed ~ 50% of leaf osmolality, concluding that high concentrations of cyclic polyols were a probable means of balancing osmotic gradients (Merchant & Adams 2005). If I apply this assumption to my own data, then the total osmolarity of leaf water may be roughly equal to twice the osmotic contribution of the inorganic ions. In this study I also estimated the total inorganic ion

concentration by doubling the inorganic cation concentration assuming an electrochemical equivalence was present. Therefore, using a mean of all trees sampled, total osmolarity would be roughly 765 mM, and contribute -1.86 MPa to leaf water potential, which is still much less than the osmotic potential in *A. aneura* estimated by pressure-volume analysis (mean π_{100} = -2.65 MPa, Table 5.3). Therefore, I conclude that neither my estimate of inorganic ion or organic solute concentrations are sufficient to account for the osmotic potential expected in the foliage of drought stressed *A. aneura* under natural conditions. While pressure-volume data are consistent with observations of other arid-zone *Acacia* species in the literature, without direct measurement of the osmolality of phyllode water, the precise contribution of osmolytes to water potential remains unclear.

Osmotic profiles among the phyllode variants at West Angelas

Acacia catenulata had the most distinct profile of cations and soluble carbohydrates, with lower concentrations of most of the measured osmotics (Table 5.1, Figure 5.2). In contrast, the osmotic profiles were more similar among the three phyllode variants of *A. aneura* and although they significantly differ from each other in multivariate space, the only measured difference was in the concentration of calcium between terete *A. aneura* and the other two phyllode forms (Table 5.1). The non-reducing cyclic polyols, ononitol and pinotol, followed by the non-reducing sugar, sucrose, were the most abundant soluble carbohydrates in all phyllode variants and species (Table 5.1). The reducing sugars glucose and fructose were the only other carbohydrates in detectable quantities in these foliage samples, but at concentrations three to five-fold lower than the cyclic polyols, and at half to one third the concentration of sucrose (Table 5.1). A high proportion of non-reducing metabolites likely fills two requirements for plants exposed to drought stress. First, they decrease osmotic potential without interfering with cellular redox potential and thus metabolic processes in the cytosol (Hare *et al.* 1998). Second, they may provide a carbon supply for respiration during prolonged drought, or immediately following a pulse rainfall event (Hare *et al.* 1998). Conversely, the low concentrations of glucose and fructose in our trees may be a consequence of low rates of photosynthesis during drought period present for three months prior to sampling, along with the consumption of starch and sucrose in the synthesis and accumulation of pinitol and ononitol once photosynthesis has slowed after the onset of drought (Hare *et al.* 1998). However, without knowing the rates of turnover and transport, these absolute concentrations are less informative.

Are differences in osmotic profiles associated with the severity of water stress?

The total concentration of organic solutes and inorganic ions per unit phyllode dry weight was not correlated with RWC, nor was concentration per unit phyllode water correlated with either Ψ_{pd} or Ψ_{md}. These data indicate a lack of coordination between the degree of drought severity (inferred from RWC, Ψ_{pd} and Ψ_{md}) and the accumulation of osmolytes in the phyllodes of either *A. aneura* or *A. catenulata*. However, as discussed above, these estimates of osmolarity derived from carbohydrate and inorganic ion analysis may fall well short of accurately estimating total cellular osmolality that could account for the osmotic potential expected in these semi-arid *Acacia* species under drought conditions. For this reason, I cannot exclude the possibility that differences may exist in the accumulation of osmolytes over the range of RWC values measured here. Nevertheless, it appears that while osmolytes are integral to the function of members of the Mulga complex during drought, large and significant differences in water potential do not reflect underlying differences in the concentration of stable osmotica. Furthermore, the consistency in pulse-response observed among members of the Mulga complex in Chapter 4 is also reflected by a consistency in the pool size and identity of osmolytes.

Chapter 6: 3D xylem networks and phyllode properties of co-occurring *Acacia*[6]

Introduction

Drought tolerance of plants in semi-arid and arid environments can be attributed to a suite of adaptations, which include modifications to both leaf and branch hydraulic architecture. Reduced leaf size is one of a suite of functionally coordinated traits correlated with increasing aridity (Givnish 1987, Wright *et al.* 2004b, Ordoñez *et al.* 2009). However, as leaf size increases so does the demand for water transported via the xylem pathway (Sperry *et al.* 2002, Brodribb 2009). An increase in mean vessel area may improve water transport efficiency but be at greater risk of cavitation, which may explain why many arid species have narrow xylem vessels (Zimmermann 1983, Hacke, Jacobsen & Pratt 2009). However, while the relationships between leaf and branch traits is well demonstrated among species and across large environmental gradients (McDonald *et al.* 2003, Wright *et al.* 2004b, Schenk *et al.* 2008, Ordoñez *et al.* 2009), it remains unclear how xylem architecture may relate to intraspecific variation in leaf level properties even though significant variability has been noted within species and at localized scales (Sack & Holbrook 2006, Choat, Sack & Holbrook 2007, Beaumont & Burns 2009).

The three-dimensional (3D) arrangement, or degree of overlap among xylem vessels, may be a significant determinant of the drought tolerance of woody species, as the connectivity among conduits will influence the continuity of the water column while under stress (Sperry *et al.* 2002). Pits on the sides and end walls of vessels facilitate the flow of water between vessels but also dictate the air-seeding pressure required to induce cavitation, as smaller pores generally require a greater pressure differential before gas enters a conduit (Zimmermann 1983, Christman, Sperry & Adler 2009). Consequently, the largest pore in a vessel will determine its vulnerability to cavitation. The 'rare pit hypothesis' states that as pit area per vessel increases, so does the probability of the occurrence of a rare larger pore (Choat *et al.* 2005, Hacke *et al.* 2006,

[6]Published as: Page G.F.M., Liu J. & Grierson P.F. (2011) Three-dimensional xylem networks and phyllode properties of co-occurring *Acacia*. *Plant, Cell & Environment*, **34**, 2149-2158.

Christman *et al.* 2009). While total pit area per vessel and vulnerability to cavitation are correlated (Wheeler *et al.* 2005, Hacke *et al.* 2006), pit area must vary independently of vessel surface area, otherwise a shift towards smaller vessels in more drought tolerant species would be confounded by an increase in vessel surface area. A decrease in pit area is thus more likely to be a function of less vessel overlap, rather than of reduced vessel surface area (Wheeler *et al.* 2005). Consequently, accurate and quantitative determination of vessel overlap will significantly improve understanding of the mechanisms of drought tolerance in any woody species.

While the 3D arrangement of xylem networks is a significant factor in the propagation or containment of hydraulic failure, most investigations of hydraulic function have been restricted to analysis of two-dimensional (2D) xylem structure. One reason for this is that physical 'pipe-based' models for understanding xylem function are primarily concerned with cross-sectional vessel attributes. According to the Hagen-Poiseuille equation, the conductivity of an individual vessel scales to the fourth power of its radius. Therefore differences in the number and diameter of vessels strongly regulate the water transport capacity of xylem (Zimmermann 1983, Zanne *et al.* 2010). However, while it is often assumed that the trade-off for having more efficient (larger) vessels is a greater risk of cavitation, the 3D arrangement of xylem is not often considered. Larger vessels may not necessarily be at greater risk of cavitation from air-seeding when isolated from other vessels (Ellmore, Zanne & Orians 2006, Zanne *et al.* 2006). A recent study across 3005 angiosperm species found that the size to number ratio of xylem vessels (S) varied independently of the proportion of branch cross-sectional area comprised of vessel lumen (F) (Zanne *et al.* 2010). Furthermore, mean vessel cross-sectional area was also negatively correlated with vessel density (Zanne *et al.* 2010). Consequently, an increase in mean vessel cross-sectional area will increase hydraulic efficiency, but not necessarily at the expense of safety if the vessel lumen fraction (F) remains constant or decreases. The degree of connectivity within a 3D xylem network may thus have a large influence on both efficiency and safety (Loepfe *et al.* 2007), although safety may not be directly related to lumen area (Zanne *et al.* 2006).

X-ray computed microtomography (micro-CT, or high resolution computed tomography, HRCT) is a rapidly developing method for investigating the 3D structure of xylem vessel networks. Only one published study so far has used micro-CT to quantitatively analyse the connectivity of xylem vessel networks (Brodersen *et al.*

2011), improving upon earlier studies that tested the technology as a visualization tool (Steppe *et al.* 2004). Micro-CT has the advantage of non-destructive and rapid capture and analysis of large volumes of 3D data, that was either impossible to attain through conventional 2D methods, or which was too time consuming to be practical. However, while there have been rapid advances in the ability to capture and analyse 3D xylem network data (e.g. Brodersen *et al.* 2011), there has been no quantitative application of this technology to studies into plant adaptation, including drought tolerance.

Here, I used micro-CT to quantify the 3D xylem connectivity of intact branch segments at 3.4 μm resolution from co-occurring forms of *Acacia aneura* F. Muel. ex Benth and *Acacia ayersiana* Maconochie. *A. aneura* (Mulga) and *A. ayersiana* are the dominant canopy species of mulga woodlands and shrublands that occur across much of semi-arid Australia (Johnson & Burrows 1994). These species exhibit large variation in their tree architecture, and in their phyllode (leaf analogue) shape and size (specific leaf area, SLA: 1.5 – 3 mm^2 mg^{-1}) (Pedley 1973, Randell 1992, Miller *et al.* 2002). Mulga are also renowned for their drought tolerance (Slatyer 1961a, Slatyer 1965, O'Grady *et al.* 2009) and their capacity to persist across a wide variety of habitats in arid and semi-arid Australia (Johnson & Burrows 1994, Miller *et al.* 2002). Previously, I showed that different phyllode shapes are not uniformly distributed across a semi-arid landscape sequence (Chapter 2; Page *et al.* 2011) . Terete phyllodes were dominant in landscape positions that received the least runoff, which we predicted was a consequence of greater drought tolerance and lower rates of water use. In this study I compared phyllode SLA, micro-structural features of xylem connectivity and estimates of hydraulic capacity with pre-dawn and midday branch water potential. I hypothesized that; (1) species with smaller and more terete phyllodes would have more negative seasonal leaf water potentials than broader phyllode types, (2) trees with more negative water potentials would exhibit less connectivity within their vessel networks, (3) measures of connectivity within vessel networks would not be correlated with differences in 2D mean vessel lumen area (A), but (4) connectivity would be sensitive to differences in the vessel lumen fraction (F).

Materials and methods

Sample site and selection of branches

I sampled phyllodes and branches from *Acacia ayersiana* and two phyllode variants of *Acacia aneura* in a low open woodland in a broad valley of the Hamersley Ranges in the Pilbara region of Western Australia (-23.045932S, 118.827095E). The two phyllode variants of *A. aneura* targeted in this study are common in the mulga woodlands of the Pilbara. Both phyllode types are typically less than 10 cm long, but differ in cross section. 'Terete' *A. aneura* has almost cylindrical phyllodes, approximately 1 x 1 mm (SLA ~ 1.5 mm^2 mg^{-1}), whereas 'broad' *A. aneura* are approximately 1 x 3 mm (SLA ~ 2 mm^2 mg^{-1}). *A. ayersiana* typically have much broader phyllodes and are 0.5 x 12 mm in cross section (SLA ~ 3 mm^2 mg^{-1}). I selected nine trees that included three replicates each of *A. aneura* (terete), *A. aneura* (broad) and *A. ayersiana*. All trees were approximately the same height (4 – 5 m) and selected for consistency in growth habit to minimize any morphological differences other than SLA (Figure 4.2). Three sub-plots spread over 100 m were selected so that they contained one of each species and phyllode variant within 25 m of one another. One branch was sampled at 2 m height from all nine trees, and selected to be within a range of 70- 100 cm long, and 5- 8 mm in diameter at the cut end. Phyllodes were collected from each branch for measurement with a leaf area meter (LI-3100, LI-COR inc., Lincoln, NE), and 10 cm from the terminal end of each branch was cut and transported back to the lab for scanning using micro-CT. All samples were collected from the field in May 2008, following two months without any effective rainfall.

Branch water potential

Water potentials were measured on the same day that samples were collected for micro-CT. Measurements were made using a Scholander pressure chamber fitted with a 10 MPa analogue gauge (PMS Instrument Co., Albany, OR). Five branches were cut from equidistant positions around the canopy 2 m above the ground at one hour before sunrise and again at 12 pm (noon). Small terminal branches ~ 10 cm long were then cut from each branch with a single sided razor blade and measured. All measurements were made within five minutes of the branch being cut from the tree.

Data acquisition using X-ray microtomography (micro-CT)

One 10 - 15 mm segment from the terminal end of each branch was scanned at a resolution of between 2.90 and 4.11 μm with a SkyScan 1172 microtomograph (SkyScan, Belgium). Each branch was scanned in 0.30° steps of a 180° rotation with 16 frame averaging. Data were output as transverse slices in a stack of 900 grayscale bitmap images with a resolution of 2000*2000 pixels (Figure 6.1). Three-dimensional data were reconstructed using Avizo 6 software (Vizualisation Sciences Group, Burlington, MA), re-sampled to a resolution of 3.40 μm and thresholded to select the xylem vessels with a minimum and maximum grayscale value of 0 and 10 (Figure 6.1b, c). While the original models output from the micro-tomograph were 900 voxels (a volumetric pixel, or 3D pixel) in length, one branch sample had split while drying for half of its length, and so all models were shortened to 450 voxels. As xylem vessels are not uniformly distributed across a transverse branch section, I expected the porosity and permeability of the branch models to vary in sections between the central axis (heartwood) and the outer layers (vascular cambium and bark). Rectangular sections were required for the model analysis, which made it difficult to ensure different axial segments were evenly represented. Therefore rectangular blocks of equal size (500*500*450 voxels) were extracted from each branch model, which bordered the heartwood and outer layers for one half of the branch (Figure 6.1a). Thresholded 3D images were then labelled in a binary format where voxels inside the threshold limits (vessel lumen) were labelled '1' and everything else labelled '0', and then exported for computational analysis following the methods of Liu *et al.* (2009) and Liu & Regenauer-Lieb (2011).

Connectivity of 3D xylem networks

Voxels labelled as vessel lumen were assigned unique cluster labels when they shared a boundary. In this way, all vessels that were 'touching' were assigned the same cluster label; vessels that were not connected at some point in the 3D vessel network were thus readily distinguished (Figure 6.2; different colours distinguish between clusters). When a cluster was present on opposite sides of the microstructural model it was determined to be 'percolating', or capable of acting as a pathway for water movement through the branch. It was then possible to determine the size and number of percolating clusters of interconnected vessels present in each branch model, as well as the overall 'porosity' of the branch (the ratio of vessel lumen to total model size).

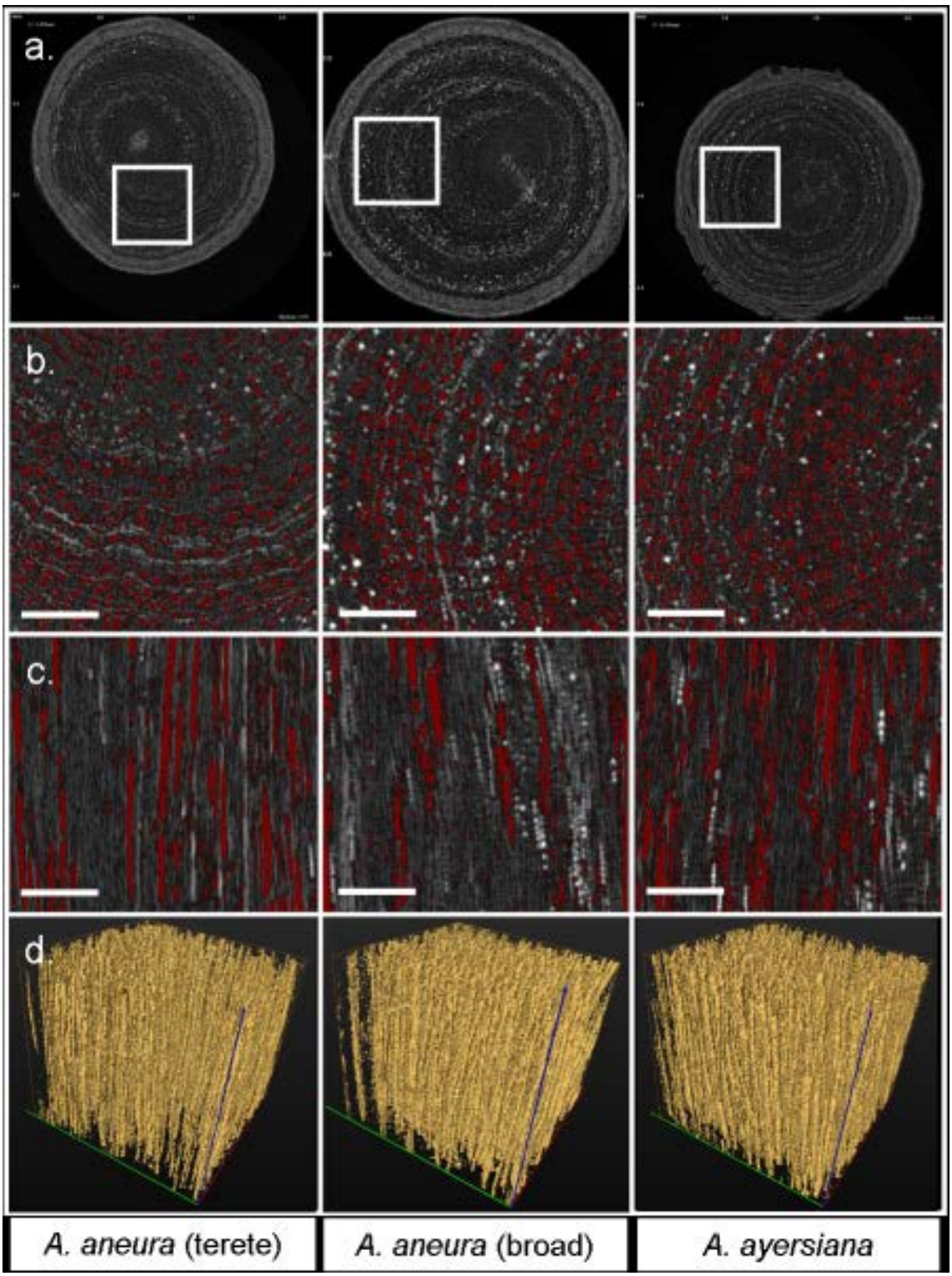

Figure 6.1 Creating 3D models of xylem networks from micro-CT data. (a) Singular transverse slices in grayscale bitmap format from micro-CT output data. 500 * 500 *450 voxel subsamples (1.75 * 1.75 * 1.575 mm) are outlined by white squares on the raw image. (b) Transverse view of subsampled blocks thresholded at 0-10. Voxels thresholded at vessel lumen are coloured red. White scale bars represent 435 μm. (c) Tangential view of subsampled blocks thresholded at 0-10, with elongated vessels clearly visible and selected in red. White scale bars represent 435 μm. (d) Visualisation of 3D vessel network model, which was then exported in binary format for computational analysis. For scale, the cube is 1.575 mm tall, and 1.75 mm along the top edge

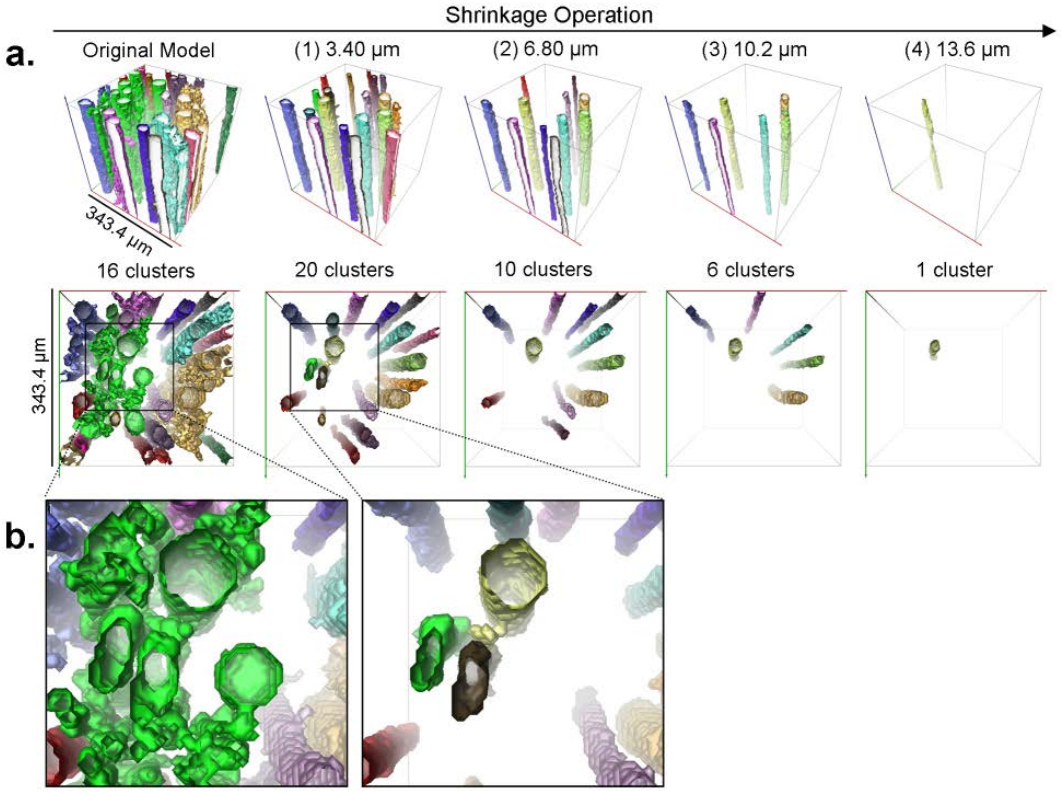

Figure 6.2 Surface models of xylem vessel clusters reconstructed from micro-CT images to demonstrate the quantification of the scale of connectivity among xylem vessels. (a) Oblique and transverse views of xylem vessel clusters over four shrinkage operations in a small sub-volume (4.05×10^7 µm^3) extracted from a branch model. Separate clusters of inter-connected vessels are identified by colour, and vessels not connected to a percolating cluster have been filtered out of the image. Voxel size of the sub-volume is 3.4 µm^3. (b) Magnified transverse sections of the sub-volume before and after the first shrinkage operation. The large green cluster of inter-connected vessels was split into three separate vessels after shrinking all sides of the cluster inwards by 3.40 µm, and non-percolating vessels filtered out of the image

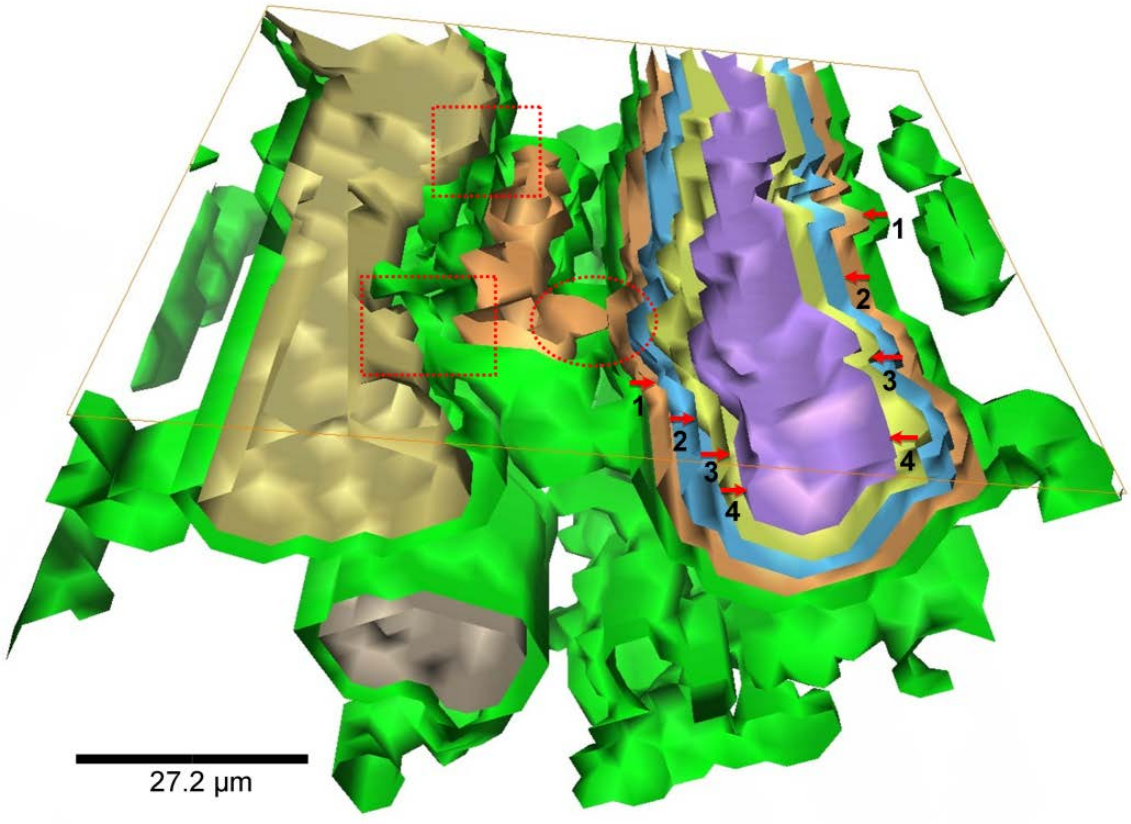

Figure 6.3 Visualising disconnection of vessel clusters by breaking connections among vessels over four shrinkage steps. The original model is green, and progressive shrinkage steps are indicated by arrows numbered according to each step. Two connections broken by the first shrinkage step are identified by red squares, and the resulting distinct vessel clusters are delineated by colour. A third, more robust connection, is only broken by the second shrinkage step (circled). Further shrinkage steps do not break apart any more clusters.

To compare the scale of connectivity, or sectorality among branches, we conducted a 'shrinkage analysis' by moving the boundaries of every cluster progressively inwards in steps of 1 to 5 voxels (3.40-17.0 µm) and then re-analysing for porosity and percolation (Liu & Regenauer-Lieb 2011). In this way, marginal, or very small connections among vessels would be disconnected by small shrinkage operations (i.e., 6.8 µm at the first shrinkage), but that more robust connections would be broken only by larger shrinkages (Figure 6.3). If sections of a cluster were separated by a shrinkage, the cluster would be differentiated in the re-analysis resulting in more clusters of smaller sizes (Figure 6.2). For example, I expected that branches with more isolated vessels, or a higher degree of sectorality, would exhibit a smaller change in the number and size of percolating clusters than branches with more interconnected vessel networks. I calculated a 'connectivity index' by dividing the number of clusters before a shrinkage by the number of clusters after. An index value <1 indicated an increase in the number of

clusters (i.e., greater connectivity), while an index value >1 indicated a decrease (less connectivity). I also calculated the minimum size of the largest cluster in each microstructural model that contained 50% of the voxels labelled as vessel lumen. I expected that this measure would provide another intuitive proxy of connectivity. Greater connectivity within a vessel network would result in less overall clusters, and so fewer but larger clusters comprising 50% of the voxels labelled as vessel lumen, and thus a larger 'minimum size'.

2D analysis of xylem and estimation of theoretical specific leaf conductivity (SLC)

The total number of vessels, and the area of each vessel lumen, were determined using particle size analysis on three 2D transverse slices from each branch taken from the output of the X-ray microtomograph using ImageJ version 1.42q (Abramoff, Megalhaes & Ram 2004). Each image was thresholded with grayscale values of 0-10 to match the 3D model analysis. The number and size of each particle in the resulting binary image was then exported into R version 2.9.2 (R Development Core Team 2010). The radius of each vessel was calculated using equation 6.1, assuming that each particle was the equivalent of a round xylem vessel. The theoretical conductivity (Φ) for each vessel was calculated using the Hagen-Poiseuille equation (equation 6.2), where η is the dynamic viscosity of water (8.90 x 10^{-4} Pa s). The branch theoretical conductivity (K_t) was calculated as the sum of K_t of all xylem vessels and had the units m^4 Pa s. This measure is also sometimes referred to as 'hydraulic capacity'(Reid *et al.* 2005).

$$radius = \sqrt{\frac{area}{\pi}} \qquad \text{(eq. 6.1)}$$

$$\Phi = \frac{\pi r^4}{8\eta} \qquad \text{(eq. 6.2)}$$

Specific leaf conductivity (SLC) was calculated for each branch by dividing K_t by the one sided leaf area. The Huber value (*Hv*) was calculated by dividing the branch cross sectional area by the one sided leaf area. I also calculated the mean vessel area (A), vessel density (N), vessel lumen fraction (F = AN) and the size to number ratio (S = A/N) for comparison with the global metrics of Zanne *et al.*, (2010).

Statistical analysis

I compared the response of 3D xylem network attributes of each *Acacia* species and phyllode variant to shrinking each cluster over five steps using repeated measures analysis. Linear mixed models (LMM) were fitted using the 'lmer' function in the lme4 package (version 0.999375) in R version 2.9.2 (R Development Core Team 2010), with a fixed effect for 'type' (*Acacia* species and phyllode variant), 'shrink step' as a fixed ordered time covariate and a random intercept for each tree. A null model and a full model including an interaction between 'shrink step' and 'type' were compared using both a pair-wise chi-squared likelihood ratio test and a comparison of Akaike's Information Criterion (AIC). When the chi-squared p-value was ≤ 0.05 and AIC values for the models differed by >10 the model with the smallest AIC value was chosen as the best fit, otherwise the most parsimonious model was preferred (Bolker *et al*. 2009). A P-value > 0.05 indicated there were no differences among the two species and phyllode variants of *Acacia*. Comparisons of all 2D branch attributes and vessel metrics were performed using one-way ANOVA, and post-hoc comparisons with Tukey's Honest Significant Difference using the multcomp package (Hothorn *et al.* 2008). Correlations among 2D vessel attributes and the connectivity index were tested using linear models fitted in R version 2.9.2.

Results

Branch water potential

Branch water potential was extremely negative in all three phyllode variants. Terete *A. aneura* was significantly less negative both at pre-dawn and midday than the broad phyllode variant or *A. ayersiana*, a result that is contradictory to my first hypothesis. Broad *A. aneura* (-8.93 MPa) and *A. ayersiana* (-9.72 MPa) also had the most negative pre-dawn water potentials. At mid-day, branch water potential of both broad *A. aneura* and *A. ayersiana* was more negative than could be measured on the Scholander pressure chamber; consequently, for all subsequent data analyses these samples were designated values of -11 MPa, which are consistent with maximum data reported for mulga elsewhere (Slatyer 1961a). In contrast to the broad phyllode variants, branch water potential of terete *A. aneura* decreased from ~ 6.91 MPa at pre-dawn to – 8.13 MPa at midday (Table 6.1; see also Chapters 4 and 5).

Table 6.1 2D branch parameters and leaf attributes of two phyllode variants of *Acacia aneura* and *Acacia ayersiana*.

Parameter	*A. aneura* (terete)	*A. aneura* (broad)	*A. ayersiana*	*p-value*
Pre-dawn Ψ (mPa)	-6.91 **a** (0.51)	-8.93 **b** (0.14)	-9.42 **b** (0.4)	<0.001
Mid-day Ψ (mPa)	-8.13 **a** (0.41)	<-11 **b** (na)	<-11 **b** (na)	<0.001
SLA (mm^2 mg^{-1})	1.45 **a** (0.06)	1.81 **a** (0.21)	2.86 **b** (0.08)	0.06
Hv **(m^2 m^{-2} x10^{-4})**	27.7 **a** (8.36)	12.8 **ab** (1.77)	7.33 **b** (0.36)	<0.001
Mean Vessel Area (A, μm^2)	260 (56.4)	245 (33.5)	210 (21.2)	0.31
Vessel Density (N, mm^{-2})	687 **a** (42.2)	587 **a** (52.0)	822 **b** (57.8)	<0.001
Vessel Lumen Fraction (F = AN)	0.18 (0.04)	0.14 (0.01)	0.17 (0.01)	0.21
Size to Number Ratio (S = A/N)	3.77 e^{-7} **ab** (7.32 e^{-8})	4.35 e^{-7} **a** (8.31 e^{-8})	2.63 e^{-7} **b** (4.54 e^{-8})	0.02
K_t **(m^4 Pa s)**	1.71 e^{-13} (5.91 e^{-14})	1.25 e^{-13} (2.70 e^{-14})	1.06 e^{-13} (1.17 e^{-14})	0.12
SLC (m^2 Pa s)	1.14 e^{-11} **a** (3.35 e^{-12})	3.59 e^{-12} **b** (2.77 e^{-13})	3.04 e^{-12} **b** (3.99 e^{-13})	<0.001

Standard errors are listed in parentheses below mean values, where n = 3 for SLA and Hv, n = 9 for water potential measurements, and n = 9 for all other parameters which were three replicate transverse branch sections from each of three trees of each type. When parameters were significantly different among tree types in a one-way ANOVA ($p \leq 0.05$), Tukey's Honest Significant Difference was computed, and significantly different tree types are denoted with different letters bolded in superscript.

3D analysis of xylem connectivity

I expected that trees with more negative water potentials (i.e. *A. ayersiana*) would exhibit less xylem connectivity. However, all three phyllode variants shared similar xylem connectivity within the vessel network over all five cluster shrinkages (LMM P > 0.05 for all 3D model parameters, full model compared to null model, Table 6.2 and Figure 6.4). Shrinking each side of the cluster by 3.40 μm resulted in an increase in the number of clusters in all branches except for one sample of the broad *A. aneura* that remained the same, and one sample of terete *A. aneura*, which decreased slightly (data not shown). Further shrinkage resulted in a decrease in the number of percolating

clusters in all branches (Figure 6.4). The connectivity index was strongly related to the porosity of the sample, where higher porosity resulted in greater connectivity among clusters. The most porous branches also exhibited the largest increase in cluster number when shrunk by 3.40 μm on each edge (Table 6.2). The minimum size of the largest clusters in each microstructural model that contained 50% of the voxels labeled as vessel lumen decreased in all branches for each progressive shrinkage step (Table 6.2). All branch segments were strongly anisotropic and were only percolating in the z-axis, as would be expected for xylem vessels.

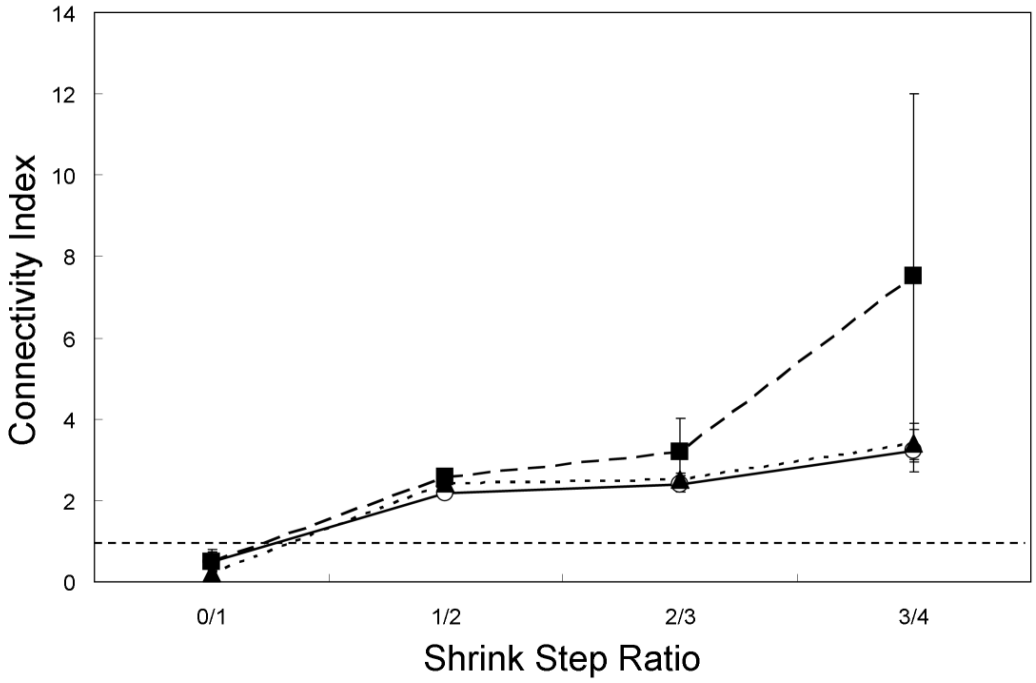

Figure 6.4 The ratio of the number of clusters before to that after a shrinkage step (connectivity index) for *Acacia ayersiana* (▲), broad *Acacia aneura* (○) and terete *A. aneura* (■). The number of clusters increased after the first shrinkage (0/1), and then decreased with further shrinkage. The fifth shrinkage step resulted in zero percolating clusters in all branches, and is not included in this figure. The dashed horizontal line indicates the 1/1 line, below which indicates an increase in clusters following a shrinkage step, and above indicates a decrease. Points are group means with n = 3, and vertical bars represent 1 standard error of the mean.

Table 6.2 3D attributes of xylem networks reconstructed from micro-CT of three closely related *Acacia* species.

		Shrink Step						
		Original	1 (3.40 µm)	2 (6.80 µm)	3 (10.2 µm)	4 (13.6 µm)	5 (17.0 µm)	p-value
Porosity (%)	A. aneura (terete)	17.5 (3.74)	7.52 (1.97)	3.08 (1.02)	1.23 (0.60)	0.43 (0.29)	0.10 (0.08)	
	A. aneura (broad)	15.1 (1.19)	7.06 (1.02)	3.27 (0.60)	1.41 (0.34)	0.49 (0.17)	0.12 (0.05)	0.99
	A. ayersiana	17.7 (1.00)	7.62 (0.51)	3.19 (0.37)	1.30 (0.22)	0.41 (0.10)	0.08 (0.04)	
Number of Active Clusters	A. aneura (terete)	86.0 (71.0)	135 (42.0)	89.7 (43.2)	40.0 (39.5)	2.33 (2.33)	0 (0)	
	A. aneura (broad)	48.3 (8.83)	134 (39.0)	88.3 (33.6)	29.7 (16.8)	3.00 (2.52)	0 (0)	0.99
	A. ayersiana	36.3 (16.4)	164 (18.8)	101 (14.8)	27.7 (10.9)	2.00 (1.00)	0 (0)	
Minimum Size of Clusters Containing 50 % of Voxels[#]	A. aneura (terete)	$8.82\ e^4$ ($7.55\ e^4$)	$3.18\ e^4$ ($2.12\ e^4$)	$9.21\ e^3$ ($5.38\ e^3$)	$5.20\ e^3$ ($4.43\ e^3$)	$1.09\ e^3$ ($9.51\ e^2$)	$1.88\ e^2$ ($1.54\ e^2$)	
	A. aneura (broad)	$2.13\ e^6$ ($1.12\ e^6$)	$1.38\ e^4$ ($3.98\ e^3$)	$7.83\ e^3$ ($2.21\ e^3$)	$3.73\ e^3$ ($1.76\ e^3$)	$1.20\ e^3$ ($6.71\ e^2$)	$2.93\ e^2$ ($1.63\ e^2$)	$0.71^{\$}$
	A. ayersiana	$2.40\ e^6$ ($1.51\ e^6$)	$1.22\ e^4$ ($1.63\ e^3$)	$6.83\ e^3$ ($6.45\ e^2$)	$3.21\ e^3$ ($9.50\ e^2$)	$1.12\ e^3$ ($4.78\ e^2$)	$3.07\ e^2$ ($1.29\ e^2$)	

All values listed are means where n = 3. Standard errors are given inside parentheses. P-values were produced from pair-wise chi-squared likelihood ratio tests between the null LMM and the interaction LMM. [#]A larger number indicates that fewer clusters compose 50% of the voxels in the microstructural model labeled as vessel lumen. [$]Minimum cluster size data was log transformed before LMM analysis.

2D analysis of xylem vessel attributes

Mean vessel area (A) was 238 μm^2 and distributions of vessel diameters in branch wood were similar among all three phyllode variants ($P > 0.05$, Table 6.1). Vessel density (N) of branch wood was highest in *A. ayersiana* (822 mm^2), while the two phyllode variants of *A. aneura* had similar vessel densities of ~ 637 mm^2 (Table 6.1). However, theoretical hydraulic conductivity (K_t,) and the fraction of branch cross sectional area occupied by vessel lumen (F) were similar among the branches of all three phyllode variants (Table 6.1). The size to number ratio (S) is a metric of the relationship commonly observed between mean vessel area (A) and density (N), where larger values are indicative of fewer but larger vessels, and small values represent many vessels with small lumen area (Zanne *et al.* 2010). I found that *A. ayersiana* had the lowest vessel size to number ratio (S) (2.63×10^{-7}), while broad *A. aneura* was significantly higher (4.53×10^{-7}); terete *A. aneura* not significantly different from either (4.35×10^{-7}) (Table 6.1).

Comparison of 2D vessel characteristics with 3D connectivity

The first shrinkage step was compared against 2D vessel characteristics as it was the only step that resulted in an increase in the number of clusters and thus measured connectivity. As expected (hypothesis three), neither mean vessel area (A) nor vessel size to number ratio (S) were correlated with the connectivity index ($P > 0.05$). However, the vessel lumen fraction (F) was negatively correlated with connectivity (Figure 6.5, $P < 0.001$). Thus, as expected (hypothesis four), there was greater connectivity in branches that had a higher proportion of the stem cross-sectional area allocated to vessel lumen.

Linking 2D vessel characteristics and 3D connectivity to physiological attributes

Contrary to hypothesis two, pre-dawn and midday branch water potentials were not correlated with the connectivity index ($P > 0.05$). However, differences in both pre-dawn and midday water potentials between terete and broad phyllode variants of *A aneura* were consistent with differences in specific leaf conductivity (SLC). SLC was more than three-fold greater in terete *A. aneura* (1.14×10^{-11}) than either broad *A. aneura* (3.59×10^{-12}) or *A. ayersiana* (3.04×10^{-12}, Table 6.1), but there were no differences in theoretical hydraulic conductivity (K_t) when not scaled for leaf (phyllode) area. While the Huber value (*Hv*) is also scaled by leaf (phyllode) area, it was consistent

both between species and among phyllode variants (Table 6.1) and thus did not correlate with water potential.

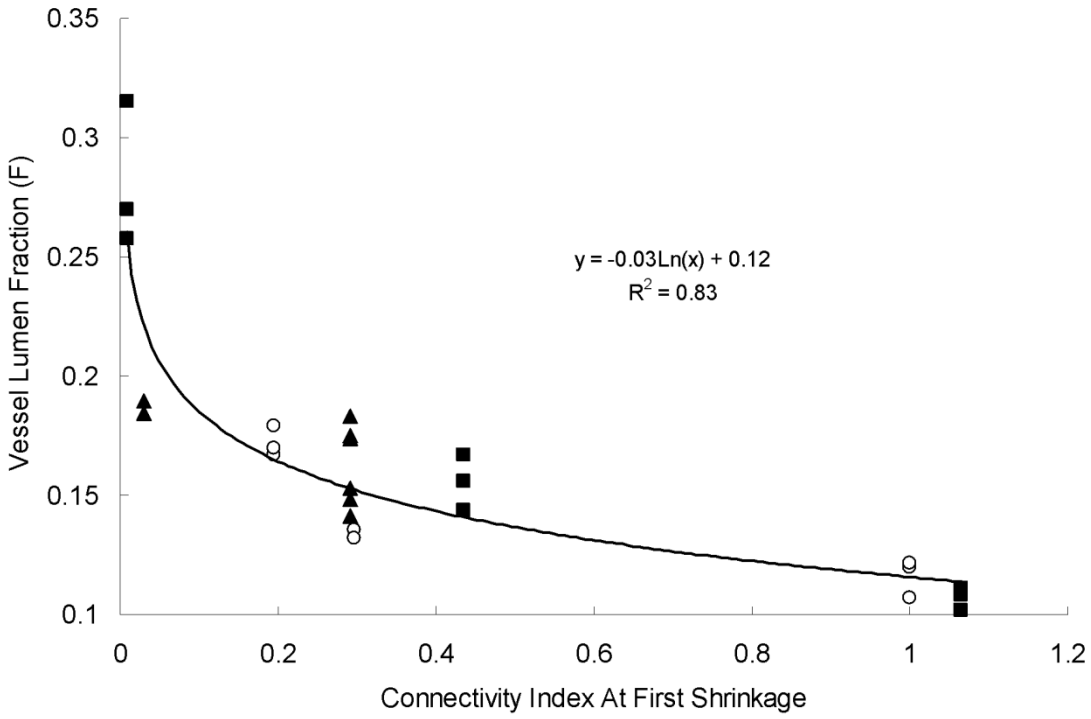

Figure 6.5 Logarithmic correlation between the vessel lumen fraction (F) and the connectivity index at the first shrinkage for all trees. Connectivity was greatest in branches with more branch cross-sectional area composed of vessel lumen. The fitted line is for all trees, but species and phyllode variants are identifiable: *Acacia ayersiana* (▲), broad *Acacia aneura* (○) and terete *A. aneura* (■).

Discussion

These results demonstrate that 3D connectivity is conserved within the xylem networks of two closely related and co-occurring *Acacia* species, regardless of phyllode type (broad or terete) and minimum branch water potential (Table 6.1, Table 6.2, Figure 6.4). Whole-plant co-ordination of drought adaptation has been suggested as an explanation for non-convergence in branch level attributes in arid environments (Meinzer *et al.* 2010). Clearly, this investigation of the role of micrometre-scale xylem connectivity in drought tolerance of terminal branches ~ 5 mm in diameter must be considered in the context of the whole transport pathway and indeed the whole plant since the selection for traits that confer fitness under the prevailing environmental conditions occurs at the organismal scale (Meinzer *et al.* 2010). Also, xylem efficiency and safety may not

necessarily always be optimized in arid environments, particularly when plants are regularly prone to conditions that induce extensive levels of cavitation (Hacke *et al.* 2009). Instead, selection in favour of traits for repair or regrowth of xylem may be more important adaptations for plants in arid and semi-arid environments. While the tolerance of hydraulic systems to stress, or maintaining function under increasing drought stress is likely a key attribute of plant fitness in arid environments, it may be equally as important to have the capacity to re-establish function after prolonged periods of hydraulic dysfunction. These closely related *Acacia* species from semi-arid Australia experience some of the most negative water potentials measured in woody vegetation and can spend large parts of the year with branch water potentials <-10 MPa (Slatyer 1961a). Whole-plant adaptation to extreme desiccation is a necessity under these conditions, as is the ability to capture very limited rainfall that only occurs unpredictably throughout the year (Chapter 4). Therefore, features of the xylem network that promote either prolonged function under extreme drought, or alternatively, rapid re-activation of the water transport pathway would be essential in these species.

While xylem connectivity was conserved at the species and phyllode variant level, our hypothesis of greater sensitivity of xylem connectivity to the vessel lumen fraction (F) was supported by a significant logarithmic correlation across all trees ($P < 0.001$, Figure 6.5). The lack of correlation of xylem connectivity with either mean vessel area (A), or the size to number ratio (S) also supports the idea that these traits may not always be closely related to xylem network connectivity (hypothesis three). My results provide further evidence that vessel lumen fraction (F) and vessel size to number ratio (S) are independent axis for adaptation at the branch level (Zanne *et al.* 2010). My data also indicate that even though only 4.8% of variation in mean vessel area (A) and density (N) at a global scale was accounted for by vessel lumen fraction (F) (Zanne *et al.* 2010), it may be a key trait in determining xylem connectivity and of particular importance at the intra-specific level and in congeneric species.

Smaller leaf size has previously been related to more negative seasonal water potentials and greater drought tolerance (Ackerly 2004, Scoffoni *et al.* 2011). However, I found the opposite; *A. aneura* with the smallest (terete) phyllodes maintained less negative branch water potentials. Terete *A. aneura* also had significantly greater specific leaf conductivity (SLC), a trait that may reflect lower rates of water use, which may reduce strain on the water column. In many species, stomatal control of transpiration limits

xylem tension to below damaging levels under non-extreme conditions (Sperry *et al.* 2002, Meinzer *et al.* 2008), which when combined with lower rates of water use may conserve resources and result in higher minimum seasonal water potentials. Alternatively, my results may be partly explained by the fact that smaller leaf sizes are also correlated with higher temperatures and light exposure owing to a thinner boundary layer that enhances convective cooling (Givnish 1987, Ordoñez *et al.* 2009). Differences in water potential among these *Acacia* species and phyllode variants may thus also reflect differences in site characteristics that are not limited to water availability (Chapter 3).

Theoretical modeling of xylem networks has concluded that higher connectivity increases efficiency but also results in a greater risk of embolisms being spread via the same pathway (Loepfe *et al.* 2007). Similarly, vessel overlap, or pit area in 2D cross sections has also been correlated with cavitation resistance (Wheeler *et al.* 2005, Hacke *et al.* 2006). Consistency among the vessel networks of the three *Acacia* studied here suggests that at the branch level, they may share a similar level of resistance to the propagation of embolisms. Analysis across a large number of species indicates that the area of overlap between adjacent vessel surfaces must be small to achieve maximal cavitation resistance, but yet merely having small pit areas does not confer similar benefits (Hacke *et al.* 2009). The lack of correlation between pit area and cavitation resistance relates to the 'rare pit hypothesis' whereby different species have different frequencies of unusually large pit membrane pores that can be a 'weak link' that reduces air-seeding thresholds (Christman *et al.* 2009). Despite interspecific differences in pit membrane properties which weaken the relationship between pit area and cavitation resistance, both pit area and vessel overlap are often used as a proxy for cavitation risk since in general the chances of encountering a 'leakier' pit increase with pit area (Wheeler *et al.* 2005, Christman *et al.* 2009). The 3D model of xylem connectivity presented here does not account for differences in membrane porosity among vessels or branches, although in such closely related species we would not expect porosity to differ greatly. However, 3D models as presented here could be further improved by incorporating stochastic simulations of the rare-pit hypothesis to further test the influence of connectivity on vulnerability to cavitation and xylem dysfunction (Loepfe *et al.* 2007, Christman *et al.* 2009). Indeed, a recent study combined analysis of 3D xylem networks using micro-CT with visualization of pore size and location with electron microscopy (Brodersen *et al.* 2011). Such elegant approaches will likely

underpin improved understanding of the anatomical adaptations in the xylem networks of species adapted to the most extremely droughted environments.

Chapter 7: General discussion

This thesis provides new understanding of the factors underpinning the biogeographical diversity of mulga woodlands and shrublands in northwest Australia. In particular, this work has identified landscape scale trends in both the composition and functional diversity of mulga woodlands. My results clearly demonstrate that the morphological diversity present within *A. aneura* and the closely related species of the Mulga complex is mirrored by differences in their capacity to both withstand prolonged periods without rain but to also rapidly respond to rainfall events when they occur. To briefly summarise, mulga communities on shaded hillslopes (south facing) tended to be dominated by individuals with terete to sub-terete phyllodes while broader phyllode forms were more common in the valley woodlands (Chapter 2). Subtle differences among mulga types in their capacity to both respond rapidly to episodic increases in rainfall (Chapter 4) and tolerance of extremes in water stress during drought (Chapter 5, 6) in part explain the landscape distribution of both morphotypes and species within the Mulga complex. These inherent but often subtle differences in physiology among Mulga types may also partly explain the co-occurrence of different species and morphotypes at the local scale; micro-site variability in underlying substrates and shading translate to small yet significant differences in the timing and availability of water to individual trees, thus creating multiple "functional niches" even within a site.

While I observed clear trends in the distribution of Mulga morphotypes, the underlying mechanisms or explanations for this variation are still largely unresolved. Patterns in soil nutrients, for example, did not correlate with patterns in morphotypes (Chapter 3). Consequently, there are many further questions, beyond the scope of the current work, regarding the as yet unresolved role that genetic factors may have in the development and functioning of co-occurring species and morphotypes. In this final chapter, I discuss my findings within the context of: (a) explaining the co-occurrence of species and processes potentially driving community assembly, (b) what is currently understood of the molecular phylogenetics and biogeography of the Mulga species complex, (c) anatomical and biochemical adaptations to extremes of water deficit in long-lived woody perennial species, and (d) the management of mulga woodlands with particular attention given to applied research into rehabilitation and restoration of disturbed

landscapes. Throughout, I will present what I consider are the most pressing avenues for future research that build upon the foundation of work presented in this thesis.

Linking form and function – can plant traits help to explain the co-occurrence of Mulga species and morphotypes?

This thesis provides new insight into the contribution of trait differentiation or similarity to species co-occurrence at particular sites or locations. Explaining the co-occurrence of different species is one of the fundamental questions in ecology. In this instance, I ask how might we explain the co-occurrence of many different phyllode shapes and growth forms of Mulga? Broadly speaking, the canopy species of mulga woodlands occupy the same "niche" and are competing for the same resources, principally water. Here, I follow the recent description of a niche as a set of abiotic and biotic conditions where a species can persist (Holt 2009, Wiens *et al.* 2010). Co-occurring Mulga species and phyllode variants thus must share a similar 'fitness' for the environmental conditions at a site indicating that competitive exclusion does not occur among many species of the Mulga complex, even though the similarity in pulse-response strategy indicates they must compete for the same resources (Chapter 4). It is therefore not so surprising that there are strong similarities in most morphological and physiological traits of the co-occurring species studied in this thesis. The "preferred" or dominant life form at West Angelas is a shallow rooted and long lived woody perennial with phyllodes. All species and/or morphotypes within this lifeform are reliant upon rainfall pulses that recharge the surface soil layers. Thus, a similarity in the dominant traits within the Mulga complex may be a good example of 'niche conservatism' (*sensu.* Wiens *et al.* 2010) . Niche conservatism refers to a situation where traits are conserved within species or clades that therefore continue to occupy the same niche, perhaps as a consequence of recent or very slow evolutionary divergence (Wiens *et al.* 2010). Alternatively, the consistency in phenotypes among more distantly related species of the Mulga complex, e.g. between *A. aneura* and *A. catenulata*, may be indicative of trait convergence (Webb *et al.* 2002). Trait convergence occurs when more distantly related species co-occur because of environmental filtering that selects for ecologically important traits (Cavender-Bares *et al.* 2009). In either case, this discussion highlights the potential of phylogenetic analysis to help explain both the co-occurrence of, and differentiation among species and phyllode variants of Mulga, a topic covered in the following section.

While most morphological traits are conserved among members of the Mulga complex, differentiation in the dominant phyllode variant of *A. aneura* between the hillslopes and valley floors at West Angelas (Chapter 2) demonstrates that there is a degree of non-random "environmental sorting" of phyllode variants occurring at the landscape scale. In community assembly theory, species are ‘sorted’ along resource gradients according to ‘environmental filters’ defined as the prevailing biotic and abiotic conditions of a site (Webb *et al.* 2002, Cavender-Bares *et al.* 2009). Species traits must suitably ‘match’ the environment or else are selectively filtered out of a community. For example, site conditions of the mulga woodlands occurring on the south facing slopes may effectively filter out broad phyllode variants of *A. aneura* in favour of terete *A. aneura*. Furthermore, it appears that the distribution or abundance of *A. catenulata* is not "sorted" in the same way (Chapter 2) despite sharing many of the same morphological and physiological traits as *A. aneura* (Chapter 5). While not directly quantified here, the distribution of terete *A. aneura* and co-occurring species and phyllode variants is also likely sorted along micro-site gradients from groves to inter-groves in many of the valley floor woodlands, which often show at least some banding (Chapter 2). For example, gradients in soil chemistry were apparent at the site level where there was clear differentiation between ‘patch’ and ‘inter-patch’ soils (Chapter 3). Likewise, differences in light availability, at a scale of meters, due to shading beneath the strike-ridges (cliffs formed by cross-cut exposed strata of a titled sedimentary landform) on the southern slopes likely influences the species composition of those sites (Chapter 2). Subtle differences in the utilization of resources including light, soil nutrient and pulse rainfall might partition resource availability and contribute to species co-occurrence (Chesson *et al.* 2004), explaining why competitive exclusion may not be a dominant process driving community assembly in the canopy of mulga woodlands at West Angelas.

This thesis also reinforces the importance of considering intra-specific variation in plant traits in vegetation assembly models. One approach to building predictive models of community assembly has used mean trait values of species to evaluate fitness for environmental conditions at particular sites (Shipley, Vile & Garnier 2006). However, it is becoming increasingly clear that incorporating intra-specific variation to trait values improves the predictive ability of community assembly models (Laughlin *et al.* 2012), as variation among individuals contributes to species co-occurrence (Albert *et al.* 2010, Clark 2010). The intra-specific variation in morphology and ecophysiology that is likely

to have influenced the landscape distribution of species at West Angelas is thus another clear example of within-species variability influencing the assembly and ecological functioning of vegetation communities. These data are important in a global context. It is becoming increasingly popular to identify commonalities in function or trade-offs between combinations of particular plant traits by analysing unified global datasets (Reich *et al.* 1997, Wright *et al.* 2004b, Diaz *et al.* 2007, Chave *et al.* 2009, Ordoñez *et al.* 2009, Kattge *et al.* 2011). However, these assessments are only as strong as the datasets that they can compile and thus are frequently skewed towards North America and Europe with relatively little representation from more arid parts of the world and, especially, the Southern Hemisphere. This is not a criticism of studies that use global datasets, but rather highlights exciting opportunities to increase their comprehensiveness and compare results from less well-studied regions including the Pilbara. Plot and stand-level studies add further value to global trait-based analyses as they provide a necessary and fundamental experimental environment for the study of trait-environment relationships.

Molecular phylogenetics and biogeography of arid-zone flora

The ancient origin and stability of the Australian arid zone provides a fascinating landscape in which to test the influence of phylogenetic similarities on trait based community assembly processes. While aridification of central Australia began 15 million years ago, climatic fluctuations in the Pleistocene produced range-shifts that created opportunities for more recent diversification (Byrne *et al.* 2008). Consequently, understanding the origin of diversity within families and clades is not straightforward (Murphy *et al.* 2003, Murphy *et al.* 2010). Coupling phylogenetics with ecological and functional trait data is a powerful way to investigate community assembly and determine the evolution of plant function (Araya *et al.* 2012, Savage & Cavender-Bares 2012). At the commencement of this research, I had hoped to include a phylogenetic analysis of the Mulga complex at West Angelas; however, owing to a number of logistic and financial constraints this aspect regrettably has not come to fruition. While development of a molecular phylogeny for Mulga is still on-going (see http://www.worldwidewattle.com/infogallery/projects/overview.php), early results suggest that divisions within Mulga closely match the ecophysiological grouping identified in this thesis (J.T. Miller, pers. comm.). For example, I found significant functional differences among co-occurring intra-specific phyllode shape variants of *A.*

aneura. Trees with terete phyllodes had less negative minimum water potentials and a more conservative strategy of water-use when compared to the broad phyllode variant (Chapter 4). However, there were no differences in either minimum water potential or water use between *A. aneura* with broad phyllodes and co-occurring *A. ayersiana*, which also has broad phyllodes (Chapter 4). Given that water is the strongest limiting resource in the semi-arid environment of the Pilbara, an obvious conclusion is that water availability (and it's many interactions with the biotic and abiotic environment including biogeochemical cycles) drives the diversity of phyllode shapes in the Mulga complex. While this hypothesis seems a plausible explanation for the differentiation of phyllode shapes within *A. aneura* (e.g., terete vs. broad), it is less applicable to differentiation among species (e.g. *A. catenulata*, *A. ayersiana* and *A. aneura*). Thus, developing a phylogeny for the co-occurring species of Mulga that identifies when and under what conditions the different lineages arose, will further improve our understanding of the reasons underlying the co-occurrence of different morphotypes and species of Mulga.

Anatomical and biochemical adaptations to extremes of water deficit in long-lived woody perennial species

My research has identified significant differences in minimum (i.e. most negative measured) water potential among co-occurring phyllode variants of *A. aneura* and other species of the Mulga complex (Chapter 4). These "threshold" values did not co-vary with other anatomical (Chapter 6) and biochemical (Chapter 5) traits. For example, I originally hypothesised that the hydraulic connectivity within the branch xylem network, and/or accumulation of stable osmotica are correlated with minimum branch water potential. However, this was not supported by my results. Therefore, the question remains: what are the functional implications, if any, of large and significant differences in minimum water potential among co-occurring species and phyllode variants of Mulga?

The lowest measurements of foliage relative water content for each species and phyllode variant of Mulga were similar (~ 40%), even among different experiments in different years (Chapter 4 & 5). These data indicate that irrespective of minimum water potential, all trees have a similar threshold of cellular dehydration. Similarly, relative water content at the turgor loss point was also consistent among the small subset of two

phyllode variants of *A. aneura* and co-occurring *A. ayersiana* (92.5%, Chapter 5). Following irrigation, all trees rehydrated to ~ 97.6% each night, before falling to ~ 90% each day at midday (Chapter 4). Therefore, I can make three interesting observations regarding phyllode water relations in Mulga: (1) the difference between relative water content during a drought period (~ 40%) and the turgor loss point (92%) is very large, therefore (2) foliage will be well below the turgor loss point for the majority of the year, and (3) when conditions are favourable, foliage must also lose and then restore turgor every day. Thus, Mulga can be classed as anisohydric, as it does not tightly regulate water potential with stomatal control of water loss, but rather allows water potential to rise and fall according to atmospheric demand and soil water availability (McDowell *et al.* 2008).

Anisohydric species are generally considered to be more drought tolerant than isohydric species, owing to their capacity to maintain photosynthesis over a larger range of water potentials (McDowell *et al.* 2008). Likewise, species that can photosynthesise over a larger range of water potentials also generally maintain greater hydraulic conductivity with decreasing water potential, i.e. are more resistant to cavitation (Maherali *et al.* 2006). A loss in either leaf, stem or root conductivity is also coordinated with stomatal closure (Brodribb & Holbrook 2003). Thus, it is likely that Mulga routinely suffers cavitation at one or multiple points along the plant hydraulic pathway that regulates daily dynamics of water loss, as well as long-term quantities of water loss during progressive dehydration during a drought period.

Consistency of 3D xylem network architecture identified in Chapter 6 indicates that co-occurring species and phyllode variants in the Mulga complex may share similar thresholds to cavitation with declining water potential, or alternatively that 3D xylem sectoriality or segmentation does not influence cavitation potential in these species. However, it remains unclear to what extent resistance to cavitation is coordinated with photosynthesis, or with absolute limits of water loss in these species. For example, is the response of photosynthesis (A) to phyllode water potential and hydraulic conductivity variable among Mulga species and phyllode variants of *A. aneura*? Similarly, are the large differences in water potential among co-occurring species and phyllode variants correlated with differences in cavitation resistance, i.e., do trees with less negative minimum water potentials also maintain higher rates of conductivity as the soil dries out following a rainfall pulse? Consequently, further work is needed to develop an explicit

understanding of the linkages between the traits that I quantified in this thesis (i.e., specific leaf area, xylem network connectivity, minimum branch water potential and pulse-response capacity) and the fundamental hydraulic and physiological processes of hydraulic conductivity, photosynthesis and respiration in order to develop a clear functional basis for the co-occurrence of species and phyllode variants along resource gradients. Replicating my pulse-response experiment (Chapter 4) would provide an ideal experimental framework in which to study photosynthesis and respiration and would also provide further details of the underlying mechanisms behind the ^{13}C dilution that was observed.

Characterisation of hydraulic limits of water transport and physiological limits of gas exchange are also relevant to the current interest in tree mortality (McDowell *et al.* 2008, Allen *et al.* 2010, McDowell 2011, McDowell *et al.* 2011, Williams *et al.* 2013). As discussed above, anisohydric species like Mulga are hypothesized to be more prone to mortality induced by hydraulic failure, where a loss of conductivity eventually results in carbon starvation following a particularly severe or prolonged drought (McDowell *et al.* 2008). However, drought-induced mortality is not well documented in Mulga and is likely rare (but see Condon 1949, Beard 1968, Fensham, Powell & Horne 2011, Fensham *et al.* 2012a). This observation contrasts with the eucalypt-dominated woodlands of semi-arid Australia, including in the northern savannas (Fensham & Fairfax 2007). This lesser susceptibility to drought-induced death of mulga woodlands may be partially attributable to adaptation to rainfall distribution patterns. In the northern eucalypt woodlands there is a strongly seasonal element to rainfall (Mott 1978, Fensham & Fairfax 2007). In contrast, mulga woodlands tend to be confined to regions that often have less rainfall but also without a regular seasonal drought (Nix & Austin 1973, Beard 1975). Thus these trees are capable of enduring prolonged droughts, the effects of which are exacerbated by the extreme soil matric potentials (i.e. <<-10 MPa) generated by the very fine textured soils as they dry out (refer to description in Chapter 4). A capacity to tolerate large hydraulic failure presumably is thus an important adaptation that allows Mulga to persist through these extended dry periods, as is a capacity to refill vessels while subject to very large negative tensions as a mechanism to restore conductivity. However, it remains unclear how long Mulga can survive without rainfall before carbon starvation may become evident, or indeed what other thresholds may induce widespread death of trees. Thus, further experiments that expand upon my quantification of carbohydrate pools in foliage over seasonal and inter-annual time

scales will help determine to what extent Mulga rely on stored carbohydrates and whether drought-induced carbohydrate starvation contributes to tree mortality in these species.

Management of mulga woodlands: applied research into rehabilitation and restoration of disturbed landscapes

How can we use plant traits and ecological theory to manage semi-arid woodlands?

There is increasing concern over the vulnerability of mulga communities to anthropogenic impacts, including from overgrazing (Fensham, Silcock & Dwyer 2011, Witt *et al.* 2011, Fensham, Fairfax & Dwyer 2012a), clearing (Fensham *et al.* 2012b), and alterations to surface hydrology (Hick, Caccetta & Corner 1997, Associates 2004, Aquaterra Consulting 2005, Muller 2005, Fortescue Metals Group Limited 2011b). This is not a trivial management question when you consider the extent of the semi-arid woodlands and shrublands in Australia (~ 1,500,000 km^2) (Johnson & Burrows 1994). In particular, the interruption of surface water flow has been hypothesized to have a detrimental impact on the health of mulga communities adjacent to linear infrastructure and other mining related earthmoving (Hick *et al.* 1997, EPA 2005). The estimated cost of constructing approximately 250 km of rail line in 2012 was US$2.09 billion (Fortescue Metals Group Limited 2011a). The additional construction cost of installing culverts specifically to manage surface hydrology in ecologically sensitive areas underpins the importance of understanding the hydrology and physiology of mulga communities. However, to predict or evaluate the impact of interruptions to water supply, it is vital to understand the environmental water requirements of the vegetation communities considered to be at risk. It is now apparent that not all mulga communities have similar canopy species and morphological variants (Chapter 2), and that these morphological differences coincide with differences in physiological attributes including minimum seasonal water potential and rates of water use (Chapters 4, 5). Therefore, understanding the relationships between morphological and functional traits of the canopy species of mulga communities might allow a “trait based” method of evaluating the vulnerability of particular woodlands to changes in the environmental conditions.

The vulnerability of mulga woodlands to interruptions to surface water flow remains largely untested and was not an objective of this thesis. However, this is certainly an

area of application of these findings. The results of Chapter 4 indicate that the contribution of a large but not infrequent rainfall event (~ 80 mm) without the contribution of surface flow from adjacent open ground is sufficient to produce a large and prolonged physiological response in mature Mulga trees. With the caveat that I cannot speculate on the impact of smaller, more frequent rainfall events (although I noted that trees responded to an earlier smaller event; Chapter 4), I would propose that surface flow may not be the most significant ecosystem process for the survival of adult Mulga trees in the Hamersley Range, largely because of the topographic complexity of the landscape. Instead, maintenance of the patch-mosaic structure that is common in semi-arid vegetation communities may be more important for the stability of Mulga woodlands. For example, retaining the grass layer beneath patches of Mulga in Queensland extended the period of water availability for Mulga following a rainfall pulse, and increased the recruitment and survival of Mulga seedlings (Anderson & Hodgkinson 1997). Retaining ground cover beneath Mulga prevents throughflow, which in effect causes the patch/interpatch or grove/intergrove woodlands to be 'closed' systems (Mabbutt & Fanning 1987, Tongway & Ludwig 1990, Dunkerley 2011). Particularly in the case of grove/intergrove mulga communities, it is likely that surface water flows only travel a distance equal to the maximum length of the intergrove width. Interruptions to surface flow that are further upslope than the boundaries of surrounding vegetation may only have a small influence on the water supply to these mulga woodlands. However, other disturbances to the patch/inter-patch structure of mulga woodlands that reduce the potential for groves to trap surface water flows (i.e., frequent fires, grazing and weed invasion) and limit the opportunity for seedling germination and recruitment potentially pose a larger risk than interruptions to surface water flow.

Restoration and rehabilitation of disturbed Mulga landscapes

One of the potential outcomes identified at the beginning of this research project was the capacity to identify particular species or "ecotypes" of Mulga for use in targeted post-mining rehabilitation projects. As discussed at the end of Chapter 3, I found most species and phyllode variants of Mulga at West Angelas appear capable of inhabiting all of the landscape positions suitable for mulga communities more generally (Chapter 2), a conclusion strengthened by the consistency of soil chemical and physical properties across the landscape sequence (Chapter 3). Thus, the soil properties quantified in this thesis provide a target envelope of conditions to be aimed for when preparing a site for the re-establishment of Mulga at West Angelas, rather than a checklist against which to

compare different substrates to match with particular species or phyllode variants. These findings also demonstrate that the soil chemistry of mulga patches, in this catchment at least, did not vary widely. Nevertheless, elsewhere, particular Mulga variants have been associated with large shifts in soil properties, including a hypothesis that a particularly distinctive morphotype called the “Christmas tree” Mulga, are restricted to calcrete platforms (Beard 1990). Post-mining conditions will encompass a large range of soil conditions, including rockiness, acidity and perhaps salinity, but it is unclear whether the local Mulga would tolerate these conditions. While soil chemistry and particle size distribution may not control the composition of the canopy of Mulga woodlands at the site scale, the other, as yet un-quantified environmental parameters that influence woodland composition will also influence the success of rehabilitation and restoration projects. These parameters are likely to include site shading, soil surface characteristics, soil depth and water storage capacity, several of which, in combination with rainfall and temperature, have been correlated with the occurrence of drought related mortality in Mulga (Fensham *et al.* 2012a).

The practical success of using the species and phyllode variants identified in this thesis in rehabilitation and restoration remains untested. An experimental test of the capacity for different species and phyllode variants of Mulga to be used in landscape restoration and rehabilitation is nevertheless critical for the development of rehabilitation plans that incorporate, or actively use the diversity within the Mulga complex. For example, how variable is the success rate of germination and establishment of particular species and phyllode variants of Mulga across a range of substrates? What is the survival rate of juvenile Mulga and for how long do they persist? While the findings presented in this thesis can provide guidance for the collection of suitable seed for restoration of particular landscapes, e.g., collecting seed from southern hillslope woodlands with a higher proportion of trees with terete phyllodes when planning to rehabilitate a south facing slope, much work remains in selecting types/provenances to optimise rehabilitation efforts.

Concluding statements

Overall, this thesis makes a significant and novel contribution to the understanding of intra- and inter-specific variation in ecophysiology of semi-arid plant species. One of the more novel aspects of this work has been the opportunity to combine new and

innovative techniques, such as 3D imaging, with more traditional methods in field ecology. Cross-disciplinary collaboration, in my case with geophysicists (Chapter 6), can lead to exciting and new understanding of the functioning of plants. Other current innovations in 3D imaging methods using synchrotron light-sources involve real-time 3D imaging that allows direct observation of the dynamics of water transport, i.e., cavitation and embolism repair (Brodersen *et al.* 2010, Kim & Lee 2010). There is much more that can be learned about the function of plants under severe and regular water stress by combining these techniques with measurement of the nature, size and flux of carbohydrate pools in plant organs (Chapter 5). Recent advances in the precision of compound specific isotope ratio mass spectrometry is now providing extremely detailed analysis of the source and fate of water and carbon in plant organs during periods of photosynthesis and respiration (Wild *et al.* 2010). Likewise, recent technological innovations in portable and robust cavity ring-down laser spectroscopy have made it possible to measure real-time dynamics of stable isotopes of oxygen, hydrogen and carbon during gas exchange at the leaf to whole plant scale in the field (Berryman *et al.* 2011). These new methods have great potential to further improve our understanding of the importance of intra- and inter-specific differences in morphology and function in arid and semi-arid vegetation communities.

Rapid and ongoing improvements in DNA sequencing technologies and phylogenetic analysis will help clarify the relationships between form and function that were developed as part of my research. In particular, DNA barcoding techniques (Cowan *et al.* 2006, Hajibabaei *et al.* 2007), hold great promise to rapidly resolve complex hierarchical patterns of genetic diversity in groups of species, in this case the Mulga species complex. DNA barcoding has the potential to greatly improve both speed and accuracy of environmental surveys and identification of species and varieties that are often difficult to delineate using morphological characters in isolation. The infrequent and brief reproductive cycle of Mulga species makes the development of a method to identify sterile material extremely important. Future work that integrates knowledge of genetic variation within and among populations at the landscape or even continental scales with functional attributes will continue to develop our understanding of the limits of plant survival, especially of Mulga and associated species growing in some of the most drought prone environments of inland Australia.

References

Abramoff M.D., Megalhaes P.J. & Ram S.J. (2004) Image processing with ImageJ. *Biophotonics International*, **11**, 36-42.

Ackerly D. (2004) Functional strategies of Chaparral shrubs in relation to seasonal water deficit and disturbance. *Ecological Monographs*, **74**, 25-44.

Ackerly D., Knight C., Weiss S., Barton K. & Starmer K. (2002) Leaf size, specific leaf area and microhabitat distribution of chaparral woody plants: contrasting patterns in species level and community level analyses. *Oecologia*, **130**, 449-457.

Albert C.H., Thuiller W., Yoccoz N.G., Soudant A., Boucher F., Saccone P. & Lavorel S. (2010) Intraspecific functional variability: extent, structure and sources of variation. *Journal of Ecology*, **98**, 604-613.

Albouchi A., Ghrir R. & El Aouni M. (1997) Endurcissement à la sécheresse et accumulation de glucides solubles et d'acides aminés libres dans les phyllodes d'Acacia cyanophylla Lindl. *Annals of Forest Science*, **54**, 155-168.

Allen C.D., Macalady A.K., Chenchouni H., Bachelet D., McDowell N., Vennetier M., Kitzberger T., Rigling A., Breshears D.D., Hogg E.H., Gonzalez P., Fensham R., Zhang Z., Castro J., Demidova N., Lim J.-H., Allard G., Running S.W., Semerci A. & Cobb N. (2010) A global overview of drought and heat-induced tree mortality reveals emerging climate change risks for forests. *Forest Ecology and Management*, **259**, 660-684.

Andersen H.D., Wang C.H., Arleth L., Peters G.H. & Westh P. (2011) Reconciliation of opposing views on membrane-sugar interactions. *Proceedings of the National Academy of Sciences of the United States of America*, **108**, 1874-1878.

Anderson M.J. (2001) A new method for non-parametric multivariate analysis of variance. *Austral Ecology*, **26**, 32-46.

Anderson M.J., Gorley R.N. & Clarke K.R. (2008) *PERMANOVA+ for PRIMER: Guide to Software and Statistical Methods*. PRIMER-E, Plymouth, UK.

Anderson M.J. & Willis T.J. (2003) Canonical analysis of principal coordinates: a useful method of contrained ordination for ecology. *Ecology*, **84**, 511-525.

Anderson V.J. & Hodgkinson K.C. (1997) Grass-mediated Capture of Resource Flows and the Maintenance of Banded Mulga in a Semi-arid Woodland. *Australian Journal of Botany*, **45**, 331-342.

Andrew R.L., Miller J.T., Peakall R., Crisp M.D. & Bayer R.J. (2003) Genetic, cytogenetic and morphological patterns in a mixed mulga population: evidence for apomixis. *Australian Systematic Botany*, **16**, 69-80.

Aquaterra Consulting (2005) *Fortescue Metals Group Pty Ltd Pilbara Iron Ore and Infrastructure Project Stage B: Mines and East-West Railway Surface Hydrology*. Aquaterra Consulting Pty. Ltd.

Araya Y.N., Silvertown J., Gowing D.J., McConway K.J., Linder H.P. & Midgley G. (2012) Do niche-structured plant communities exhibit phylogenetic conservatism? A test case in an endemic clade. *Journal of Ecology*, **100**, 1434-1439.

Arndt N.T., Nelson D.R., Compston W., Trendall A.F. & Thorne A.M. (1991) The age of the Fortescue Group, Hamersley Basin, Western Australia, from ion microprobe zircon U-Pb results. *Australian Journal of Earth Sciences*, **38**, 261-281.

Arndt S.K., Livesley S.J., Merchant A., Bleby T. & Grierson P.F. (2008) Quercitol and osmotic adaptation of field-grown *Eucalyptus* under seasonal drought stress. *Plant, Cell & Environment*, **31**, 915-924.

Aronson J., Floret C., Le Floc'h E., Ovalle C. & Pontanier R. (1993) Restoration and Rehabilitation of Degraded Ecosystems in Arid and Semi-Arid Lands. I. A View from the South. *Restoration Ecology*, **1**, 8-17.

Associates T. (2004) *Pilbara Iron Ore and Infrastructure Project Stage B - Evaulation of Alternative Rail Routes. Report Prepared for Fortescue Metals Group Limited.* http://reports.fmgl.com.au/ENVIRO/Stage%20B%20PER/App%20E%20Analysis%20of%20Altern%20Rail.pdf.

Baayen R.H., Davidson D.J. & Bates D.M. (2008) Mixed-effects modeling with crossed random effects for subjects and items. *Journal of Memory and Language*, **59**, 390-412.

Barron-Gafford G.A., Scott R.L., Jenerette G.D., Hamerlynck E.P. & Huxman T.E. (2012) Temperature and precipitation controls over leaf- and ecosystem-level CO2 flux along a woody plant encroachment gradient. *Global Change Biology*, **18**, 1389-1400.

Bartlett M.K., Scoffoni C. & Sack L. (2012) The determinants of leaf turgor loss point and prediction of drought tolerance of species and biomes: a global meta-analysis. *Ecology Letters*, **15**, 393-405.

Beard J.S. (1968) Drought effects in the Gibson Desert. *Journal of the Royal Society of Western Australia*, **51**, 39-50.

Beard J.S. (1975) *Pilbara. Explanatory Notes to Sheet 5, 1:1000000 Vegetation Series*. University of Western Australia Press, Nedlands.

Beard J.S. (1990) *Plant Life of Western Australia*. Kangaroo Press, Kenthurst, NSW.

Beaumont S. & Burns K. (2009) Vertical gradients in leaf trait diversity in a New Zealand forest. *Trees - Structure and Function*, **23**, 339-346.

Behrens T., Zhu A.X., Schmidt K. & Scholten T. (2010) Multi-scale digital terrain analysis and feature selection for digital soil mapping. *Geoderma*, **155**, 175-185.

Bennett L.T. & Adams M.A. (1999) Indices for characterising spatial variability of soil nitrogen semi-arid grasslands of northwestern Australia. *Soil Biology and Biochemistry*, **31**, 735-746.

Bentham G. (1855) Plantae Muellerianae. Mimoseae. *Linnaea*, **26**, 603-630.

Bentham G. (1864) Flora Australiensis: A Description of the Plants of the Australian Territory. In: *Leguminosae to Combretaceae*, pp. 402. Lovell Reeve & Co, London.

Bentley D., Grierson P.F., Bennett L.T. & Adams M.A. (1999) Evaluation of anion exchange membranes to estimate bioavailable phosphorus in native grasslands of semi-arid Northwestern Australia. *Communications in Soil Science and Plant Analysis*, **30**, 2231 - 2244.

Berg S.S. & Dunkerley D.L. (2004) Patterned Mulga near Alice Springs, central Australia, and the potential threat of firewood collection on this vegetation community. *Journal of Arid Environments*, **59**, 313-350.

Berryman E.M., Marshall J.D., Rahn T., Cook S.P. & Litvak M. (2011) Adaptation of continuous-flow cavity ring-down spectroscopy for batch analysis of δ13C of CO2 and comparison with isotope ratio mass spectrometry. *Rapid Communications in Mass Spectrometry*, **25**, 2355-2360.

Beven K.J. & Kirkby M.J. (1979) A physically based, variable contributing area model of basin hydrology. *Hydrological Sciences Bulletin*, **24**, 43-69.

Bezdek C.J. (1981) *Pattern Recognition with Fuzzy Objective Function Algorithms*. Plenum Press, New York.

Blake G.R. & Hartge K.H. (1986) Bulk Density. In: *Methods of Soil Analysis Part 1* (ed A. Klute), pp. 363-376. Soil Science Society of America, Madison, Wisconsin USA.

Boer M., del Barrio G. & Puigdefabregas J. (1996) Mapping soil depth classes in dry Mediterranean areas using terrain attributes derived from a digital elevation model. *Geoderma*, **72**, 99-118.

Bolker M.B., Brooks M.E., Clark C.J., Geange S.W., Poulson J.R., Stevens M.H.H. & White J.S.S. (2009) Generalized linear mixed models: a practical guide for ecology and evolution. *Trends in Ecology & Evolution*, **24**, 127-135.

Boughton V.H. (1986) Phyllode structure, taxonomy and distribution in some Australian acacias. *Australian Journal of Botany*, **34**, 663-674.

Bowman R.A. & Cole C.V. (1978) An exploratory method for fractionation of organic phosphorus from grassland soils. *Soil Science Society of America Journal*, **125**, 95-101.

Brodersen C.R., Lee E.F., Choat B., Jansen S., Phillips R.J., Shackel K.A., McElrone A.J. & Matthews M.A. (2011) Automated analysis of three-dimensional xylem networks using high-resolution computed tomography. *New Phytologist*, **191**, 1168-1179.

Brodersen C.R., McElrone A.J., Choat B., Matthews M.A. & Shackel K.A. (2010) The dynamics of embolism repair in xylem: in vivo visualizations using high-resolution computed tomography. *Plant Physiology*, **154**, 1088-1095.

Brodribb T. & Hill R.S. (1993) A physiological comparison of leaves and phyllodes in *Acacia melanoxylon*. *Australian Journal of Botany*, **41**, 293-305.

Brodribb T.J. (2009) Xylem hydraulic physiology: The functional backbone of terrestrial plant productivity. *Plant Science*, **177**, 245-251.

Brodribb T.J. & Holbrook N.M. (2003) Stomatal closure during leaf dehydration, correlation with other leaf physiological traits. *Plant Physiology*, **132**, 2166-2173.

Brugnoli E., Hubick K.T., von Caemmerer S., Wong S.C. & Farquhar G.D. (1988) Correlation between the Carbon Isotope Discrimination in Leaf Starch and Sugars of C3 Plants and the Ratio of Intercellular and Atmospheric Partial Pressures of Carbon Dioxide. *Plant Physiol.*, **88**, 1418-1424.

Bureau of Meteorology (2011a) Climate averages for Australian sites: Newman Aero. Commonwealth of Australia.

Bureau of Meteorology (2011b) Climate averages for Australian sites: Wittenoom. Commonwealth of Australia.

Burrough P.A., van Gaans P.F.M. & Hootsmans R. (1997) Continuous classification in soil survey: spatial correlation, confusion and boundaries. *Geoderma*, **77**, 115-135.

Burrough P.A., van Gaans P.F.M. & MacMillan R.A. (2000) High-resolution landform classification using fuzzy k-means. *Fuzzy Sets and Systems*, **113**, 37-52.

Burrough P.A., Wilson J.P., van Gaans P.F.M. & Hansen A.J. (2001) Fuzzy *k*-means classification of topo-climatic data as an aid to forest mapping in the Greater Yellowstone Area, USA. *Landscape Ecology*, **16**, 523-546.

Byrne M., Yeates D.K., Joseph L., Kearny M., Bowler J., Williams M.A.J., Cooper S., Donnellan S.C., Keogh J.S., Leys R., Melville J., Murphy D.J., Porch N. & Wyrwoll K.-H. (2008) Birth of a biome: insights into the assembly and maintenance of the Australian arid zone biota. *Molecular Ecology*, **17**, 4398-4417.

Cavender-Bares J., Kitajima K. & Bazzaz F.A. (2004) Multiple trait associations in relation to habitat differentiation among 17 Floridian oak species. *Ecological Monographs*, **74**, 635-662.

Cavender-Bares J., Kozak K.H., Fine P.V.A. & Kembel S.W. (2009) The merging of community ecology and phylogenetic biology. *Ecology Letters*, **12**, 693-715.

Cernusak L.A., Tcherkez G., Keitel C., Cornwell W.K., Santiago L.S., Knohl A., Barbour M.M., Williams D.G., Reich P.B., Ellsworth D.S., Dawson T.E., Griffiths H.G., Farquhar G.D. & Wright I.J. (2009) Why are non-photosynthetic tissues generally 13C enriched compared with leaves in C3 plants? Review and synthesis of current hypotheses. *Functional Plant Biology*, **36**, 199-213.

Cernusak L.A., Winter K., Aranda J. & Turner B.L. (2008) Conifers, Angiosperm Trees, and Lianas: Growth, Whole-Plant Water and Nitrogen Use Efficiency, and Stable Isotope Composition (Δ13C and Δ18O) of Seedlings Grown in a Tropical Environment. *Plant Physiology*, **148**, 642-659.

Chave J., Coomes D., Jansen S., Lewis S.L., Swenson N.G. & Zanne A.E. (2009) Towards a worldwide wood economics spectrum. *Ecology Letters*, **12**, 351-366.

Chen S.P., Lin G.H., Huang J.H. & Jenerette G.D. (2009) Dependence of carbon sequestration on the differential responses of ecosystem photosynthesis and respiration to rain pulses in a semiarid steppe. *Global Change Biology*, **15**, 2450-2461.

Chesson P., Gebauer R.L.E., Schwinning S., Huntly N., Wiegand K., Ernest M.S.K., Sher A., Novoplansky A. & Weltzin J.F. (2004) Resource pulses, species interactions, and diversity maintenance in arid and semi-arid environments. *Oecologia*, **141**, 236-253.

Choat B., Lahr E.C., Melcher P.J., Zwieniecki M.A. & Holbrook N.M. (2005) The spatial pattern of air seeding thresholds in mature sugar maple trees. *Plant, Cell & Environment*, **28**, 1082-1089.

Choat B., Sack L. & Holbrook N.M. (2007) Diversity of hydraulic traits in nine Cordia species growing in tropical forests with contrasting precipitation. *New Phytologist*, **175**, 686-698.

Christman M.A., Sperry J.S. & Adler F.R. (2009) Testing the 'rare pit' hypothesis for xylem cavitation resistance in three species of *Acer*. *New Phytologist*, **182**, 664-674.

Clark J.S. (2010) Individuals and the Variation Needed for High Species Diversity in Forest Trees. *Science*, **327**, 1129-1132.

Clarke K.R. & Gorley R.N. (2006) *PRIMER v6: User Manual/Tutorial*. PRIMER-E Ltd, Plymouth, UK.

Cochard H., Coll L., Le Roux X. & Ameglio T. (2002) Unraveling the Effects of Plant Hydraulics on Stomatal Closure during Water Stress in Walnut. *Plant Physiology*, **128**, 282-290.

Cody M.L. (1989) Morphological variation in mulga I. Variation and covariation within and among *Acacia aneura* populations. *Israel Journal of Botany*, **38**, 241-257.

Conde A., Chaves M.M. & Gerós H. (2011) Membrane Transport, Sensing and Signaling in Plant Adaptation to Environmental Stress. *Plant and Cell Physiology*, **52**, 1583-1602.

Condon R.W. (1949) Mulga death in the west Darling country. *Journal of the Soil Conservation Service of New South Wales*, **5**, 7-14.

Cooke J.A. & Johnson M.S. (2002) Ecological restoration of land with particular reference to the mining of metals and industrial minerals: A review of theory and practice. *Environmental Reviews*, **10**, 41-71.

Coplen T.B., Brand W.A., Gehre M., Gröning M., Meijer H.A.J., Toman B. & Verkouteren R.M. (2006) After two decades a second anchor for the VPDB δ13C scale. *Rapid Communications in Mass Spectrometry*, **20**, 3165-3166.

Cornwell W.K. & Ackerly D.D. (2009) Community assembly and shifts in plant trait distributions across an environmental gradient in coastal California. *Ecological Monographs*, **79**, 109-126.

Cowan R.S., Chase M.W., Kress W.J. & Savolainen V. (2006) 300,000 species to identify: problems, progress, and prospects in DNA barcoding of land plants. *Taxon*, **55**, 611-616.

Creed I.F. & Sass G.Z. (2011) Digital Terrain Analysis Approaches for Tracking Hydrological and Biogeochemical Pathways and Processes in Forested Landscapes

Forest Hydrology and Biogeochemistry. (eds D.F. Levia, D. Carlyle-Moses, & T. Tanaka), pp. 69-100. Springer Netherlands.

Cullen L. & Grierson P. (2007) A stable oxygen, but not carbon, isotope chronology of Callitris columellaris reflects recent climate change in north-western Australia. *Climatic Change*, **85**, 213-229.

Díaz S. & Cabido M. (1997) Plant functional types and ecosystem function in relation to global change. *Journal of Vegetation Science*, **8**, 463-474.

Diaz S., Lavorel S., McIntyre S.U.E., Falczuk V., Casanoves F., Milchunas D.G., Skarpe C., Rusch G., Sternberg M., Noy-Meir I., Landsberg J., Zhang W.E.I., Clark H. & Campbell B.D. (2007) Plant trait responses to grazing – a global synthesis. *Global Change Biology*, **13**, 313-341.

Dogramaci S., Skrzypek G., Dodson W. & Grierson P.F. (2012) Stable isotope and hydrochemical evolution of groundwater in the semi-arid Hamersley Basin of subtropical northwest Australia. *Journal of Hydrology*, **475**, 281-293.

DRDL (2011) *Pilbara: a region in profile*. Department of Regional Development and Lands, Government of Western Australia.

DRDL (2012) *Future Development of the Pilbara*. Department of Regional Development and Lands, Government of Western Australia.

Dunkerley D.L. (2002) Infiltration rates and soil moisture in a groved mulga community near Alice Springs, arid central Australia: evidence for complex internal rainwater redistribution in a runoff-runon landscape. *Journal of Arid Environments*, **51**, 199-219.

Dunkerley D.L. (2011) Desert Soils. In: *Arid Zone Geomorphology: Process, Form and Change in Drylands* (ed D.S.G. Thomas), pp. 101-129. John Wiley & Sons Ltd, West Sussex, UK.

Duranceau M., Ghashghaie J., Badeck F., Deleens E. & Cornic G. (1999) $\delta^{13}C$ of CO_2 respired in the dark in relation to $\delta^{13}C$ of leaf carbohydrates in *Phaseolus vulgaris* L. under progressive drought. *Plant, Cell & Environment*, **22**, 515-523.

Dyer J. (2009) Assessing topographic patterns in moisture use and stress using a water balance approach. *Landscape Ecology*, **24**, 391-403.

Ellmore G.S., Zanne A.E. & Orians C.M. (2006) Comparative sectoriality in temperate hardwoods: hydraulics and xylem anatomy. *Botanical Journal of the Linnean Society*, **150**, 61-71.

EPA (2005) *Pilbara Iron Ore and Infrastructure Project: Port and North-South Railway (Stage A) - Report and recommendations of the Environmental Protection Authority* *http://www.epa.wa.gov.au/docs/B1173/B1173.pdf*.

EPA (2006) *Rehabilitation of Terrestrial Ecosystems*.

Erskine P.D., Stewart G.R., Schmidt S., Turnbull M.H., Unkovich M. & Pate J.S. (1996) Water availability - a physiological constraint on nitrate utilization in plants of Australian semi-arid mulga woodlands. *Plant, Cell and Environment*, **19**, 1149-1159.

Espino S. & Schenk H.J. (2009) Hydraulically integrated or modular? Comparing whole-plant-level hydraulic systems between two desert shrub species with different growth forms. *New Phytologist*, **183**, 142-152.

ESRI (2006) ArcGIS 9.0. Environmental Systems Research Institute, Redlands, California.

Evans J.R. (1989) Photosynthesis and nitrogen relationships in leaves of C3 plants. *Oecologia*, **78**, 9-19.

Everist S.L. (1949) Mulga (*Acacia aneura* F.Muell.) in Queensland. *The Queensland Journal of Agricultural Science*, **6**, 87-131.

Falster D.S. & Westoby M. (2003) Leaf size and angle vary widely across species: what consequences for light interception? *New Phytologist*, **158**, 509-525.

Farquhar G.D., Ehleringer J.R. & Hubick K.T. (1989) Carbon isotope discrimination and photosynthesis. *Annual Review of Plant Physiology and Plant Molecular Biology*, **40**, 503-537.

Farrell T.P. & Ashton D.H. (1978) Population studies on *Acacia melanoxylon* R. Br. I. Variation in seed and vegetative characteristics. *Australian Journal of Botany*, **26**, 365-379.

Fensham R., Fairfax R. & Dwyer J. (2012a) Potential aboveground biomass in drought-prone forest used for rangeland pastoralism. *Ecological Applications*, **22**, 894-908.

Fensham R.J., Dwyer J.M., Eyre T.J., Fairfax R.J. & Wang J. (2012b) The effect of clearing on plant composition in mulga (Acacia aneura) dry forest, Australia. *Austral Ecology*, **37**, 183-192.

Fensham R.J. & Fairfax R.J. (2007) Drought-related tree death of savanna eucalypts: Species susceptibility, soil conditions and root architecture. *Journal of Vegetation Science*, **18**, 71-80.

Fensham R.J., Powell O. & Horne J. (2011) Rail survey plans to remote sensing: vegetation change in the Mulga Lands of eastern Australia and its implications for land use. *The Rangeland Journal*, **33**, 229-238.

Fensham R.J., Silcock J.L. & Dwyer J.M. (2011) Plant species richness responses to grazing protection and degradation history in a low productivity landscape. *Journal of Vegetation Science*, **22**, 997-1008.

Ford D.J., Cookson W.R., Adams M.A. & Grierson P.F. (2007) Role of soil drying in nitrogen mineralization and microbial community function in semi-arid grasslands of north-west Australia. *Soil Biology and Biochemistry*, **39**, 1557-1569.

Fortescue Metals Group Limited (2011a) Fortescue Rail Expansion Factsheet: http://www.fmgl.com.au/UserDir/Documents/Fact%20Sheets/FACT%20SHEET%20Rail%20Expansion%20-%20Sept%202011.pdf.

Fortescue Metals Group Limited (2011b) *Railway Corridor Disturbance Management Plant - Pilbara Iron Ore and Infrastructure Project.* *http://reports.fmgl.com.au/ENVIRO/Additional%20Rail%20EPBC/Appendices/Appendix%209%20Rail%20Corridor%20Disturbance%20MP.pdf*.

Fox J.E.D. (1986) Vegetation: Diversity of the Mulga Species. In: *The Mulga Lands* (ed P.S. Sattler), pp. 27-32. Royal Society of Queensland.

Fravolini A., Hultine K.R., Brugnoli E., Gazal R., English N.B. & Williams D.G. (2005) Precipitation pulse use by an invasive woody legume: the role of soil texture and pulse size. *Oecologia*, **144**, 618-627.

Gaff D. & Latz P. (1978) The Occurrence of Resurrection Plants in the Australian Flora. *Australian Journal of Botany*, **26**, 485-492.

Gebauer R.L.E. & Ehleringer J.R. (2000) Water and nitrogen uptake patterns following moisture pulses in a cold desert community. *Ecology*, **81**, 1415-1424.

Gee G.W. & Bauder J.W. (1986) Particle-size analysis. In: *Methods of Soil Analysis Part 1* (ed A. Klute), pp. 383-411. Soil Science Society of America, Madison, Wisconsin USA.

Gessler A., Brandes E., Buchmann N., Helle G., Rennenberg H. & Barnard R.L. (2009) Tracing carbon and oxygen isotope signals from newly assimilated sugars in the leaves to the tree-ring archive. *Plant, Cell & Environment*, **32**, 780-795.

Gessler A., Keitel C., Kodama N., Weston C., Winters A.J., Keith H., Grice K., Leuning R. & Farquhar G.D. (2007) δ13C of organic matter transported from the leaves to the roots in Eucalyptus delegatensis: short-term variations and relation to respired CO2. *Functional Plant Biology*, **34**, 692-706.

Ghashghaie J., Badeck F.-W., Lanigan G., Nogués S., Tcherkez G., Deléens E., Cornic G. & Griffiths H. (2003) Carbon isotope fractionation during dark respiration and photorespiration in C3 plants. *Phytochemistry Reviews*, **2**, 145-161.

Givnish T.J. (1987) Comparative studies of leaf form: assessing the relative roles of selective pressures and phylogenetic constraints. *New Phytologist*, **106**, 131-160.

González-Orozco C.E., Laffan S.W. & Miller J.T. (2011) Spatial distribution of species richness and endemism of the genus Acacia in Australia. *Australian Journal of Botany*, **59**, 601-609.

Gouveia A. & Freitas H. (2009) Modulation of leaf attributes and water use efficiency in *Quercus suber* along a rainfall gradient. *Trees - Structure and Function*, **23**, 267-275.

Greene R.S.B. (1992) Soil physical properties of three geomorphic zones in a semiarid mulga woodland. *Australian Journal of Soil Research*, **30**, 55-69.

Grigg A., Lambers H. & Veneklaas E. (2010) Changes in water relations for *Acacia ancistrocarpa* on natural and mine-rehabilitation sites in response to an experimental wetting pulse in the Great Sandy Desert. *Plant and Soil*, **326**, 75-96.

Hacke U.G., Jacobsen A.L. & Pratt R.B. (2009) Xylem function of arid-land shrubs from California, USA: an ecological and evolutionary analysis. *Plant, Cell & Environment*, **32**, 1324-1333.

Hacke U.G., Sperry J.S., Wheeler J.K. & Castro L. (2006) Scaling of angiosperm xylem structure with safety and efficiency. *Tree Physiology*, **26**, 689-701.

Hajibabaei M., Singer G.A.C., Hebert P.D.N. & Hickey D.A. (2007) DNA barcoding: how it complements taxonomy, molecular phylogenetics and population genetics. *Trends in Genetics*, **23**, 167-172.

Hare P.D., Cress W.A. & Van Staden J. (1998) Dissecting the roles of osmolyte accumulation during stress. *Plant, Cell & Environment*, **21**, 535-553.

Hellmuth E.O. (1969) Eco-Physiological Studies on Plants in Arid and Semi-Arid Regions in Western Australia: II. Field Physiology of Acacia Craspedocarpa F. Muell. *Journal of Ecology*, **57**, 613-634.

Heyting M. (2011) *Hydrological processes in sheetflow dependent Mulga groves, Honours Thesis*, The University of Western Australia.

Hick P., Caccetta M. & Corner R. (1997) *An Assessment Of Vegetation Condition And Monitoring Strategy For Hamersley Iron's Central Pilbara Railway (CPR) Through Karijini National Park Using Remotely-Sensed And Ancillary Data*. CSIRO.

Hodge R., Brasington J. & Richards K. (2009) Analysing laser-scanned digital terrain models of gravel bed surfaces: linking morphology to sediment transport processes and hydraulics. *Sedimentology*, **56**, 2024-2043.

Holt R.D. (2009) Bringing the Hutchinsonian niche into the 21st century: Ecological and evolutionary perspectives. *Proceedings of the National Academy of Sciences*, **106**, 19659-19665.

Hothorn T., Bretz F. & Westfall P. (2008) Simultaneous inference in general parametric models. *Biometrical Journal*, **50**, 346-363.

Hsiao T.C., Acevedo E., Fereres E. & Henderson D.W. (1976) Water stress, growth, and osmotic adjustment. *Philosophical Transactions of the Royal Society of London. Series B, Biological Sciences*, **273**, 479-500.

Huggett R.J. (1975) Soil landscape systems: A model of soil Genesis. *Geoderma*, **13**, 1-22.

Hummel I., Pantin F., Sulpice R., Piques M., Rolland G., Dauzat M., Christophe A., Pervent M., Bouteillé M., Stitt M., Gibon Y. & Muller B. (2010) Arabidopsis Plants Acclimate to Water Deficit at Low Cost through Changes of Carbon Usage: An Integrated Perspective Using Growth, Metabolite, Enzyme, and Gene Expression Analysis. *Plant Physiology*, **154**, 357-372.

Hutchinson M.F. (1989) A new procedure for gridding elevation and stream line data with automatic removal of spurious pits. *Journal of Hydrology*, **106**, 211-232.

Huxman T.E., Cable J.M., Ignace D.D., Eilts J.A., English N.B., Weltzin J. & Williams D.G. (2004a) Response of net ecosystem gas exchange to a simulated precipitation pulse in a semi-arid grassland: the role of native versus non-native grasses and soil texture. *Oecologia*, **141**, 295-305.

Huxman T.E., Snyder K.A., Tissue D., Leffler A.J., Ogle K., Pockman W.T., Sandquist D.R., Potts D.L. & Schwinning S. (2004b) Precipitation pulses and carbon fluxes in semiarid and arid ecosystems. *Oecologia*, **141**, 254-268.

Isbell R.F. (1996) *The Australian Soil Classification*. CSIRO Publishing, Collingwood, VIC 3066.

Jaindl M. & Popp M. (2006) Cyclitols protect glutamine synthetase and malate dehydrogenase against heat induced deactivation and thermal denaturation. *Biochemical and Biophysical Research Communications*, **345**, 761-765.

John R., Dalling J.W., Harms K.E., Yavitt J.B., Stallard R.F., Mirabello M., Hubbell S.P., Valencia R., Navarrete H., Vallejo M. & Foster R.B. (2007) Soil nutrients influence spatial distributions of tropical tree species. *Proceedings of the National Academy of Sciences*, **104**, 864-869.

Johnson R.W. & Burrows W.H. (1994) Acacia open-forests, woodlands and shublands. In: *Australian Vegetation* (ed R.H. Groves), pp. 257-290. Cambridge University Press, Cambridge, England.

Kalapos T. & Csontos P. (2003) Variation in leaf structure and function of the Mediterranean tree *Fraxinus ornus* L. growing in ecologically contrasting habitats at the margin of its range. *Plant Biosystems*, **137**, 73-82.

Kattge J., DÍAz S., Lavorel S., Prentice I.C., Leadley P., BÖNisch G., Garnier E., Westoby M., Reich P.B., Wright I.J., Cornelissen J.H.C., Violle C., Harrison S.P., Van Bodegom P.M., Reichstein M., Enquist B.J., Soudzilovskaia N.A., Ackerly D.D., Anand M., Atkin O., Bahn M., Baker T.R., Baldocchi D., Bekker R., Blanco C.C., Blonder B., Bond W.J., Bradstock R., Bunker D.E., Casanoves F., Cavender-Bares J., Chambers J.Q., Chapin Iii F.S., Chave

J., Coomes D., Cornwell W.K., Craine J.M., Dobrin B.H., Duarte L., Durka W., Elser J., Esser G., Estiarte M., Fagan W.F., Fang J., FernÁNdez-MÉNdez F., Fidelis A., Finegan B., Flores O., Ford H., Frank D., Freschet G.T., Fyllas N.M., Gallagher R.V., Green W.A., Gutierrez A.G., Hickler T., Higgins S.I., Hodgson J.G., Jalili A., Jansen S., Joly C.A., Kerkhoff A.J., Kirkup D., Kitajima K., Kleyer M., Klotz S., Knops J.M.H., Kramer K., KÜHn I., Kurokawa H., Laughlin D., Lee T.D., Leishman M., Lens F., Lenz T., Lewis S.L., Lloyd J., LlusiÀ J., Louault F., Ma S., Mahecha M.D., Manning P., Massad T., Medlyn B.E., Messier J., Moles A.T., MÜLler S.C., Nadrowski K., Naeem S., Niinemets Ü., NÖLlert S., NÜSke A., Ogaya R., Oleksyn J., Onipchenko V.G., Onoda Y., OrdoÑEz J., Overbeck G., Ozinga W.A. (2011) TRY – a global database of plant traits. *Global Change Biology*, **17**, 2905-2935.

Kent M. & Coker P. (1992) *Vegetation description and analysis: a practical approach*. CRC Press, London.

Kim H.K. & Lee S.J. (2010) Synchrotron X-ray imaging for nondestructive monitoring of sap flow dynamics through xylem vessel elements in rice leaves. *New Phytologist*, **188**, 1085-1098.

King D.A. (1990) The adaptive significance of tree height. *The American Naturalist*, **135**, 809-828.

Koch G.W., Sillett S.C., Jennings G.M. & Davis S.D. (2004) The limits to tree height. *Nature*, **428**, 851-854.

Kranendonk M.J.V., Hickman A.H., Smithies R.H., Nelson D.R. & Pike G. (2002) Geology and Tectonic Evolution of the Archean North Pilbara Terrain, Pilbara Craton, Western Australia. *Economic Geology*, **97**, 695-732.

Laughlin D.C., Joshi C., van Bodegom P.M., Bastow Z.A. & Fulé P.Z. (2012) A predictive model of community assembly that incorporates intraspecific trait variation. *Ecology Letters*, **15**, 1291-1299.

Liu J. & Regenauer-Lieb K. (2011) Application of percolation theory to microtomography of structured media: Percolation threshold, critical exponents, and upscaling. *Physical Review E*, **83**, 016106.

Liu J., Regenauer-Lieb K., Hines C., Liu K., Gaede O. & Squelch A. (2009) Improved estimates of percolation and anisotropic permeability from 3-D X-ray microtomography using stochastic analyses and visualization. *Geochemistry Geophysics Geosystems*, **10**.

Liu L.X., Xu S.M., Wang D.L. & Woo K.C. (2008) Accumulation of pinitol and other soluble sugars in water-stressed phyllodes of tropical *Acacia auriculiformis* in northern Australia. *New Zealand Journal of Botany*, **46**, 119-126.

Liu Y.B., Wang G., Liu J., Zhao X., Tan H.J. & Li X.R. (2007) Anatomical, morphological and metabolic acclimation in the resurrection plant Reaumuria soongorica during dehydration and rehydration. *Journal of Arid Environments*, **70**, 183-194.

Loepfe L., Martinez-Vilalta J., Piñol J. & Mencuccini M. (2007) The relevance of xylem network structure for plant hydraulic efficiency and safety. *Journal of Theoretical Biology*, **247**, 788-803.

Loeppert R.H. & Inskeep W.P. (1996) Iron. In: *Methods of Soil Analysis Part 3 - Chemical Methods* (ed D.L. Sparks), pp. 639-664. Soil Science Society of America, Madison, Wisconsin USA.

Lottermoser B.G. (2011) Recycling, Reuse and Rehabilitation of Mine Wastes. *Elements*, **7**, 405-410.

Ludwig J.A., Wilcox B.P., Breshears D.D., Tongway D.J. & Imeson A.C. (2005) Vegetation patches and runoff-erosion as interacting ecohydrological processes in semiarid landscapes. *Ecology*, **86**, 288-297.

Lynch J. (1995) Root architecture and plant productivity. *Plant Physiology*, **109**, 7-13.

Maathuis F.J.M. & Amtmann A. (1999) K+Nutrition and Na+Toxicity: The Basis of Cellular K+/Na+Ratios. *Annals of Botany*, **84**, 123-133.

Mabbutt J.A. & Fanning P.C. (1987) Vegetation banding in arid Western Australia. *Journal of Arid Environments*, **12**, 41-59.

Maestre F.T., Bowker M.A., Escolar C., Puche M.D., Soliveres S., Maltez-Mouro S., García-Palacios P., Castillo-Monroy A.P., Martínez I. & Escudero A. (2010) Do biotic interactions modulate ecosystem functioning along stress gradients? Insights from semi-arid plant and biological soil crust communities. *Philosophical Transactions of the Royal Society B: Biological Sciences*, **365**, 2057-2070.

Maherali H., Moura C.F., Caldeira M.C., Willson C.J. & Jackson R.B. (2006) Functional coordination between leaf gas exchange and vulnerability to xylem cavitation in temperate forest trees. *Plant, Cell & Environment*, **29**, 571-583.

Maslin B.R., O'Leary M., Reid J.E. & Miller J.T. (2012) The type of *Acacia aneura* (Mulga: Fabaceae) and ambiguities concerning the application of this name. *Nuytsia*, **22**, 269-294.

Maslin B.R. & Reid J.E. (2012) A taxonomic revision of Mulga (*Acacia aneura* and its close relatives: Fabaceae) in Western Australia. *Nuytsia*, **22**, 129-267.

Mattiske E. & Havel J. (1998) Vegetation Complexes of the South-west Forest Region of Western Australia. *Maps and report prepared as part of the Regional Forest Agreement, Western Australia for the Department of Conservation and Land Management and Environment Australia*.

McArdle B.H. & Anderson M.J. (2001) Fitting multivariate models to community data: a comment on distance-based redundancy analysis. *Ecology*, **82**, 290-297.

McConnaughay K.D.M. & Coleman J.S. (1999) Biomass allocation in plants: ontogeny or optimality? A test along three resource gradients. *Ecology*, **80**, 2581-2593.

McDonald P.G., Fonseca C.R., Overton J.M. & Westoby M. (2003) Leaf-size divergence along rainfall and soil-nutrient gradients: is the method of size reduction common among clades? *Functional Ecology*, **17**, 50-57.

McDowell N., Pockman W.T., Allen C.D., Breshears D.D., Cobb N., Kolb T., Plaut J., Sperry J., West A., Williams D.G. & Yepez E.A. (2008) Mechanisms of plant survival and mortality during drought: why do some plants survive while others succumb to drought? *New Phytologist*, **178**, 719-739.

McDowell N.G. (2011) Mechanisms Linking Drought, Hydraulics, Carbon Metabolism, and Vegetation Mortality. *Plant Physiology*, **155**, 1051-1059.

McDowell N.G., Beerling D.J., Breshears D.D., Fisher R.A., Raffa K.F. & Stitt M. (2011) The interdependence of mechanisms underlying climate-driven vegetation mortality. *Trends in Ecology & Evolution*, **26**, 523-532.

McIntyre R.E.S., Adams M.A. & Grierson P.F. (2009) Nitrogen mineralization potential in rewetted soils from a semi-arid stream landscape, north-west Australia. *Journal of Arid Environments*, **73**, 48-54.

McKenzie N.L., van Leeuwen S.J. & Pinder A.M. (2009) Introduction to the Pilbara Biodiversity Survey, 2002-2007. *Records of the Western Australian Museum*, **Supplement 78**, 3-89.

McLeish M., Chapman T. & Schwarz M. (2007) Host-driven diversification of gall-inducing *Acacia* thrips and the aridification of Australia. *BMC Biology*, **5**, 3.

Meier I. & Leuschner C. (2008) Leaf size and leaf area index in *Fagus sylvatica* forests: competing effects of recipitation, temperature, and nitrogen availability. *Ecosystems*, **11**, 655-669.

Meinzer F., McCulloh K., Lachenbruch B., Woodruff D. & Johnson D. (2010) The blind men and the elephant: the impact of context and scale in evaluating conflicts between plant hydraulic safety and efficiency. *Oecologia*, **164**, 287-296.

Meinzer F., Woodruff D., Domec J.-C., Goldstein G., Campanello P., Gatti M. & Villalobos-Vega R. (2008) Coordination of leaf and stem water transport properties in tropical forest trees. *Oecologia*, **156**, 31-41.

Merchant A. & Adams M. (2005) Stable osmotica in *Eucalyptus spathulata* - responses to salt and water deficit stress. *Functional Plant Biology*, **32**, 797-805.

Merchant A., Ladiges P.Y. & Adams M.A. (2007) Quercitol links the physiology, taxonomy and evolution of 279 eucalypt species. *Global Ecology and Biogeography*, **16**, 810-819.

Merchant A., Peuke A.D., Keitel C., Macfarlane C., Warren C.R. & Adams M.A. (2010) Phloem sap and leaf $\delta^{13}C$, carbohydrates, and amino acid concentrations in *Eucalyptus globulus* change systematically according to flooding and water deficit treatment. *Journal of Experimental Botany*, **61**, 1785-1793.

Merchant A., Richter A., Popp M. & Adams M. (2006a) Targeted metabolite profiling provides a functional link among eucalypt taxonomy, physiology and evolution. *Phytochemistry*, **67**, 402-408.

Merchant A., Tausz M., Arndt S.K. & Adams M.A. (2006b) Cyclitols and carbohydrates in leaves and roots of 13 *Eucalyptus* species suggest contrasting physiological responses to water deficit. *Plant, Cell and Environment*, **29**, 2017-2029.

Merritt D.J. & Dixon K.W. (2011) Restoration seed banks–a matter of scale. *Science*, **332**, 424-425.

Miller J.T., Andrew R.A. & Maslin B.R. (2002) Towards an understanding of variation in the Mulga complex (*Acacia aneura* and relatives). *Conservation Science Western Australia*, **4**, 19-35.

Milne G. (1935) Some suggested units of classification and mapping, particularly for East African soils. *Soil Research*, **4**, 183-198.

Mokany K., McMurtrie R.E., Atwell B.J. & Keith H. (2003) Interaction between sapwood and foliage area in alpine ash (*Eucalyptus delegatensis*) trees of different heights. *Tree Physiology*, **23**, 949-958.

Moore I.D. & Burch G.J. (1986) Physical basis of the length-slope factor in the Universal Soil Loss Equation. *Soil Science Society of America Journal*, **50**, 1294-1298.

Moore I.D., Gessler P.E., Nielsen G.A. & Peterson G.A. (1993) Soil attribute prediction using terrain analysis. *Soil Science Society of America Journal*, **57**, 443-452.

Moreno-de las Heras M., Saco P.M., Willgoose G.R. & Tongway D.J. (2012) Variations in hydrological connectivity of Australian semiarid landscapes indicate abrupt changes in rainfall-use efficiency of vegetation. *Journal of Geophysical Research: Biogeosciences*, **117**, G03009.

Morton S.R., Stafford Smith D.M., Dickman C.R., Dunkerley D.L., Friedel M.H., McAllister R.R.J., Reid J.R.W., Roshier D.A., Smith M.A., Walsh F.J., Wardle G.M., Watson I.W. & Westoby M. (2011) A fresh framework for the ecology of arid Australia. *Journal of Arid Environments*, **75**, 313-329.

Mott J. (1978) Dormancy and Germination in Five Native Grass Species From Savannah Woodland Communities of the Northern Territory. *Australian Journal of Botany*, **26**, 621-631.

Muller C. (2005) *Water Flow in Mulga Areas Adjoining Fortescue Marsh*. Unpublished Report of Observations From Field Trials Undertaken for Fortescue Metals Group Limited.

Murphy D.J., Brown G.K., Miller J.T. & Ladiges P.Y. (2010) Molecular phylogeny of Acacia Mill. (Mimosoideae: Leguminosae): Evidence for major clades and informal classification. *Taxon*, **59**, 7-19.

Murphy D.J., Miller J.T., Bayer R.J. & Ladiges P.Y. (2003) Molecular phylogeny of *Acacia* subgenus *Phyllodineae* (Mimosoideae: Leguminosae) based on DNA sequences of the internal transcribed spacer region. *Australian Systematic Botany*, **16**, 19-26.

Nicolau J.M., Solé-Benet A., Puigdefábregas J. & Gutiérrez L. (1996) Effects of soil and vegetation on runoff along a catena in semi-arid Spain. *Geomorphology*, **14**, 297-309.

Niinemets Ü., Kull O. & Tenhunen J.D. (1999) Variability in leaf morphology and chemical composition as a function of canopy light environment in coexisting deciduous trees. *International Journal of Plant Sciences*, **160**, 837-848.

Niinemets U., Portsmuth A., Tena D., Tobias M., Matesanz S. & Valladares F. (2007a) Do we underestimate the importance of leaf size in plant economics? Disproportional scaling

of support costs within the spectrum of leaf physiognomy. *Annals of Botany*, **100**, 283-303.

Niinemets U., Portsmuth A. & Tobias M. (2007b) Leaf shape and venation pattern alter the support investments within leaf lamina in temperate species: a neglected source of leaf physiological differentiation? *Functional Ecology*, **21**, 28-40.

Niinemets Ü. & Tenhunen J.D. (1997) A model separating leaf structural and physiological effects on carbon gain along light gradients for the shade-tolerant species *Acer saccharum*. *Plant, Cell and Environment*, **20**, 845-866.

Nix H.A. & Austin M.P. (1973) Mulga: a bioclimatic analysis. *Tropical Grasslands*, **7**, 9-21.

Noble I.R. & Slatyer R.O. (1980) The use of vital attributes to predict successional changes in plant communities subject to recurrent disturbances. *Plant Ecology*, **43**, 5-21.

North G.B. & Nobel P.S. (1998) Water uptake and structural plasticity along roots of a desert succulent during prolonged drought. *Plant, Cell & Environment*, **21**, 705-713.

Northcote K.H. (1971) *A factual key for the recognition of Australian soils*. Rellim Technical Publications, Glenside, South Australia.

Noy-Meir I. (1973) Desert ecosystems: environment and producers. *Annual Review of Ecology and Systematics*, **4**, 25-51.

O'Grady A., Cook P., Eamus D., Duguid A., Wischusen J., Fass T. & Worldege D. (2009) Convergence of tree water use within an arid-zone woodland. *Oecologia*, **160**, 643-655.

Ordoñez J.C., Bodegom P.M.v., Witte J.-P.M., Wright I.J., Reich P.B. & Aerts R. (2009) A global study of relationships between leaf traits, climate and soil measures of nutrient fertility. *Global Ecology and Biogeography*, **18**, 137-149.

Orthen B. & Popp M. (2000) Cyclitols as cryoprotectants for spinach and chickpea thylakoids. *Environmental and Experimental Botany*, **44**, 125-132.

Orthen B., Popp M. & Smirnoff N. (1994) Hydroxyl radical scavenging properties of cyclitols. *Proceedings of the Royal Society of Edinburgh Section B: Biology*, **102**, 269-272.

Padilla F.M., Ortega R., Sánchez J. & Pugnaire F.I. (2009) Rethinking species selection for restoration of arid shrublands. *Basic and Applied Ecology*, **10**, 640-647.

Page G.F.M., Cullen L.E., van Leeuwen S. & Grierson P.F. (2011) Inter- and intra-specific variation in phyllode size and growth form among closely related Mimosaceae Acacia species across a semiarid landscape gradient. *Australian Journal of Botany*, **59**, 426-439.

Paul D., Skrzypek G. & Fórizs I. (2007) Normalization of measured stable isotopic compositions to isotope reference scales – a review. *Rapid Communications in Mass Spectrometry*, **21**, 3006-3014.

Paul M.J. & Foyer C.H. (2001) Sink regulation of photosynthesis. *Journal of Experimental Botany*, **52**, 1383-1400.

PCRaster (2006) PCRaster - software for environmental modelling. Faculty of Geosciences, Utrecht University, Utrecht, The Netherlands.

Pedley L. (1973) Taxonomy of the *Acacia aneura* complex. *Tropical Grasslands*, **7**, 3-8.

Pedley L. (2001) *Acacia aneura* and relatives. In: *Flora of Australia 11B, Mimosaceae, Acacia part 1* (eds A.E. Orchard & A.J.G. Wilson), pp. 309-328. CSIRO Publishing / Australian Biological Resources Study, Canberra.

Pepper M., Doughty P., Arculus R. & Keogh J.S. (2008) Landforms predict phylogenetic structure on one of the world's most ancient surfaces. *BMC Evolutionary Biology*, **8**, 152.

Perroni-Ventura Y., Montaña C. & García-Oliva F. (2006) Relationship between soil nutrient availability and plant species richness in a tropical semi-arid environment. *Journal of Vegetation Science*, **17**, 719-728.

Pickup M., Westoby M. & Basden A. (2005) Dry mass costs of deploying leaf area in relation to leaf size. *Functional Ecology*, **19**, 88-97.

Pockman W.T. & Small E.E. (2010) The Influence of Spatial Patterns of Soil Moisture on the Grass and Shrub Responses to a Summer Rainstorm in a Chihuahuan Desert Ecotone. *Ecosystems*, **13**, 511-525.

Poorter H., Niinemets Ü., Poorter L., Wright I.J. & Villar R. (2009) Causes and consequences of variation in leaf mass per area (LMA): a meta-analysis. *New Phytologist*, **182**, 565-588.

Popp M., Lied W., Meyer A.J., Richter A., Schiller P. & Schwitte H. (1996) Sample preservation for determination of organic compounds: microwave versus freeze-drying. *Journal of Experimental Botany*, **47**, 1469-1473.

Potts D.L., Huxman T.E., Cable J.M., English N.B., Ignace D.D., Eilts J.A., Mason M.J., Weltzin J.F. & Williams D.G. (2006) Antecedent moisture and seasonal precipitation influence the response of canopy-scale carbon and water exchange to rainfall pulses in a semi-arid grassland. *New Phytologist*, **170**, 849-860.

Preece P.B. (1971a) Contributions to the biology of mulga I. Flowering. *Australian Journal of Botany*, **19**, 21-38.

Preece P.B. (1971b) Contributions to the biology of mulga II. Germination. *Australian Journal of Botany*, **19**, 39-49.

Pressland A.J. (1973) Rainfall partitioning by an arid woodland (*Acacia aneura* F. Muell.) in south-western Queensland. *Australian Journal of Botany*, **21**, 235-245.

Pressland A.J. (1975) Productivity and management of Mulga in south-western Queensland in relation to tree structure and density. *Australian Journal of Botany*, **23**, 965-975.

Pressland A.J. (1976) Effect of stand density of water use of Mulga (*Acacia aneura* F. Muell.) woodlands of south-western Queensland. *Australian Journal of Botany*, **24**, 177-191.

Prior L.D., Bowman D.M.J.S. & Eamus D. (2005) Intra-specific variation in leaf attributes of four savanna tree species across a rainfall gradient in tropical Australia. *Australian Journal of Botany*, **53**, 323-335.

Prior L.D., Eamus D. & Bowman D.M.J.S. (2003) Leaf attributes in the seasonally dry tropics: a comparison of four habitats in northern Australia. *Functional Ecology*, **17**, 504-515.

Pugnaire F.I. & Lázaro R. (2000) Seed Bank and Understorey Species Composition in a Semi-arid Environment: The Effect of Shrub Age and Rainfall. *Annals of Botany*, **86**, 807-813.

Quinn P., Beven K., Chevallier P. & Planchon O. (1991) The prediction of hillslope flow paths for distributed hydrological modelling using digital terrain models. *Hydrological Processes*, **5**, 59-79.

R Development Core Team (2010) R: A language and environment for statistical computing. R Foundation for Statistical Computing, Vienna, Austria.

Randell B.R. (1992) Key to the varieties of *A. aneura*. *Journal of the Adelaide Botanic Gardens*, **14**, 120-121.

Raunkiaer C. (1934) *Life forms of plants and statistical plant geography*. Clarendon Press, Oxford, UK.

Reich P.B., Ellsworth D.S. & Walters M.B. (1998) Leaf structure (specific leaf area) modulates photosynthesis-nitrogen relations: evidence from within and across species and functional groups. *Functional Ecology*, **12**, 948-958.

Reich P.B., Walters M.B. & Ellsworth D.S. (1997) From tropics to tundra: global convergence in plant functioning. *Proceedings of the National Academy of Sciences*, **94**, 13730-13734.

Reid D.E.B., Silins U., Mendoza C. & Lieffers V.J. (2005) A unified nomenclature for quantification and description of water conducting properties of sapwood xylem based on Darcy's law. *Tree Physiology*, **25**, 993-1000.

Resco V., Ewers B.E., Sun W., Huxman T.E., Weltzin J.F. & Williams D.G. (2009) Drought-induced hydraulic limitations constrain leaf gas exchange recovery after precipitation pulses in the C_3 woody legume, *Prosopis velutina*. *New Phytologist*, **181**, 672-682.

Resco V., Ignace D.D., Sun W., Huxman T.E., Weltzin J.F. & Williams D.G. (2008) Chlorophyll fluorescence, predawn water potential and photosynthesis in precipitation pulse-driven ecosystems - implications for ecological studies. *Functional Ecology*, **22**, 479-483.

Reynolds H.L., Packer A., Bever J.D. & Clay K. (2003) Grassroots ecology: plant-microbe-soil interactions as drivers of plant community structure and dynamics. *Ecology*, **84**, 2281-2291.

Richardson M.C., Fortin M.J. & Branfireun B.A. (2009) Hydrogeomorphic edge detection and delineation of landscape functional units from lidar digital elevation models. *Water Resources Research*, **45**, W10441.

Rossi B.E. & Villagra P.E. (2003) Effects of Prosopis flexuosa on soil properties and the spatial pattern of understorey species in arid Argentina. *Journal of Vegetation Science*, **14**, 543-550.

Sack L. & Holbrook N.M. (2006) Leaf hydraulics. *Annual Review of Plant Biology*, **57**, 361-381.

Sack L., Pasquet-Kok J. & PrometheusWiki contributors (2011) Leaf pressure-volume curve parameters. PrometheusWiki, http://prometheuswiki.publish.csiro.au/tiki-index.php?page=Leaf+pressure-volume+curve+parameters.

Savage J.A. & Cavender-Bares J. (2012) Habitat specialization and the role of trait lability in structuring diverse willow (genus Salix) communities. *Ecology*, **93**, S138-S150.

Scatena F.N. & Lugo A.E. (1995) Geomorphology, disturbance, and the soil and vegetation of two subtropical wet steepland watersheds of Puerto Rico. *Geomorphology*, **13**, 199-213.

Schenk H.J., Espino S., Goedhart C.M., Nordenstahl M., Cabrera H.I.M. & Jones C.S. (2008) Hydraulic integration and shrub growth form linked across continental aridity gradients. *Proceedings of the National Academy of Sciences*, **105**, 11248-11253.

Schwender J., Ohlrogge J. & Shachar-Hill Y. (2004) Understanding flux in plant metabolic networks. *Current Opinion in Plant Biology*, **7**, 309-317.

Schwinning S. & Osvaldo E.S. (2004) Hierarchy of responses to resource pulses in arid and semi-arid ecosystems. *Oecologia*, **141**, 211-220.

Scoffoni C., Rawls M., McKown A., Cochard H. & Sack L. (2011) Decline of leaf hydraulic conductance with dehydration: relationship to leaf size and venation architecture. *Plant Physiology*, **156**, 832-843.

Scott P. (2000) Resurrection Plants and the Secrets of Eternal Leaf. *Annals of Botany*, **85**, 159-166.

Seigler D.S. (2003) Phytochemistry of Acacia - sensu lato. *Biochemical Systematics and Ecology*, **31**, 845-873.

Shepherd D.P., Beeston G.R. & Hopkins A.J.M. (2001) *Native Vegetation in Western Australia. Technical Report 249* Department of Agriculture, Western Australia.

Shim J.H., Pendall E., Morgan J.A. & Ojima D.S. (2009) Wetting and drying cycles drive variations in the stable carbon isotope ratio of respired carbon dioxide in semi-arid grassland. *Oecologia*, **160**, 321-333.

Shipley B. (1999) Testing causal explanations in organismal biology: causation, correlation and structural equation modelling. *Oikos*, **86**, 374-382.

Shipley B., Vile D. & Garnier É. (2006) From Plant Traits to Plant Communities: A Statistical Mechanistic Approach to Biodiversity. *Science*, **314**, 812-814.

Skrzypek G. & Paul D. (2006) δ13C analyses of calcium carbonate: comparison between the GasBench and elemental analyzer techniques. *Rapid Communications in Mass Spectrometry*, **20**, 2915-2920.

Slatyer R.O. (1960) Aspects of the tissue water relationship of an important arid zone species (*Acacia aneura* F.Muell.) in comparison with two mesophytes. *Bullentin of the Research Council of Israel*, **8D**, 159-168.

Slatyer R.O. (1961a) Internal Water Balance of *Acacia aneura* F. Muell. in Relation to Environmental Conditions. In: *Plant-water Relationships in Arid and Semi-Arid Conditions: Proceedings of the Madrid Symposium* (ed UNESCO), pp. 137-146. UNESCO, Paris, France.

Slatyer R.O. (1961b) Methodology of a Water Balance Study Conducted on a Desert Woodland (*Acacia aneura* F. Muell.) Community in Central Australia. In: *Plant-Water*

Relationships in Arid and Semi-Arid Conditions: Proceedings of the Madrid Symposium (ed UNSECO), pp. 15-26. UNESCO, Paris, France.

Slatyer R.O. (1965) Measurements of precipitation interception by an arid zone plant community (*Acacia aneura* F. Muell). *Arid Zone Research*, **25**, 181-192.

Sperry J.S. (2000) Hydraulic constraints on plant gas exchange. *Agricultural and Forest Meteorology*, **104**, 13-23.

Sperry J.S., Hacke U.G., Oren R. & Comstock J.P. (2002) Water deficits and hydraulic limits to leaf water supply. *Plant, Cell & Environment*, **25**, 251-263.

Stafford Smith D.M. & Morton S.R. (1990) A framework for the ecology of arid Australia. *Journal of Arid Environments*, **18**, 255-278.

Steppe K., Cnudde V., Girard C., Lemeur R., Cnudde J.-P. & Jacobs P. (2004) Use of X-ray computed microtomography for non-invasive determination of wood anatomical characteristics. *Journal of Structural Biology*, **148**, 11-21.

Thomas G.W. (1996) Soil pH and Soil Acidity. In: *Methods of Soil Analysis Part 3 - Chemical Methods* (ed D. Sparks), pp. 475-490. Soil Science Society of America, Madison, Wisconsin USA.

Tongway D.J. & Ludwig J.A. (1990) Vegetation and soil patterning in semi-arid mulga lands of Eastern Australia. *Australian Journal of Ecology*, **15**, 23-34.

Tongway D.J. & Ludwig J.A. (1997) The Conservation of Water and Nutrients Within Landscapes. In: *Landscape Ecology, Function and Management: Principles From Australian Rangelands.* (eds J.A. Ludwig, D.J. Tongway, D. Freudenberger, J. Noble, & K.C. Hodgkinson), pp. 13-22. CSIRO Publishing, Collingwood.

Tunstall B. & Connor D. (1975) Internal water balance of Brigalow (*Acacia harpophylla* F. Muell.) under natural conditions. *Functional Plant Biology*, **2**, 489-499.

Turner N.C. & Jones M.M. (1980) Turgor maintenance by osmotic adjustment: a review and evaluation. In: *Adaptations of Plants to Water and High Temperature Stress* (eds N.C. Turner & P.J. Kramer), pp. 155-172. Wiley-Interscience, New York.

Tyree M.T. & Ewers F.W. (1991) Tansley Review No. 34. The hydraulic architecture of trees and other woody plants. *New Phytologist*, **119**, 345-360.

Tyree M.T. & Hammel H.T. (1972) The measurement of the turgor pressure and the water relations of plants by the pressure-bomb technique. *Journal of Experimental Botany*, **23**, 267-282.

van Dam O. (2000) *Modelling incoming Potential Radiation on a land surface with PCRaster: POTRAD5.MOD manual*. Utrecht Centre for Environment and Landscape dynamics, Utrecht University, the Netherlands.

Van Vreeswyk A.M.W., Payne A.L., Leighton K.A. & Hennig P. (2004) *An inventory and condition survey of the Pilbara region, Western Australia*. Department of Agriculture Western Australia.

Vicré M., Farrant J.M. & Driouich A. (2004) Insights into the cellular mechanisms of desiccation tolerance among angiosperm resurrection plant species. *Plant, Cell & Environment*, **27**, 1329-1340.

Voss I., Sunil B., Scheibe R. & Raghavendra A.S. (2013) Emerging concept for the role of photorespiration as an important part of abiotic stress response. *Plant Biology*, In Press.

Vriend S.P., van Gaans P.F.M., Middelburg J. & De Nijs A. (1988) The application of fuzzy c-means cluster analysis and non-linear mapping to geochemical datasets: examples from Portugal. *Applied Geochemistry*, **3**, 213-224.

Walters M.B. & Gerlach J.P. (2013) Intraspecific growth and functional leaf trait responses to natural soil resource gradients for conifer species with contrasting leaf habit. *Tree Physiology*, **33**, 297-310.

Warren C.R., Aranda I. & Cano F.J. (2011) Responses to water stress of gas exchange and metabolites in Eucalyptus and Acacia spp. *Plant, Cell & Environment*, **34**, 1609-1629.

Warwick N.W.M. & Thukten (2006) Water relations of phyllodinous and non-phyllodinous Acacias, with particular reference to osmotic adjustment. *Physiologia Plantarum*, **127**, 393-403.

Webb C.O., Ackerly D.D., McPeek M.A. & Donoghue M.J. (2002) Phylogenies and Community Ecology. *Annual Review of Ecology and Systematics*, **33**, 475-505.

Weiher E., Werf A.v.d., Thompson K., Roderick M., Garnier E. & Eriksson O. (1999) Challenging Theophrastus: a common core list of plant traits for functional ecology. *Journal of Vegetation Science*, **10**, 609-620.

Westoby M. & Wright I.J. (2006) Land-plant ecology on the basis of functional traits. *Trends in Ecology & Evolution*, **21**, 261-268.

Whalley W.R. (1993) Considerations on the use of time-domain reflectometry (TDR) for measuring soil water content. *Journal of Soil Science*, **44**, 1-9.

Wheeler J.K., Sperry J.S., Hacke U.G. & Hoang N. (2005) Inter-vessel pitting and cavitation in woody Rosaceae and other vesselled plants: a basis for a safety versus efficiency trade-off in xylem transport. *Plant, Cell & Environment*, **28**, 800-812.

Wiens J.J., Ackerly D.D., Allen A.P., Anacker B.L., Buckley L.B., Cornell H.V., Damschen E.I., Jonathan Davies T., Grytnes J.-A., Harrison S.P., Hawkins B.A., Holt R.D., McCain C.M. & Stephens P.R. (2010) Niche conservatism as an emerging principle in ecology and conservation biology. *Ecology Letters*, **13**, 1310-1324.

Wild B., Wanek W., Postl W. & Richter A. (2010) Contribution of carbon fixed by Rubisco and PEPC to phloem export in the Crassulacean acid metabolism plant *Kalanchoe daigremontiana*. *Journal of Experimental Botany*, **61**, 1375-1383.

Williams A.P., Allen C.D., Macalady A.K., Griffin D., Woodhouse C.A., Meko D.M., Swetnam T.W., Rauscher S.A., Seager R., Grissino-Mayer H.D., Dean J.S., Cook E.R., Gangodagamage C., Cai M. & McDowell N.G. (2013) Temperature as a potent driver of regional forest drought stress and tree mortality. *Nature Climate Change*, **3**, 292-297.

Williams C., Hanan N., Scholes R. & Kutsch W. (2009) Complexity in water and carbon dioxide fluxes following rain pulses in an African savanna. *Oecologia*, **161**, 469-480.

Williams J. (2002) *Fire Regimes and their Impacts in the Mulga (Acacia aneura) Landscapes of Central Australia* (State of the Environment Second Technical Paper Series (Biodiversity), Series 2). Department of Environment and Heritage.

Williams O.B. & Calaby J.H. (1985) The hot deserts of Australia. In: *Ecosystems of the World 12A: Hot Deserts and Arid Shrublands* (eds M. Evenari, I. Noy-Meir, & D.W. Goodall), pp. 269-312. Elsevier.

Winkworth R.E. (1973) Eco-physiology of mulga (*Acacia aneura*). *Tropical Grasslands*, **7**, 43-48.

Witt G.B., Noël M.V., Bird M.I., Beeton R.J.S. & Menzies N.W. (2011) Carbon sequestration and biodiversity restoration potential of semi-arid mulga lands of Australia interpreted from long-term grazing exclosures. *Agriculture, Ecosystems & Environment*, **141**, 108-118.

Wohlfahrt G., Fenstermaker L.F. & Arnone J.A. (2008) Large annual net ecosystem CO2 uptake of a Mojave Desert ecosystem. *Global Change Biology*, **14**, 1475-1487.

Wright I.J., Groom P.K., Lamont B.B., Poot P., Prior L.D., Reich P.B., Schulze E.-D., Veneklaas E.J. & Westoby M. (2004a) Leaf trait relationships in Australian plant species. *Functional Plant Biology*, **31**, 551-558.

Wright I.J., Reich P.B., Westoby M., Ackerly D.D., Baruch Z., Bongers F., Cavender-Bares J., Chapin T., Cornelissen J.H.C., Diemer M., Flexas J., Garnier E., Groom P.K., Gulias J., Hikosaka K., Lamont B.B., Lee T., Lee W., Lusk C., Midgley J.J., Navas M.-L., Niinemets U., Oleksyn J., Osada N., Poorter H., Poot P., Prior L., Pyankov V.I., Roumet C., Thomas S.C., Tjoelker M.G., Veneklaas E.J. & Villar R. (2004b) The worldwide leaf economics spectrum. *Nature*, **428**, 821-827.

Xu D., Su P., Zhang R., Li H., Zhao L. & Wang G. (2010) Photosynthetic parameters and carbon reserves of a resurrection plant *Reaumuria soongorica* during dehydration and rehydration. *Plant Growth Regulation*, **60**, 183-190.

Xu Z., Zhou G. & Shimizu H. (2009) Are plant growth and photosynthesis limited by pre-drought following rewatering in grass? *Journal of Experimental Botany*, **60**, 3737-3749.

Yancey P.H. (2005) Organic osmolytes as compatible, metabolic and counteracting cytoprotectants in high osmolarity and other stresses. *Journal of Experimental Biology*, **208**, 2819-2830.

Yazaki K., Sano Y., Fujikawa S., Nakano T. & Ishida A. (2010) Response to dehydration and irrigation in invasive and native saplings: osmotic adjustment versus leaf shedding. *Tree Physiology*, **30**, 597-607.

Zanne A.E., Sweeney K., Sharma M. & Orians C.M. (2006) Patterns and consequences of differential vascular sectoriality in 18 temperate tree and shrub species. *Functional Ecology*, **20**, 200-206.

Zanne A.E., Westoby M., Falster D.S., Ackerly D.D., Loarie S.R., Arnold S.E.J. & Coomes D.A. (2010) Angiosperm wood structure: Global patterns in vessel anatomy and their relation to wood density and potential conductivity. *American Journal of Botany*, **97**, 207-215.

Ziadat F.M. (2010) Prediction of Soil Depth from Digital Terrain Data by Integrating Statistical and Visual Approaches. *Pedosphere*, **20**, 361-367.

Zimmermann M.H. (1983) *Xylem Structure and the Ascent of Sap*. Springer-Verlag, Berlin.

Appendix A: A preliminary landscape stratification of the Hamersley Ranges for investigating the landscape distribution of mulga woodlands at West Angelas

Introduction

Landscape classification based on digital terrain modeling can be highly informative when investigating the ecology and distribution of plant species and relating it to subtle differences in topography. Digital terrain modeling is routinely used in earth science to map and predict soil attributes (Moore *et al.* 1993, Boer, del Barrio & Puigdefabregas 1996, Behrens *et al.* 2010, Ziadat 2010) and hydrological features including catchment boundaries and flow dynamics at both coarse (Quinn *et al.* 1991, Creed & Sass 2011) and fine scales (Hodge, Brasington & Richards 2009). As water is the most limiting resource in semi-arid and arid environments (Noy-Meir 1973, Morton *et al.* 2011), digital terrain analysis is particularly useful in these landscapes as it allows the modeling of redistribution and availability of water from readily available digital elevation models (DEM). Comparisons among landscape positions can be made quantitatively and similar locations identified using multivariate landform classification (Burrough *et al.* 2000, Burrough *et al.* 2001, Richardson, Fortin & Branfireun 2009). My objective was to stratify the landscape at West Angelas using a classification analysis based on terrain attributes derived from a digital elevation model (DEM) that predict the redistribution and availability of water and solar irradiance. The resulting classification can then be used to delineate among different landscape positions in the hills and valleys of the West Angelas area as a basis for on-ground surveying of the distribution and morphological composition of mulga woodlands in the area (Chapters 2 and 3).

Methods

Interpolation of raw point-elevation data

Raw point-elevation data with a resolution of 12 m (x,y) that covered an area of 105 km^2 of the West Angelas area in the Pilbara region of Western Australia was supplied by Pilbara Iron Pty. Ltd. A digital elevation model (DEM) with a cell size of 15 m was generated using the TopotoRaster tool in ArcGIS 9.0 (ESRI 2006). TopotoRaster is a data-interpolation method that produces a hydrologically accurate DEM by eliminating spurious 'sinks' and 'pits' in raw point-elevation data, and is based on the ANUDEM program developed by Hutchinson (1989). Owing to the large extent of the DEM, it was resampled to 30 m with PCRaster software (PCRaster 2006) to reduce the computational requirements of subsequent processing.

Calculation of terrain attributes

Five terrain attributes that modelled the potential redistribution and availability of light and water across the landscape were calculated using dynamic simulation models in PCRaster. Elevation (*ELEV*), local slope angle (*SLO*), and the specific catchment area draining to each cell (*ARE*) were primary terrain attributes derived from the 30 m DEM. The soil wetness index (*WI*) was calculated as an estimate of the capacity of each cell in the DEM to accumulate the runoff from its specific catchment area (ARE) and store it as a function of the local slope (SLO) (equation A.1, following Bevan & Kirkby 1979, Burrough, van Gaans & MacMillan 2000, Moore *et al.* 2000) . The length-slope factor (*LSF*, equation A.2) estimates the potential volume and flow velocity of runoff analogous to the length-slope factor of the Universal Soil Loss Equation (USLE) and derived from the unit stream power theory by Moore and Burch (1986)(1986)(1986)(1986)(1986)(1986).

$$WI = \ln(ARE/\tan SLO) \qquad \text{(eq. A.1)}$$

$$LSF = \left(\frac{ARE}{22.13}\right)^{0.4} \cdot \left(\frac{\sin SLO}{0.0896}\right)^{1.3} \qquad \text{(eq. A.2)}$$

Potential annual incident solar radiation was calculated using the program POTRAD5 for PCRaster, at six time periods each day for four days in 12 months (van Dam 2000). All primary and secondary terrain attributes were averaged over 40 iterations where a

random normal error of ± 15 m was assigned to the z-axis to account for the reported vertical error of the DEM. Averages were used to 'smooth out' any artefacts in the primary terrain attributes that result from minor errors in the elevation and have a disproportionally large influence on resulting analyses, particularly in flat terrain (Burrough *et al.* 2000, Burrough *et al.* 2001)

Landscape classification

'Landscape units' of similar topographic character were determined using fuzzy *k*-mean cluster analysis with the FUZNLM program (Vriend *et al.* 1988). Fuzzy *k*-mean cluster analysis of multivariate data has an advantage over 'hard' clustering methods in a geographic context owing to the continuous and often overlapping nature of environmental data (Burrough *et al.* 2000). Continuous (or fuzzy) classification assigns every cell in a DEM a 'membership value' between 0 and 1 for each cluster, where membership is strongest as the value approaches 1, and the membership across all clusters sums to 1. Comparison of the membership values of a particular cell for every cluster allows quantification of the degree of certainty when then assigning each cell to a particular cluster.

A random sample of 10 000 cells (0.28% total area) from the DEM were used for fuzzy *k*-mean cluster analysis. The cluster centre *C* of the c^{th} cluster for the j^{th} attribute *x* was determined for between 2 and 9 clusters over 500 iterations on untransformed data using equation A.3. The exponent *q* controls the extent of membership between fuzzy clusters (Bezdek 1981) or 'fuzziness' of the model (Vriend *et al.* 1988). When $q = 1$ the fuzzy *k*-mean clustering converges to conventional hard clustering (i.e. values of 0 and 1 only), and while there is no theoretical basis for the selection of *q*, it is usually a value between 1.5 and 3 (Vriend *et al.* 1988), in this case *q* was set at 1.5 following Burrough *et al.* (2000).

$$C_{cj} = \frac{\sum_{i=1}^{N} (u_{ic})^q * x_{ij}}{\sum_{i=1}^{N} (u_{ic})^q} \qquad \text{(eq. A.3)}$$

The classification entropy (*H*-scaled, equation A.4) and partition coefficient (*F*-scaled, equation A.5) were used to determine the optimal number of clusters. While the formulae for calculating *H* and *F* are provided here (reproduced from Vriend *et al.* 1998), values were provided in the output from FUZNLM. The partition coefficient is

comparable to the *F*-ratio of pooled within cluster to between cluster covariance, with stronger clustering when the value approaches 1. Similarly, the classification entropy is analogous to thermodynamic entropy and indicates more significant clustering as it approaches 0 (Vriend *et al.* 1988).

$$H = -\sum_{k=1}^{N}\sum_{i=1}^{C}[u_{ki}.\log(u_{ki})/N] \quad \text{(eq. A.4)}$$

$$F = \sum_{k=1}^{N}\sum_{i=1}^{C}[(u_{ki})^2/N] \quad \text{(eq. A.5)}$$

Once the optimal number of clusters was determined, the cluster centroids produced by the fuzzy *k*-mean classification were then used to assign membership values for all cells in the DEM. Membership of each cell (μ) of the i^{th} object to the c^{th} cluster was calculated with equation A.6, where *d* is the distance measure used, which in this case was the diagonal metric (equation A.7) and where s_j is the standard deviation of the j^{th} variable. The diagonal metric was selected because it allows scale invariance by standardizing each variable by its standard deviation (Vriend *et al.* 1988).

$$\mu_{ic} = \frac{[(d_{ic})^2]^{-1/(q-1)}}{\sum_{c'=1}^{K}[(d_{ic'})^2]^{-1/(q-1)}} \quad \text{(eq. A.6)}$$

$$(d_{ic})^2 = \sum_{j=1}^{V}\left[(x_{ij} - C_{cj})/s_j\right]^2 \quad \text{(eq. A.7)}$$

A ‘confusion index’ was used to quantify the strength of the classification for each cell (equation A.8). When the ratio of the second highest membership value to the highest membership value was ≥ 0.7 the cell was assigned to the cluster with the strongest membership value. When the value was <0.7 the cell was not assigned to any cluster. A

confusion index has been applied in comparable terrain classifications, and is a useful index of class overlap (Burrough *et al.* 2001), particularly when spatial correlation is strong (Burrough, van Gaans & Hootsmans 1997).

$$CI = \mu_i, \max 2/\mu_i, \max 1 \qquad \text{(eq. A.8)}$$

Outcomes of the classification analysis

Fuzzy k-mean classification

Optimal clustering of the five terrain attributes was achieved with two clusters (maximum *H* and minimum *F* indices, Appendix A.1), which distinguished between the hills and the flat plains of the DEM. However, a classification of the landscape into two very broad terrain units was not considered the most useful approach for designing a sampling regime to describe and map the distribution of plant species. Therefore, a heuristic approach was used to instead select seven clusters as the optimal number in this study. Seven clusters was a 'local' maximum and minimum for *H* and *F* indices respectively (Appendix A.1), and when mapped on the DEM provided a more useful stratification of the landscape. A heuristic method to select optimal clustering can be part of a multivariate analysis, as the *H* and *F* indices only describe properties of the model rather than of the data, and thus can be considered in the context of the overall objectives of the analysis (Vriend *et al.* 1988). Similarly, the fuzzy *k*-mean cluster analysis initially contains no information on the geographical continuity of the final 'classes', but if the source data are spatially correlated then the final membership values are also likely to be spatially correlated (Burrough *et al.* 1997, Burrough *et al.* 2000). When terrain units were mapped it was clear that they were spatially correlated, as terrain units were clearly classifying particular landscape features (i.e. upper and lower hill slopes and drainage features, Appendix A.2).

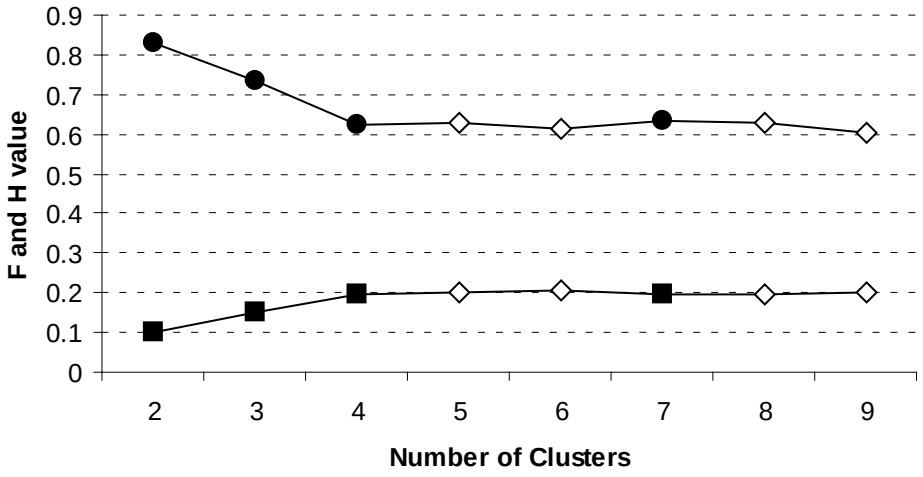

Appendix A.1 Classification entropy ■, *H*-scaled[1-F<H<max]) and participation coefficient (●, *F*-scaled [min<F<1]) for 2 – 9 clusters produced by *k*-mean cluster analysis over 500 iterations. 5, 6, 8 and 9 clusters were not able to resolve after 500 iterations (◊).

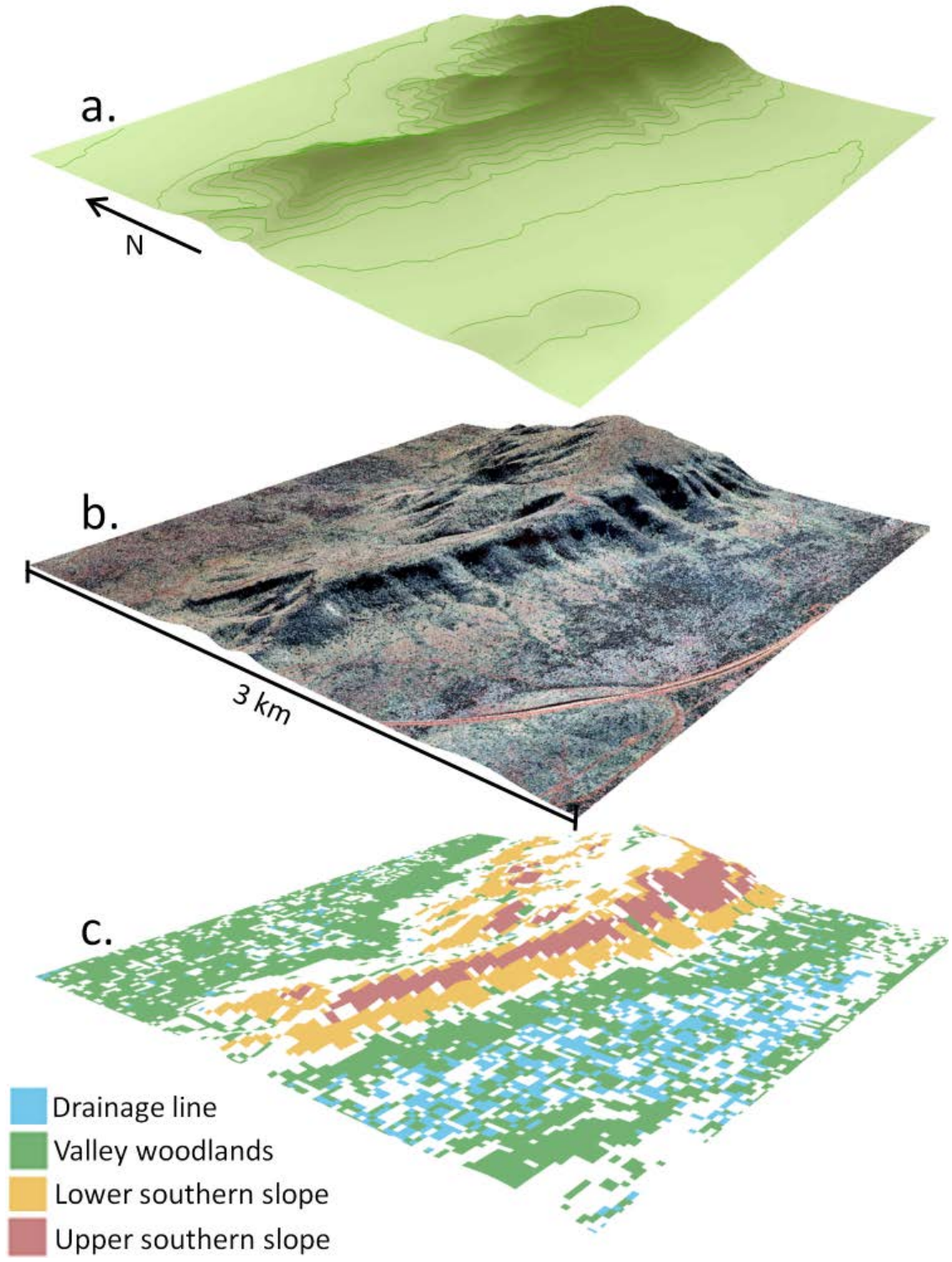

Appendix A.2 Terrain classification of the Hamersley Ranges produced using fuzzy *k*-mean cluster analysis compared with digital terrain model and aerial photography for a small subset of the spatial dataset processed in this study. (a) Digital elevation model (DEM) with 30 m contours. Elevation range is 506 – 754 m a.s.l. (b) Aerial photograph draped over DEM demonstrating differences in vegetation distribution. (c) Terrain classification draped over DEM. Four terrain units containing mulga communities, chosen from a total of seven (not including the confusion index) produced by the fuzzy *k*-mean cluster analysis.

Evaluation of classification analysis for a landscape sampling regime

This landscape classification successfully delineated between seven discrete landscape positions and also identified areas that were unable to be categorically assigned to one particular unit based on the 'confusion index'. Consequently, these terrain units provide a very useful guide when traversing the landscape at West Angelas for the purpose of surveying the diversity of mulga woodlands across the range of landscape features (Chapter 2). For example, this terrain classification demonstrated a clear differentiation of major drainage features with higher cumulative flow from the surrounding low-relief valley floor woodlands. However, *Acacia aneura* (Mulga) does not occur ubiquitously over the landscape at West Angelas. Instead, Mulga is very common in the broad valleys, but absent on plateaux and north facing hill slopes (Figure 2.1). Therefore, the four landscape units that likely contained Mulga were selected from the landscape classification, and assigned a general name based on their geographic position: Upper southern slopes, lower southern slopes, valleys and drainage lines (Appendix B.1, Appendix A.2). Finally, while Mulga occurred in all four terrain units, the majority of the woodlands were captured by the "valley" landscape unit. Therefore, the valleys were further stratified into three woodland structural types based on the spatial patterning and estimated projected foliage cover of the tallest stratum, and is described in greater detail in Chapter 2.

Appendix B: Supplementary figures and tables from Chapter 2[7]

Appendix B.1 Modelled landscape attributes by landscape position in the Hamersley Ranges.

Landscape Position	Elevation (m)	Length/ Slope Factor	Slope (Degrees)	Incident Solar Radiation (MJ m^{-2} day^{-1})	Soil Wetness Index
Drainage Line	**692** (0.36)	**27.0** (0.11)	**4.62** (0.02)	**6.81 e^3** (1.02)	**12.0** (0.008)
Valley	**747** (0.21)	**8.85** (0.07)	**4.12** (0.02)	**6.86 e^3** (0.72)	**10.9** (0.004)
Lower Southern Slope	**822** (0.62)	**36.9** (0.10)	**19.8** (0.03)	**6.14 e^3** (1.75)	**8.81** (0.003)
Upper Southern Slope	**921** (0.48)	**63.5** (0.10)	**30.1** (0.03)	**5.52 e^3** (2.09)	**8.61** (0.003)

Mean values are bolded and standard errors are in parentheses.

[7] These two tables and two figures were published as Appendices 1 -4 in the published version of Chapter 2:
Page G.F.M., Cullen L.E., van Leeuwen S. & Grierson P.F. (2011) Inter- and intra-specific variation in phyllode size and growth form among closely related Mimosaceae *Acacia* species across a semiarid landscape gradient. *Australian Journal of Botany*, **59**, 426-439.

Appendix B.2 Mean values of branching attributes for each growth form of species in the Mulga complex at West Angelas.

	Growth Forms										
	Shrubs		Multi-stemmed trees			Single-stemmed trees					
	S1	S2	T1	T2	T4C	T3A	T3B	T4A	T4B	T5	p-value
Number of individuals	***6***	***14***	***98***	***4***	***302***	***98***	***160***	***50***	***53***	***6***	
Basal diameter (mm)	**137** (21.7)	**127** (8.76)	**116** (5.56)	**215** (46.3)	**196** (4.19)	**126** (5.60)	**92** (2.57)	**214** (8.63)	**137** (5.51)	**87** (15.03)	**<0.001**
Number of stems	**5.66** (0.80)	**3.50** (0.70)	**2.56** (0.13)	**8.00** (2.12)	**2.34** (0.06)	**1.06** (0.02)	**1.02** (0.01)	**1.00** (0.00)	**1.00** (0.00)	**1.00** (0.00)	**<0.001**
Diameter of stem 50 cm from ground	**75.6** (9.43)	**61.0** (5.38)	**83.5** (3.74)	**153** (32.4)	**139** (2.96)	**102** (5.10)	**68.2** (2.01)	**175** (7.5)	**105** (3.22)	**67.3** (11.09)	**<0.001**
Height to first stem division (m)	**0.08** (0.03)	**0.36** (0.13)	**0.30** (0.05)	**0.07** (0.05)	**0.27** (0.02)	**1.44** (0.09)	**2.06** (0.10)	**2.25** (0.16)	**2.76** (0.19)	**1.75** (0.34)	**<0.001**
Height to crown break (m)	**0.53** (0.15)	**1.60** (0.13)	**1.84** (0.10)	**0.75** (0.22)	**3.20** (0.13)	**2.29** (0.11)	**3.54** (0.14)	**4.44** (0.36)	**5.84** (0.25)	**1.15** (0.23)	**<0.001**
Canopy Area (m^2)	**11.2** (1.76)	**7.39** (1.14)	**9.33** (0.68)	**28.2** (8.59)	**19.6** (0.72)	**13.4** (0.82)	**6.98** (0.61)	**25.0** (1.79)	**9.18** (0.62)	**8.10** (2.46)	**<0.001**
Tree Height (m)	**3.13** (0.34)	**3.92** (0.18)	**5.06** (0.16)	**6.15** (0.56)	**6.96** (0.11)	**5.76** (0.13)	**6.07** (0.13)	**8.69** (0.34)	**8.63** (0.24)	**4.46** (0.68)	**<0.001**

Mean values are bolded, and standard errors are given in parentheses. *P*-values denote significance for one-way ANOVA tests for differences among forms for each attribute. Pair-wise comparisons not shown. See text in Chapter 2 for definitions of growth forms.

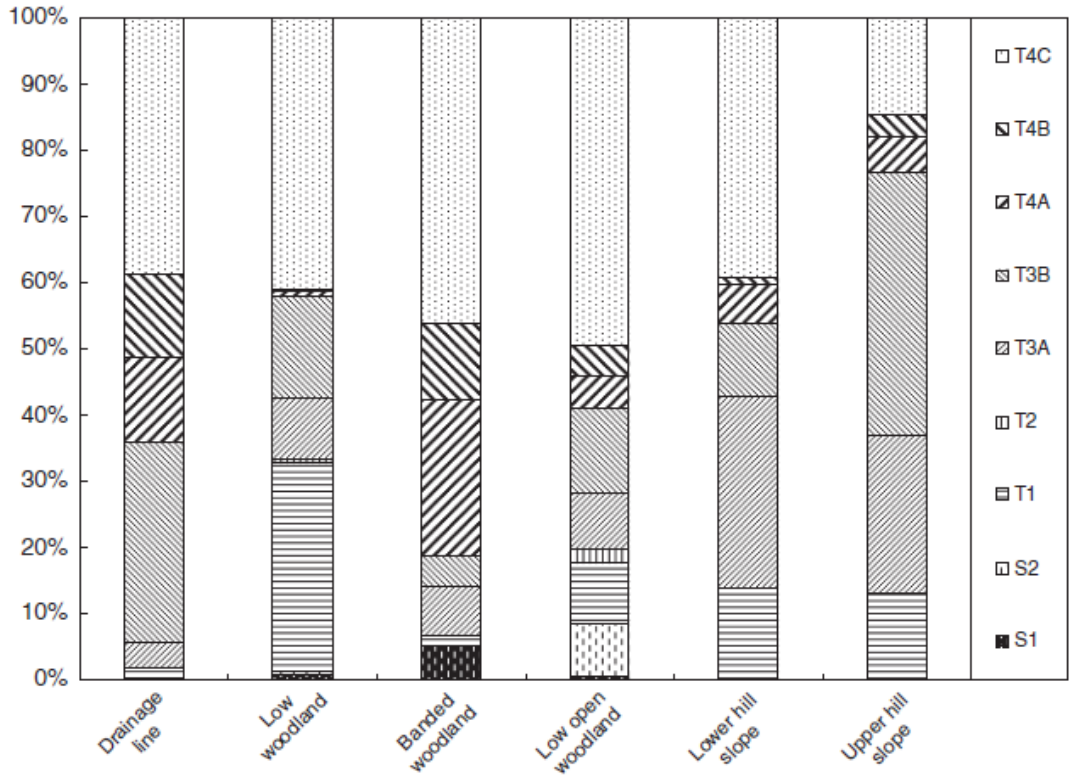

Appendix B.3 Relative dominance (%) of growth forms of species in the Mulga complex in each landscape position at West Angelas. The dominant growth form T4C is represented by black dots, bolded diagonal lines represent single-stemmed tall trees, fine diagonal lines represent single-stemmed small trees, and horizontal and vertical lines represent all other multi-stemmed forms (S1, S2, T1, T2).

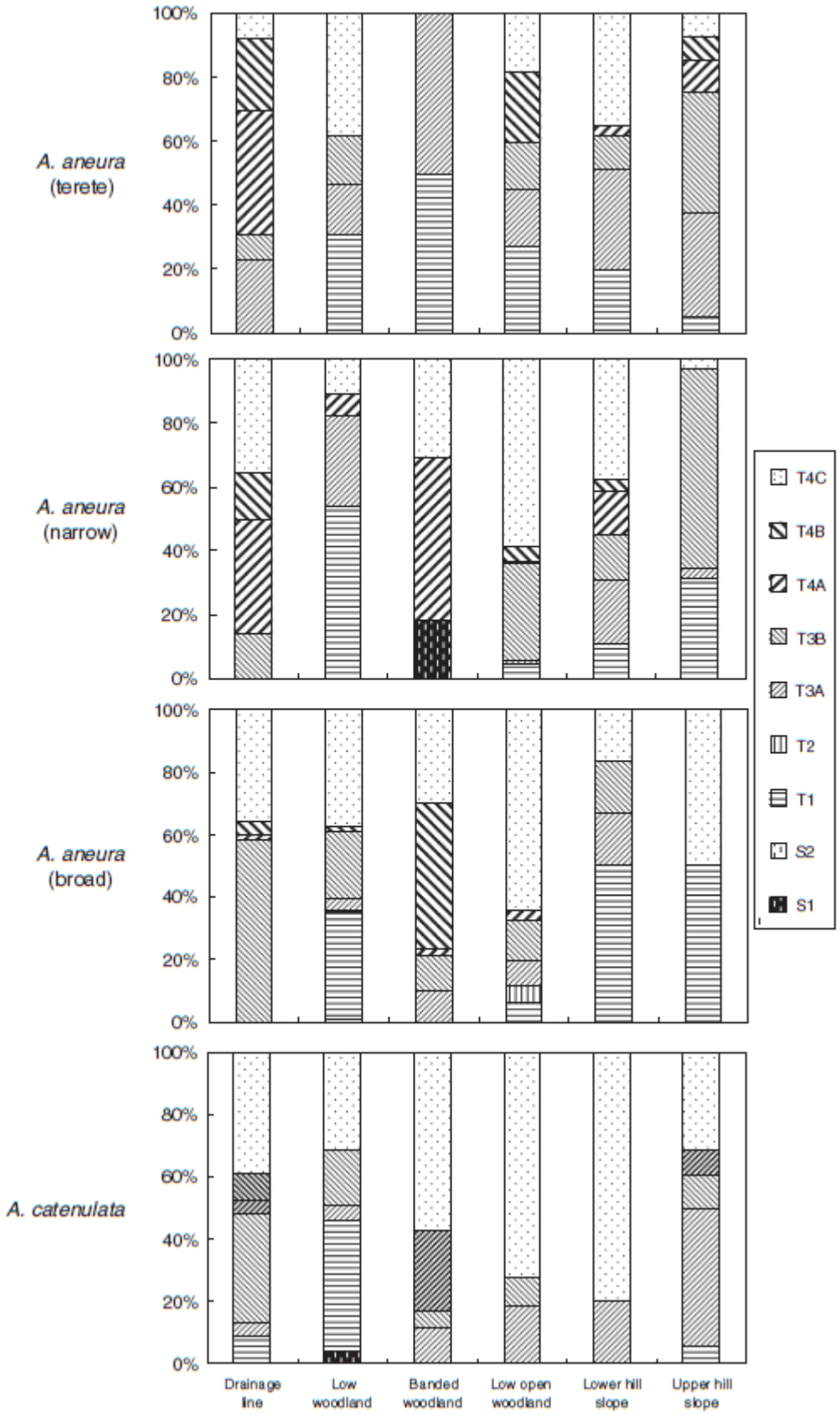

Appendix B.4 Relative abundance (%) of each growth form in each landscape position of two species in the Mulga complex at West Angelas including three phyllode variants of *A. aneura*. Diagonal lines represent single-stemmed growth forms, dots represent the multi-stemmed tall tree 'T4C' and horizontal and vertical lines represent all other multi-stemmed growth forms.

Appendix C: Table of synonyms applied in this thesis revised against the treatment of Maslin & Reid (2012)

Chapter 2 and 6 of this thesis were published in scientific journals before the publication of Maslin & Reid (2012). Therefore, the species name *A. aneura* was used in the broad sense (*s. lat.*) in these papers and *A. aneura* was subdivided into "phyllode shape variants" (Chapter 2 onwards). The broad usage of *A. aneura* was therefore adopted in the remaining chapters of this thesis for consistency.

I have recently re-examined representative sterile specimens collected as part of the thesis. Species were provisionally identified by Jordan Reid and checked by Bruce Maslin from the Western Australian Herbarium. Maslin & Reid had also vouchered replicate specimens of my study trees at the Western Australian Herbarium. Appendix C.1, below, provides the Maslin & Reid (2012) species names along with a voucher number for material lodged at the Western Australian Herbarium against the synonyms used in this thesis when referring to "phyllode shape variants" of *A. aneura*.

In some instances, synonyms that described "phyllode shape variants" of *A. aneura* did not consistently correspond to particular species following Maslin & Reid (2012). For example, "terete" *A. aneura* found at Site 7 were identified as *A. aptaneura*, whereas trees sharing the same phyllode shape at Site 20 were *A. macraneura*. *Acacia aneura* with "narrow" phyllodes were the most variable; trees were identified as three different species: *A. aptaneura, A. incurvaneura* and *A. paraneura*, not including hybrids. Perhaps most interestingly, *A. aptaneura* appears to have the most variable phyllode morphology of the species captured by this study at West Angelas; trees had "terete", "narrow" and "broad" phyllodes.

Appendix C.1 Table of synonyms used in this thesis and corresponding species names according to Maslin & Reid (2013) based on representative sterile collections.

Synonym used in thesis	Species	Voucher Number – Western Australian Herbarium	Collection Sites (Page, PhD Thesis)
A. aneura (terete)	*A. aptaneura* Maslin & J.E.Reid	BRM 9425	GP7
	A. macraneura Maslin & J.E.Reid	BRM 9213	GP20
A. aneura (narrow)	*A. aptaneura* Maslin & J.E.Reid	BRM 9428, 9422, 9432	GP12, 13, 26
	A. aptaneura x paraneura	BRM 9427	GP13
	A. incurvaneura Maslin & J.E.Reid	Not vouchered	GP13
	A. paraneura Randell	BRM 9421	GP12
A. aneura (broad)	*A. aneura* s.s.	BRM 9423	GP12
	A. aptaneura Maslin & J.E. Reid	BRM 9430	GP20, 21